

https://dspace.org/

Taxonomy, taphonomy, and biostratigraphic significance of a basal sauropodomorph from the lower elliot formation, Eastern Cape, South Africa

Dinter, Cory Michaela

2018

https://hdl.handle.net/10539/32774

Downloaded from a DSpace repository. https://dspace.org/

TAXONOMY, TAPHONOMY, AND BIOSTRATIGRAPHIC SIGNIFICANCE OF A BASAL SAUROPODOMORPH FROM THE LOWER ELLIOT FORMATION, EASTERN CAPE, SOUTH AFRICA

A dissertation presented to the Faculty of Science, University of the Witwatersrand, in fulfillment of the requirements for the degree of Master of Science (Palaeontology)

By: Cory Michaela Dinter
Student number: 1533829
Supervisor: Prof. Jonah Choiniere
Co-Supervisors: Dr. Blair McPhee & Dr. Pia Viglietti

School of Geosciences and Evolutionary Studies Institute (ESI), University of the Witwatersrand, Private Bag 3, WIT 2050, Johannesburg, South Africa.

Declaration page

I declare that this dissertation is my own work. It is being submitted for the degree of Master of Science at the University of the Witwatersrand, Johannesburg. It has not been submitted before for any degree or examination at any other university.

Signature: _____ Date: 12th July 2018

Abstract

South Africa's lower Elliot Formation is notably depauperate in fossils relative to the upper strata. These lower layers, however, are important because they preserve Triassic deposits leading up to a mass extinction event at the Triassic-Jurassic boundary. A new, associated skeleton of a single specimen of basal sauropodomorph recently collected from the lower Elliot Formation represents an extremely rare find from this stratum. This project investigates the systematic position, taphonomy, and stratigraphic context of this specimen through anatomical description, phylogenetic systematics, and sedimentological interpretation. This dissertation shows that the specimen was preserved in a sequence of low-energy stream deposits and overbank/oxbow lakes suggestive of a local death instead of one of transportation. The new specimen represents a new species that is part of a small clade of specimens referred to "*Melanorosaurus*". However, due to poor provenance data and poor association within the syntype and referred material calls into question the validity of "*Melanorosaurus*". This clade, and the taxa within it, require taxonomic revision.

Acknowledgements:

The completion of this dissertation would not have been possible without the support, generosity, kindness, and friendship provided by friends and family worldwide.

Paramount to this project and its completion was my primary supervisor, Professor Jonah Choiniere, who provided a wealth of knowledge, insight, advice, tasty tacos, speedy edits, and all sorts of inspiration. A wholehearted thank you is given for an incredible two years.

Huge thanks is given to Dr. Blair McPhee, co-supervisor for this project. Thank you for your immense erudition, your remarkable patience, and your friendship, Blair. Thanks is also given to my other co-supervisor, Dr. Pia Viglietti, for irreplaceable assistance in the field, for helpful edits and ideas, and for being an all-around superb friend!

Thank you so much to all the funders who made this endeavor financially possible: PAST, NRF, AOP, NRF CPRR, the Friedel Sellschop Award, and COE.

To Hannie, Nelly, and Redvis: Moerse groot dankie vir julle gasvryheid en toegang tot julle grond – sonder julle sou hierdie projek nie moontlik gewees het nie!

I would like to thank Chalton Dube and everyone down in the fossil preparation lab for the assistance, advice, and friendship. A special thank you is given to Cynthia Kemp for all the beautiful preparation work on BP/1/7811 – your work is indispensable!

Thank you to Bronwyn Quinn, Tandi Scott-Turner, Nelly Nkosi for solving every problem and putting up with all my silly postcards and thank you to Professor Marion Bamford for keeping ESI running smoothly!

Choinere Bone Lab (Jonah Choiniere, Kimi Chapelle, Kat Clayton, Kathleen Dollman, Christophe Hendrickx, Blair McPhee, Cebisa Mdekazi, Isabel Meyer, Casey Staunton, Vik Radermacher, Rick Tolchard, Gina Viglietti, Pia Viglietti, Kelsey Glennon, Freyja, Midas, and Mella), you guys are amazing. I couldn't have asked for a better, more fun, group of colleagues. Each of you are completely brilliant and inspiring. Thank you for everything. Special thank as well to Dave Groenewald for being my friend from day one, you and the rest of the Tequila Friday regulars made South Africa home.

Thanks is also given to Dr. Mark Loewen who provided valuable conversation pertaining to this project as well as an abundance of Illustrator knowhow.

And finally thank you to my family: Margo Collier and David Dinter, thank you for all the unconditional love and support. You guys are amazing parents and I am so lucky to have you in my life. Noah, thank you for putting up with all the late nights and craziness. You are the very best partner.

TABLE OF CONTENTS

DECLARATION ii

ABSRACT iii

ACKNOWLEDGEMENTS iv

Chapter 1: INTRODUCTION AND LITERATURE REVIEW 1

1.1 General Introduction 1

1.2 Overview of the Elliot Formation 4

1.3 History of Sauropodomorpha 6

1.4 Systematics and Evolution 7

1.5 Sauropodomorph Biostratigraphy in the Elliot Formation 9

1.5.1 Lower Elliot Taxa Taxonomy and Legitimacy 11

1.5.1.1 *Euskelosaurus brownii* Huxley, 1867 12

1.5.1.2 *Plateosauravus cullingworthi* Haughton, 1924 12

1.5.1.3 *Eucnemesaurus* van Hoepen, 1920 13

1.5.1.4 *Blikanasaurus cromptoni* Galton & van Heerden, 1985 14

1.5.1.5 The "Bloem/Maphutseng dinosaur" 14

1.5.1.6 *Melanorosaurus readi* Haughton, 1924 15

1.5.1.7 Summary 17

1.5.1.8 BP/1/7811 17

Chapter 2: MATERIALS AND METHODOLOGY 21

2.1 Taphonomic Materials and Methodology 21

2.2 Geological Field Methodology 25

2.3 Specimen Excavation and Preparation 25

2.4 Taxonomic and Anatomical Materials and Methodology 26

2.5 Phylogenetic Systematics 27

2.5.1 Selection of Problematic LEF Specimens for Cladistical Analysis 28

2.6 Institutional Abbreviations 29

Chapter 3: RESULTS **31**

3.1 H5 Lithofacies 31

3.2 Taphonomy 32

3.3 Preparation Observations 34

3.4 Facies Association Overview 34

3.5 Anatomical Descriptions 36

3.5.1 Axial Skelton 36

3.5.1.1 Cervical Vertebrae 36

3.5.1.2 Dorsal Vertebrae 41

3.5.1.3 Caudal Vertebrae 47

3.5.2 Appendicular Skeleton 48

3.5.2.1 Scapula 48

3.5.2.2 Humerus 50

3.5.2.3 Radius 54

3.5.2.4 Ulna 55

3.5.2.5 Manus 57

3.5.2.5.1 Metacarpal 1 57

3.5.2.5.2 Metacarpal 2 59

3.5.2.5.3 Non-terminal ?manual phalanges 61

3.5.2.5.4 ?manual ungual phalanx 62

3.5.2.6 Ilium 62

3.5.2.7 Pubis 66

3.5.2.8 Femur 68

3.5.2.9 Tibia 71

3.5.2.10 Fibula 74

3.5.2.11 Pes 76

3.6 Taxonomy 78

3.7 Phylogenetics 83

3.8 BP/1/7811 Differentiation 83
3.8.1 BP/1/7811 vs. NMQR 1551 83
3.8.2 BP/1/7811 vs. NMQR 3314 83
3.8.3 BP/1/7811 vs. *Plateosauravus* 84
3.8.4 BP/1/7811 vs. *Sefapanosaurus* 84
3.8.5 BP/1/7811 vs. *Eucnemesaurus* 85

Chapter 4: SYSTEMATICS 88

4.1. Systematic Paleontology 88
4.2 Gen. et. Spec. nov. 88
4.3 Holotype 88
4.4 Type Locality 88
4.5 Horizon and Age 89
4.6 Diagnosis 89

Chapter 5: DISCUSSION 91

5.1 Taphonomy Through Depositional Environment 91
5.2 Taxonomy and Phylogenetic Analysis 94
5.2.3 Functional Morphology 97

Chapter 6: CONCLUSIONS 99

REFERENCES 100
APPENDIX 112
Tables 112
Matrix 116

FIGURE LIST

Figure 1: The Elliot Formation of South Africa 3
Figure 2: Range zones from Kitching & Raath's (1984) 11

Figure 3: H5 Stratigraphic Column 19
Figure 4: Full skeleton (excluding ribs and gastralia) 20
Figure 5: H5 Quarry map 21
Figure 6: Hindlimb jacket 22
Figure 7: Rib distribution rose diagram 23
Figure 8: Long bone distribution rose diagram 23
Figure 9: All bones (excluding rib) distribution rose diagram 23
Figure 10: Bone weathering stages from Behrensmeyer (1978) 24
Figure 11: Predation/scavenging marks on pubes 33
Figure 12: Cervical vertebra 5? 37
Figure 13: Cervical vertebra 7? 38
Figure 14: Dorsal vertebra 1? 42
Figure 15: Dorsal vertebra 2? 42
Figure 16: Dorsal vertebra 4?.. 43
Figure 17: Dorsal vertebra 5?.. 44
Figure 18: Dorsal vertebra 6?.. 44
Figure 19: Dorsal vertebra 8?. 45
Figure 20: Dorsal vertebra 12? 45
Figure 21: Dorsal vertebra 13? 46
Figure 22: Posterior caudal vertebrae 47
Figure 23: Left scapula 49
Figure 24: Right humerus 53
Figure 25: Right radius (distal) 55
Figure 26: Left ulna (proximal)... 56
Figure 27: Metacarpal 1 58
Figure 28: Metacarpal 2 60
Figure 29: Non-terminal ?manual phalanges (3).... 61
Figure 30: ?Manual ungual phalanx 62
Figure 31: Left ilium 65

Figure 32: Left pubis..... 67
Figure 33: Left femur..... 69
Figure 34: Left tibia..... 72
Figure 35: Right fibula..... 74
Figure 36: Right pedal ungual..... 77
Figure 37: Time-calibrated strict consensus..... 82

TABLE LIST

Table 1: H5 Jackets..... 112
Table 2: Vertebral measurements..... 113
Table 3: Appendicular measurements..... 114

Chapter 1: Introduction and Literature Review

1.1 General Introduction

Sauropodomorph dinosaurs were one of the most successful clades of terrestrial animals to walk this planet. They diverged from other dinosaurian lineages during the Carnian stage (Sereno et al., 1993; Langer et al., 1999; Wilson, 2002; Martínez & Alcober, 2009; Müller et al., 2018), during which time they were small, gracile, bipedal animals (e.g., *Saturnalia*, *Panphagia*, *Eoraptor*) relatively undifferentiated from the plesiomorphic saurischian condition (Langer et al., 1999; Sereno et al., 1993; Martínez & Alcober, 2009). However, due to recent finds, the affinity of these Carnian taxa remain relatively undetermined in comparison to their Norian counterparts (Martinez & Alcober, 2009). By the earliest Jurassic, they had become the first dinosaurian bulk-browsers to gain cosmopolitan distribution (Novas, 2009), and they remained the dominant herbivores in many areas until the end of the Cretaceous (Sander et al., 2011).

From the Norian stage onwards, sauropodomorph evolution is marked by a general increase in body size accompanied by the development of a quadrupedal locomotory habit and herbivorous feeding strategy (Raath, 1972; Buffetaut et al., 2000; Yates and Kitching, 2003; Upchurch & Barrett, 2005; Sander et al, 2011; Benson et al., 2014). While the earliest members of the clade weighed only 10-35 kilograms, maximum body mass increased dramatically over the course of sauropodomorph evolution (Benson et al., 2014), ultimately making them the

largest animals to have ever walked on Earth (Bonaparte & Coria, 1993; Haines & Chambers, 2007; Sander et al., 2011).

Many non-sauropodan sauropodomorph taxa are well known (e.g., *Plateosaurus, Massospondylus*, *Antetonitrus*) but the complexities of their early transition into derived, quadrupedal, massive sauropodans are still not entirely clear. This is particularly true of the Triassic South African representatives which are marred by poor provenance data, incomplete specimens, and chimaeric specimens which obscure understanding of the transition (McPhee et al., 2017). There is also a great deal of confusion regarding the specific evolutionary history and relationships of taxa occupying a more central position on the sauropodomorph stem (basal to Sauropoda).

In the last 20 years there has been a dramatic resurgence in work on non-sauropodan sauropodomorphs (e.g., Yates, 2003; Martínez & Alcober, 2009; Smith & Pol, 2007; Ezcurra, 2010; Yates et al., 2010; Pol et al., 2011; McPhee et al., 2014, 2015 a&b, 2017; Müller et al., 2018). This research has precipitated further understanding of the evolution of the earliest members of this group, which will ultimately provide vital information on how these initially light, bipedal animals evolved into the largest terrestrial animals in Earth's history, and how they were able to dominate the large-bodied herbivore niche for almost 150 million years (Tidwell & Carpenter, 2005; Sander et al., 2011; Langer et al., 2010).

A key stratum for addressing these issues is the Elliot Formation of South Africa (Fig. 1). The Triassic component of this rock unit, known informally as the lower Elliot Formation (Bordy et al., 2004a, 2004b, 2004c), is understudied. The associated fossil assemblage that will form the basis of this study (BP/1/7811) was collected the Eastern Cape Province of South Africa from the lower Elliot Formation. Representative elements of most of the appendicular skeleton, along with multiple vertebrae, were collected from this assemblage.

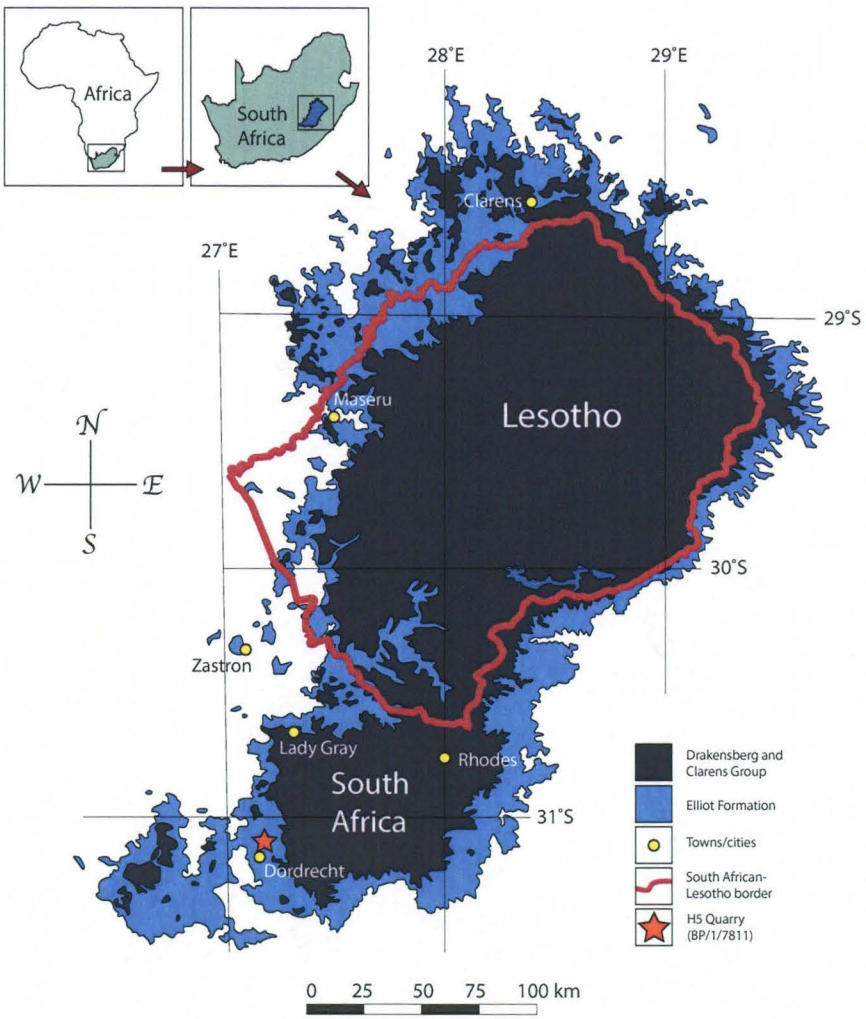

Figure 1: (Modified from Bordy & Erikkson, 2015) Map depicting Elliot Formation outcrops in South Africa and Lesotho and the location of the H5 Quarry in the southeast (marked by orange star).

1.2 Overview of the Elliot Formation

The Late Triassic to Early Jurassic Elliot Formation is the middle unit of the Stormberg Group sequence and crops out in both South Africa and Lesotho, surrounding the Drakensberg Massif. The formation stretches across approximately 20 million years, spanning the late Norian to Sinemurian stages of the Mesozoic (Bordy & Eriksson, 2015; Sciscio & Bordy, 2016). The Elliot Formation is underlain by the Molteno Formation and overlain by the Clarens Formation (Bordy & Catuneanu, 2001; Catuneanu et al., 2005). The Molteno/Elliot Formation contact is a disconformity, whereas the contact between the Elliot and Clarens Formations is conformable and gradational (Bordy & Eriksson, 2015), as observed in the Eastern Cape, Free State, and Kwa-Zulu Natal provinces (Fig. 1).

The Elliot Formation preserves a depositionally continuous record of the non-marine Triassic-Jurassic boundary (Bordy et al., 2004a; Bordy & Eriksson, 2015). Diverse vertebrate fossils are known from the Elliot at this time, which is an important period in the evolution of dinosaurs and mammals (Brusatte et al., 2008). In particular, it contains one of the richest known record of basal sauropodomorphs, the ancestors to the iconic long-necked Jurassic sauropods (McPhee et al., 2017).

Earlier work divided the Elliot Formation "Red-Beds" succession of mud-and-siltstones and sandstones into three informal members: lower, middle, and upper (Haughton, 1924; Olsen & Galton, 1977; Kitching & Raath, 1984; Smith & Kitching, 1997). More recent work by Bordy

(2004 a&b, 2005) and Bordy and Eriksson (2015) recognizes just two informal subdivisions within the Elliot – the upper Elliot Formation (UEF) and the lower Elliot Formation (LEF). These divisions have been widely adopted (e.g., Otero et al., 2015; Bordy et al., 2017; McPhee et al., 2015 a&b) but no formal subdivision has been proposed as of yet (Bordy & Eriksson, 2015).

The LEF is characterized by asymmetrical, isolated channel sandstone and alternating thick mudstone deposits. These have been interpreted as a perennial meandering fluvial system (Bordy et al., 2004a; 2005; Bordy & Eriksson, 2015). The southern LEF outcrops preserve up to 300 meters of section but they dramatically thin northward, which is possibly due to its close proximity with the Kaapvaal Craton (Bordy et al., 2004a). The depositional environment interpretations made by Bordy et al. (2004a, 2005) suggest a semi-arid climatic setting (McPhee et al., 2017).

The UEF is characterized by laterally continuous sandstones and interbedded mudstones which have been interpreted as ephemeral, flash flood-dominated fluvial systems suggesting a progressively more arid climatic setting (Bordy et al., 2004a). The now-disused "middle Elliot", which was originally marked by a layer of small, calcareous concretions (Smith & Kitching, 1997), has now been incorporated solely into the UEF. This consolidation was argued on the grounds that the middle Elliot could not be traced on a regional scale (Bordy et al., 2004a, 2004b, 2004c; Bordy & Eriksson, 2015). While relative aging places the LEF between 210 and 200 and the UEF between 200 and 190 m.y.a. (e.g., Visser & Botha, 1984; Lucas & Hancox,

2001; Butler, 2005; Bordy & Eriksson, 2015), no radiometric dates have been published for these strata (Sciscio et al., 2017).

1.3 History of Sauropodomorpha

The clade Dinosauria diverged from their archosaurian relatives towards the end of the middle Triassic (Upchurch, 1995; Nesbitt et al., 2012). During this time, Pangaea was still whole (Kent et al., 1995). Just prior to the breakup of Pangaea, the Triassic-Jurassic extinction (TJB) occurred, possibly due to a changing climate (Quan et al., 2008) and/or widespread volcanism (Tanner et al., 2001; Whiteside et al., 2010; Blackburn et al., 2013). This event lasted ~10,000 years and marks the boundary between the Triassic and Jurassic periods (Ryder et al., 1996; Whiteside et al., 2010; Roff, 2011). During this extinction event most non-dinosaurian archosaurs, therapsids, and large amphibians were wiped out, but sauropodomorph diversity appears to have been relatively unaffected (Olsen et al., 2002; Barrett & Upchurch, 2005; Barrett, 2009; McPhee et al., 2017). While it remains uncertain why this clade survived this event, research indicates that this after extinction, open niche space was able to accommodate a vastly accelerated radiation of the dinosaurs throughout the Early Jurassic (Hallam, 1990; Wilson & Sereno, 1998; Wilson, 2002; Barrett & Upchurch, 2005; Pol et al., 2011).

Soon after the TJB extinction event, rifting of Pangaea began, which ultimately created two separate supercontinents, Laurasia and Gondwana (Collins & Windley, 2002). This rifting created shallow continental tropical seas which led to generally warmer global temperatures

(Sellwood & Valdes, 2006). It is within this global context that the derived sauropodan bauplan first appears, with all sauropods primarily distinguished by exceptionally long necks and tails, proportionally small skulls, an obligatory quadrupedal locomotor habit and, in later-branching members of the group, an enormous body plan (Upchurch et al., 2004; Sander et al., 2011; Langer et al., 2010; McPhee et al., 2015a).

1.4 Systematics and Evolution

Saurischian dinosaurs are traditionally divided into two major groups: Theropoda and Sauropodomorpha (e.g., Marsh, 1882; Seeley, 1887; von Huene, 1932; Benton, 2004; Weishampel et al., 2004). Although this relationship has been contested (Baron et al. 2017), the precise interrelationships of these groups remains in a state of flux (Langer et al., 2017; Müller & Dias-da-Silva, 2017). The 'traditional' arrangement will be observed throughout this dissertation, and has no impact on the conclusions reached here.

The earliest phylogenetic work done in regard to Sauropodomorpha can be traced back to von Huene, who coined the clade Sauropodomorpha in the early 20th century (1932). Although pre-cladistical hypotheses of sauropodomorph relationships suggested a close affinity between Prosauropoda (von Huene, 1920) and Sauropoda (Marsh, 1898), the details of this remained a point of contention throughout the 20th century (Carpenter & Currie, 1990; Yates et al., 2012).

The widespread adoption of cladistics (from the early work of Hennig in 1966) beginning in the 1980s introduced a fundamental shift in how hypotheses of evolutionary relationships between taxa were made and tested. Early systematic work on dinosaurs (Gauthier, 1986) built upon von Huene's (1932) conception of the group, originally assigning a sister-taxon relationship between a reciprocally monophyletic Prosauropoda and Sauropoda (e.g., Galton, 1976, 1990; Upchurch, 1995, 1998; Sereno 1998, 1999; Wilson, 2002; Galton & Upchurch, 2004). This arrangement was formalized in early phylogenetic definitions of the group: i.e., Prosauropoda = all taxa closer to *Plateosaurus*, Sauropoda = all taxa closer to *Saltasaurus* (Wilson & Sereno, 1998). This work predated an era of discovery of new sauropodomorph taxa, particularly in South America, but also in China and the USA (e.g., Sertich & Loewen, 2010; Wang et al., 2017; Apaldetti et al., 2014).

The first cladistical analyses to employ a wide sample of both basal sauropods and traditional 'prosauropod' taxa were conducted by Yates (2003) and Yates & Kitching (2003). This work differed from previous studies that focused on the inter-relationships exclusively within Prosauropoda (e.g., Galton, 1990; Sereno, 1999; Benton et al., 2000). Yates & Kitching's 2003 analysis suggested a prosauropod paraphyly, the result of which echoes through most other subsequent analyses. One exception to this trend is Upchurch et al. (2007) where a small monophyletic group of taxa once considered prosauropods was recovered. Ensuing works using Yates and Kitching's dataset (i.e., with prosauropod paraphyly) generally recovered early branching sauropodomorphs (e.g., *Saturnalia, Thecodontosaurus, Efraasia*), "core prosauropods" now forming reciprocally monophyletic groups (Plateosauridae, Riojasauridae,

and Massospondylidae), that occupied various positions on the stem, and "near-sauropod" taxa demonstrating a more sauropod-like anatomical structure (e.g., *Anchisaurus*, *Mussaurus*, *"Melanorosaurus"*) (Benton et al., 2000; Galton & Upchurch, 2004; Galton, 2005; Yates, 2007; Otero et al., 2015)

Yates (2007a) named a clade Massopoda comprising of Massospondylidae, Riojasauridae, and all Sauropoda, the definition being all sauropodomorph dinosaurs more closely related to *Saltasaurus loricatus* than to *Plateosaurus* (*engelhardti*). Yates (2007b) built upon this definition by specifically excluding *"Melanorosaurus"* from Sauropoda (Sauropoda = all sauropodomorphs closer to *Saltosaurus* than *"Melanorosaurus"*) and many others followed suit (e.g., Ezcurra, 2010; Pol et al., 2011).

More recent work conducted by McPhee et al. (2014) defined Sauropodomorpha as "the most inclusive clade containing *Saltasaurus* but not *Tyrannosaurus rex*". Massopoda retained the Yates (2007b) definition but the definition for Sauropodiformes was changed to "the most inclusive clade containing *Saltasaurus* but not *Massospondylus"*. Otero et al. (2015) favors "the most inclusive clade containing *Saltasaurus* but not *Passer* or *Triceratops*" from the Sereno (2007) sauropodomorpha definition and defines Sauropodiformes as "the least inclusive clade containing *Mussaurus* and *Saltasaurus*" but shares the McPhee et al. (2014)'s (Yates, 2007b) definition of Massopoda.

1.5 Sauropodomorph Biostratigraphy in the Elliot Formation

Kitching and Raath proposed the first systematic, influential biostratigraphical partitioning of the Elliot Formation in 1984. They divided the Elliot and lower Clarens Formations into two distinct range zones based upon the supposedly exclusive stratigraphic occurrence of two sauropodomorph genera: *Massospondylus* and *"Euskelosaurus"* (Fig. 2) (see below regarding the current taxonomic status of *"Euskelosaurus"*). The *"Euskelosaurus"* Range Zone correlates with Upper Triassic strata elsewhere in the world, which contain a similar fauna of early branching non-sauropodan sauropodomorphs (Letourneau & Olsen, 2003). The *Massospondylus* Range Zone comprises the middle and upper Elliot (now both informally considered UEF; see above) and basal beds of the Clarens Formation, and correlates with the Lower Jurassic (Hettangian–Pliensbachian) global biostratigraphic records. These zones were based on the interpretation (Haughton, 1924; Kitching & Raath, 1984) that the lower sections of the formation tended to preserve the remains of a large-bodied "prosauropods" (*"Euskelosaurus"*) where the upper sections had an abundance of the small-bodied *Massospondylus.*

However, based on recent and ongoing work on Elliot Formation fieldwork and taxonomic revision, it is becoming increasingly evident that this early two-range zone classification was an oversimplification, which has raised questions regarding the stratigraphic provenance data of a number of historically collected lower Elliot Formation taxa (McPhee et al., 2017). Many of the early studies of these animals contain sparse locality information, and there has been a great deal of confusion and debate on which taxa are valid and how many distinct species are

represented (Kitching and Raath, 1984; Sereno et al., 1993; Yates, 2003, 2007; McPhee et al. 2015b).

Previous work on the Elliot Formation has put a great deal of emphasis on the greater taxonomic diversity of the LEF saurpodomorph assemblage and the perceived lack of diversity in the UEF (e.g., Kitching & Raath, 1984). However, more recent work by McPhee et al. (2017) has shown the UEF to be far more taxonomically diverse than previously thought (Yates et al., 2010 & 2011; McPhee et al., 2015 a&b). Below I review these taxa in brief (see more comprehensive review in McPhee et al., 2017).

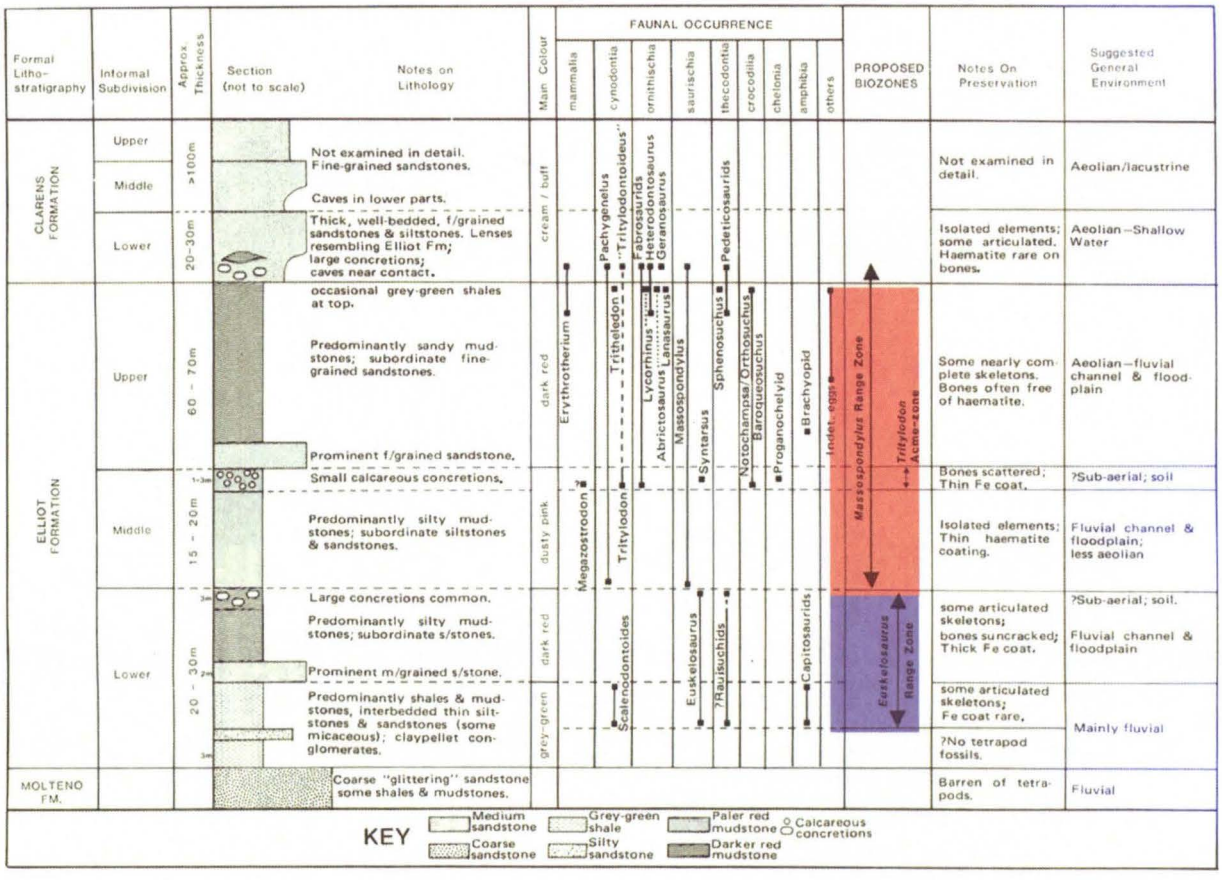

Figure 2: Kitching & Raath's (1984) Massospondylus (red) and "Euskelosaurus" (purple) Range Zones.

1.5.1 Lower Elliot Taxa Taxonomy and Legitimacy

1.5.1.1 *Euskelosaurus brownii* Huxley, 1867

Euskelosaurus brownii was first described by Huxley (1867) and was based primarily on an isolated proximal femur (now housed at the Natural History Museum, London) collected from the Elliot Formation (previously known as the Stormberg "Red-Beds") by Brown in 1863. This genus is the basis for the "*Euskelosaurus* Range Zone" of Kitching and Raath (1984) (see History of Sauropodomorpha). The holotype lacks diagnostic features and contains duplicate referred elements with different morphologies, therefore it is both not diagnosable and it cannot pertain to a single taxon. For this reason, "*Euskelosaurus*" has been considered a *nomen dubium* by Yates & Kitching (2003) and Yates (2003). Due to the chimeric nature of "*Euskelosaurus*", the use of this taxa as a range zone indicator is not viable.

1.5.1.2 *Plateosauravus cullingworthi* Haughton, 1924

Plateosauravus was originally named *Plateosaurus cullingworthi* by Haughton (1924) and re-designated as a distinct genus by von Huene (1932). Van Heerden (1979) reassigned the genus to "*Euskelosaurus*", but Yates (2003) recommended abandoning "*Euskelosaurus*" altogether (see above) in favor of the name *Plateosauravus*. This animal is currently hypothesized to be the earliest-branching sauropodomorph within the Elliot formation (Yates, 2007a, 2007b, 2010). This animal is known primarily from a disarticulated fossil assemblage recovered in 1918

in the Eastern Cape (Haughton, 1924) on a hillside near Kromme Spruit. The assemblage is composed of at least three different sized individuals with dubious association. Within this assemblage, no reliable autapomorphies can be found. These issues suggest that *Plateosauravus* is a *nomen dubium*. Despite taxonomic concerns (Yates, 2003; McPhee et al., 2015b; McPhee et al., 2017) the geologic data places *Plateosauravus cullingworthi* within the LEF.

1.5.1.3 *Eucnemesaurus* van Hoepen, 1920

Eucnemesaurus was named by van Hoepen (1920) based on postcranial material collected from northern exposures of the lower Elliot Formation near Bethlehem, Orange Free State. The partial skeleton, which includes a coracoid, several vertebrae, a pubis, femur, and two tibiae, represents the type species *Eucnemesaurus fortis.* Until recently, most workers considered *Eucnemesaurus* to be synonymous with *Euskelosaurus* (van Heerden, 1979); however, Yates (2007b) identified *Eucnemesaurus* as a distinct genus and assigned it to a new family, Riojasauridae, at the base of Massopoda. Yates (2007b) also synonymized the problematic 'herrerasaurid' *'Aliwalia rex'* with *Eucnemesaurus*. A second species, *Eucnemesaurus entaxonis,* was recently recognized and is distinguished from *E. fortis* based on differing features of the femoral shaft and distal tibia. The holotype of that species was excavated in 2003 from Cannon Rock Farm in the lower Elliot Formation 40 meters above the Elliot-Molteno contact within gray-brown mudstones (McPhee et al., 2015b & 2017).

1.5.1.4 *Blikanasaurus cromptoni* Galton & van Heerden, 1985

Blikanasaurus cromptoni was collected from the 'Passage Beds' of Blikana Mountain in the Herschel District (Charig et al., 1965; Galton & van Heerden, 1985; Yates, 2008) at the southern end of the Elliot Formation. It is known from an isolated epipodium and pes. This material is unique in the Elliot formation due to its extreme stockiness (Yates, 2003) excluding a hyper-robust ilium recently described by McPhee & Choiniere (2016). Although the precise stratigraphic location that the hindlimb was collected from is not known, there are no UEF outcrops within the immediate area, which places it safely within the lowermost LEF (McPhee et al., 2017).

1.5.1.5 The "Bloem/Maphutseng dinosaur"

The "Bloem/Maphutseng dinosaur" is a multi-specimen (as many as a dozen individuals) assemblage of sauropodomorph remains retrieved from the lower Elliot Formation of Maphutseng, Lesotho, over three separate excavations from 1955 to 1970 (Ellenberger and Ellenberger, 1956; Ellenberger, 1970). Its attribution is problematic. The excavators, Ellenberger and Ellenberger) describe the animal as a quadrupedal prosauropod "similar to *Melanorosaurus* or *Euskelosaurus*". Gauffre (1993a) noted that it conforms to the diagnostic criterion for *Euskelosaurus* (van Heerden, 1979), in that length of the humerus approaches 80% of that of the femur, but later considered it to represent a new taxon, *Kholumolumosaurus* (Gauffre, 1996). However, the excavation was poorly documented and Maphutseng material is now

distributed among the National Museum in Bloemfontein, the University of Cape Town, and the Museum National d'Histoire Naturelle in Paris. The correct attribution of this material is currently the subject of two PhD projects.

1.5.1.6 *Melanorosaurus readi* Haughton, 1924

"Melanorosaurus" is an important taxon within this study as well as within sauropodomorph systematics, being the basis for Melanorosauridae, as well as the external specifier in Yate's (2007a, b) definition of Sauropoda. Despite the historical importance of this taxon, there is now doubt as to the stratigraphic provenance(s) of this taxon as well as its generic validity (Yates, 2008; McPhee et al., 2015a, McPhee et al., 2017).

"Melanorosaurus" was first named and described by Haughton (1924) and is based on material collected from lower Elliot beds on the north slope of Thaba Nyama in Transkei, South Africa (SAM-PK 3449-3450, SAM-PK 3532 referred). SAM-PK 3449-3450 constitute the *"Melanorosaurus"* syntype. This syntype is problematic because it comes from two separate localities and might contain other disassociated material (Galton et al., 2005, McPhee et al., 2015b; de Fabrègues & Allain, 2016). The referred SAM-PK 3532 is from a different locality and consists of (possibly disassociated) forelimb bones that provide little insight into the analyses conducted in this dissertation (Bonnan & Yates, 2007).

There are two specimens in the National Museum, Bloemfontein that are ascribed to *"Melanorosaurus"*: NMQR 1551 and 3314. NMQR 1551 was collected over the course of two field seasons (1967 and 1971) from the LEF (Galton et al., 2005). Work done by McPhee et al. (2017) confirms the LEF placement for NMQR 1551. Although represented by at least two individuals, there is currently little evidence to suggest that the assemblage is not monospecific (e.g., there is no character conflict in overlapping bones, and no major differences in preservation). NMQR 3314 comes from the Damplaats 55 Farm and was collected in 1994 (Yates, 2007; McPhee et al., 2017). It was found in articulation and at the time was the only LEF sauropodomorph with a preserved skull. It has since been shown to be from the UEF by McPhee et al. (2017).

'Melanorosaurus' thabanensis was described by Gauffre (1993b) and consisted of a single femur. It has since been expanded to include associated, fragmentary material (one partial right ilium, one left pubis, and one right metatarsal. The specimen comes from the Mafeteng district in Lesotho and was originally thought to be from the UEF. It is now presumed to be from the LEF and has been referred to *Meroktenos thabanensis* (MNHN.F.LES16) (de Fabrègues & Allain, 2016).

The *"Melanorosaurus"* syntype lacks autapomorphies, it is not a single specimen, and does not all come from the same locality, making *"Melanorosaurus"* a *nomen dubium*. The only member of the hypodigm from the UEF was a referred specimen, NMQR 3314, which is either a preexisting UEF animal or an entirely new taxon. Due to poor provenance data, poor

association, and general anatomical distinction, it is the recommendation of this author that "*Melanorosaurus*" should be abandoned.

1.5.1.7 Summary

From these listed taxa, only *Blikanasaurus* and *Eucnemesaurus* are unquestionably valid LEF taxa. Based on the section above, "*Melanorosaurus*" is a *nomen dubium*. Work conducted by McPhee et al. (2017) shows that, in one case (NMQR 3314), referred material doesn't come from the same time period. From these rationale, the specimens currently referred to "*Melanorosaurus*" are in need of taxonomic revision. On a broader scale, after more than 150 years of collection efforts, the depauperate LEF sauropodomorph fauna is in need of revision. This underscores the significance of the specimen described below.

1.5.1.8 BP/1/7811

BP/1/7811 represents an associated individual discovered by McPhee and Phillips (2014) on Driefontein Farm in the Eastern Cape of South Africa. Based upon work conducted by myself and Dr. Viglietti, the precise stratigraphic location (Fig. 3) is known and this specimen is confidently placed within the LEF. The specimen consists forelimb, pelvic, and hindlimb elements as well as cervical, dorsal, and caudal vertebrae.

Owing to their general rarity and excellent preservation, these fossils (Fig. 4) provide a unique opportunity to greatly enhance our understanding of early sauropodomorph evolution prior to the emergence of Sauropoda. The study of this specimen and its taphonomic history along with

the strata in which they are buried will add to the understanding of the fluvial/lacustrine deposits within the Elliot Formation. The morphology of these specimens will provide new insight into current taxonomic uncertainties surrounding specific LEF sauropodomorph genera listed above (McPhee et al., 2015a, 2017). This dissertation addresses these issues and topics.

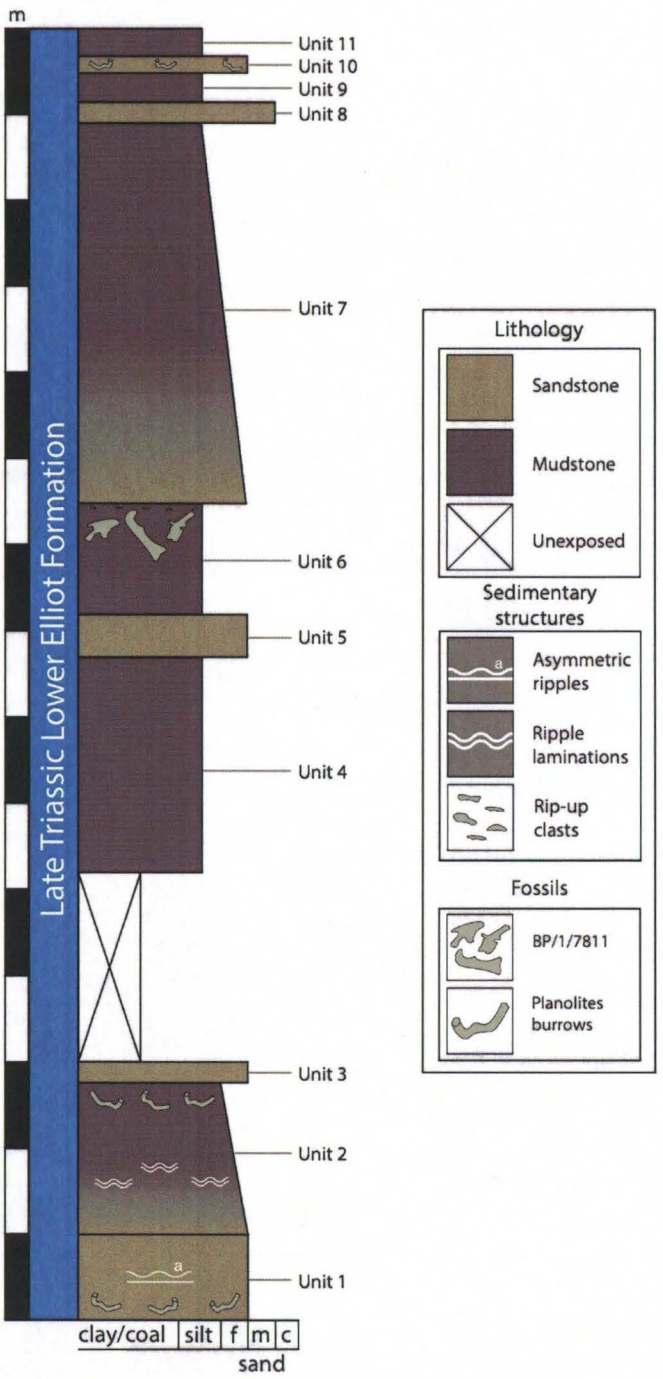

Figure 3: Stratigraphic column (15 m) depicting the lithostratigraphy of the H5 Quarry, Dreifontein Farm, Eastern Cape, South Africa.

Figure 4: Silhouette showing the preserved skeletal remains of BP/1/7811 modified from Scott Hartman.

2.1 Taphonomic Materials and Methodology

Taphonomic and geological data were gathered in and around the quarry and a quarry map (Fig. 5) was created to preserve *in situ* bone orientations and distributions. From the quarry, four large jackets were removed, along with three smaller jackets (Table 1) and weathered natural material collected as sub-aerially exposed float on the original erosional surface. None of the elements collected were in articulation, but most material was found in association.

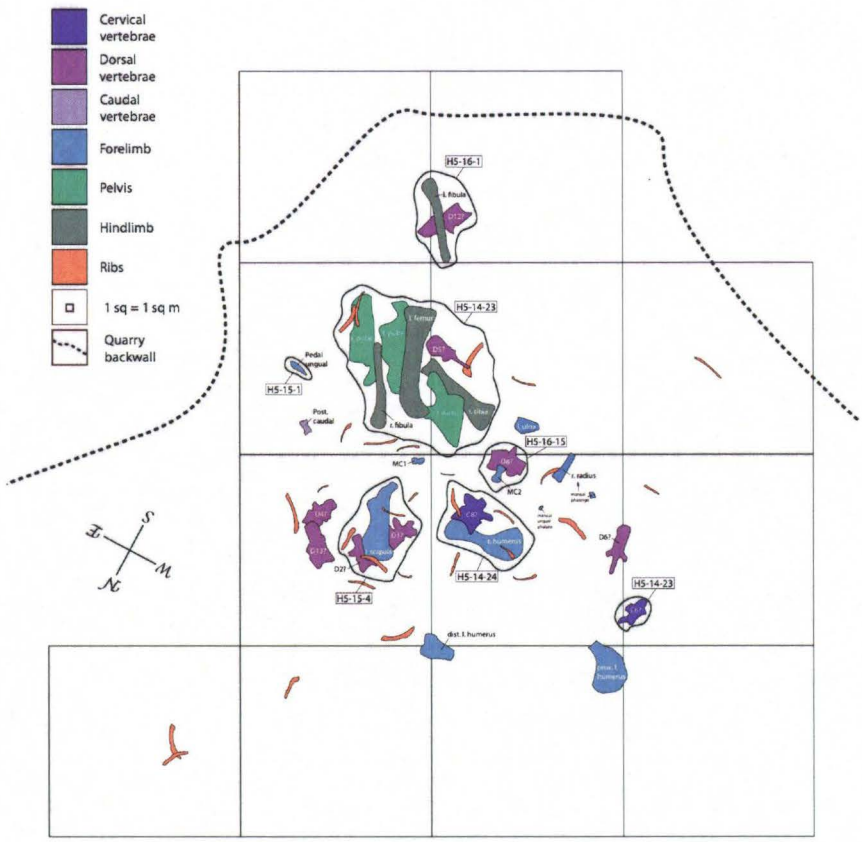

Figure 5: H5 Quarry map, Dreifontein Farm, Eastern Cape, South Africa. 1 grid square = 1 sqare meter. Rectangles around "HN" text indicate field numbers.

The geological data collected was used to determine depositional environments to be used in taphonomic interpretation. To preserve detailed positional information of the bones (e.g., disarticulation, preservation, association), photographs and measurements were taken of the opened jackets before each element was removed and cleaned. For the largest of the jackets, a high-resolution 3D model was created with Agisoft Photoscan Professional Version 1.2.6 (Fig. 6) (Agisoft LLC, St. Petersburg, Russia).



Figure 6: BP/1/7811 Hindlimb jacket from the H5 Quarry.

To determine the degree of transportation within the H5 Quarry, proximal trend data was taken for each element from the quarry map (Fig.5). These measurements were compiled in a spreadsheet (Microsoft Excel 15.40) and copied into a rose diagram plotting program (GeoRose 0.5.0.). Rose diagrams were used instead of a sterographic projection because all elements within the quarry were found horizontally and in the same layer, with roses being the preferred

diagram for two dimensional phenomena (Toots, 1965 a&b). Three rose diagrams were generated from this data: only ribs (Fig. 7), only large, elongate elements (Fig. 8), and all bones excluding ribs (Fig. 9).

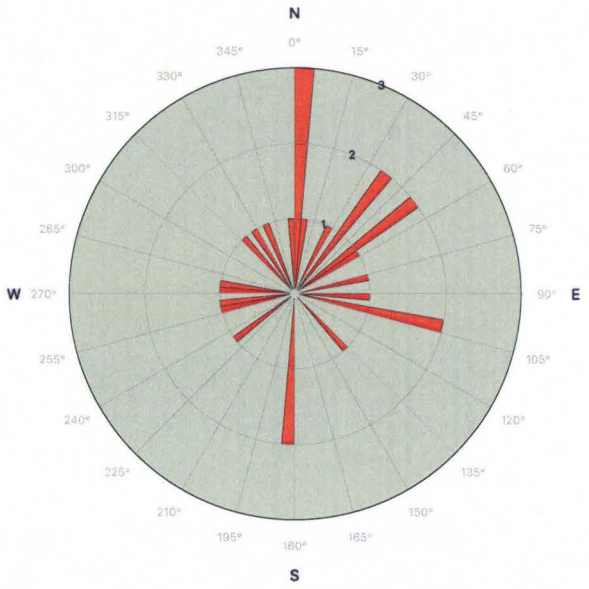

Figure 7: Rose diagram depicting BP/1/7811 rib distribution within the H5 Quarry. Image generated by GeoRose 0.5.0 software.

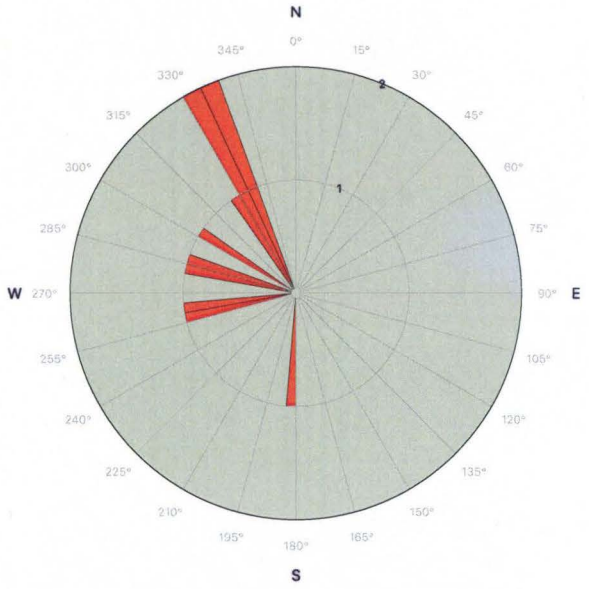

Figure 8: Rose diagram depicting BP/1/7811 long bone distribution within the H5 Quarry. Image generated by GeoRose 0.5.0 software.

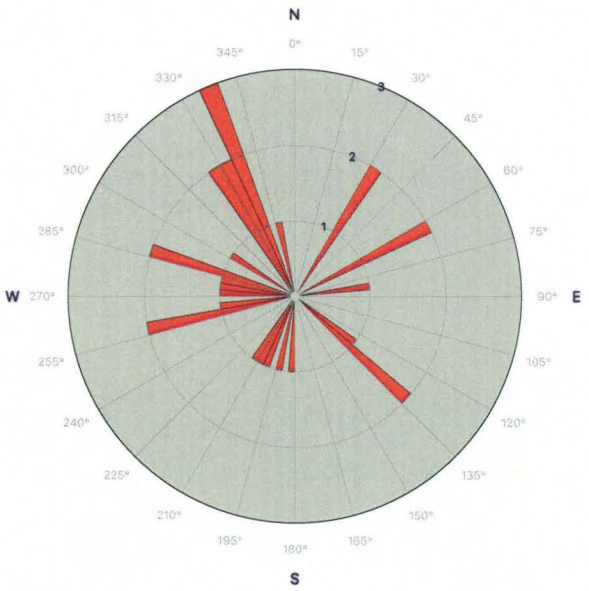

Figure 9: Rose diagram depicting BP/1/7811 all bone excluding rib distribution within the H5 Quarry. Image generated by GeoRose 0.5.0 software.

Detailed lithological notes were taken throughout the preparation process, and all elements were checked for distortion, weathering, and predation marks. The Bone Weathering Stages defined by Behrensmeyer (1978) was used in this study to guide in the taphonomic analysis of BP/1/7811. While intended for modern bone, these stages assist in providing a rough depositional timeline (Fig. 10). BP/1/7811 is an isolated individual so a Minimum Number of Individuals present (MNI) analysis was not conducted for this study.

Stage Description:	Weathering stage:	Possible range in years since death:
0	Bone surface shows no sign of cracking or flaking due to weathering. Usually bone is still greasy, marrow cavities contain tissue, skin, and muscle/ligament may cover part or all of the bone surface.	0-1
1	Bone shows cracking, normally parallel to the fiber structure (e.g., longitudinal in long bones). Articular surfaces may show mosaic cracking of covering tissue as well as in the bone itself. Fat, skin, and other tissue may or may not be present.	0-3
2	Outermost concentric thin layers of bone show flaking, usually associated with cracks, in that the bone edges along the crack tend to separate and flake first. Long thin flakes, with one or more sides still attached to the bone are common in the initial part of Stage 2. Deeper and more extensive flaking follows, until most of the outermost bone is gone. Crack edges are usually angular in cross-section. Remnants of ligaments, cartilage, and skin may be present.	2-6
3	Bone surface is characterized by patches of rough, homogeneous weathered compact bone, resulting in a fibrous texture. In these patches, all the external, concentrically layered bone has been removed. Gradually the patches extend to cover the entire bone surface. Weathering does not penetrate deeper than 1.0-1.5 mm at this stage and bone fibers are still firmly attached to each other. Crack edges usually are rounded in cross-section. Tissue rarely present at this stage.	4-15+
4	The bone surface is coarsely fibrous and rough in texture; large and small splinters occur and may be loose enough to fall away from the bone when it is moved. Weathering penetrates into inner cavities. Cracks are open and have splintered or rounded edges.	6-15+
5	Bone is falling apart in situ with large splinters lying around what remains of the whole, which is fragile and easily broken by moving. Original bone shape may be difficult to determine. Cancellous bone usually exposed, when present, and may outlast all traces of the former more compact, outer parts of the bones.	6-15

Figure 10: Bone Weathering Stages reformatted from Behrensmeyer (1978).

2.2 Geological Field Methodology

Approximately 15 meters of Late Triassic Lower Elliot Formation (LEF) sedimentary strata are exposed in and around the H5 quarry. These were divided into 11 specific lithostratigraphic units consisting primarily of alternating fluvial mudstones and fining-upward sandstones. Lithology and texture of each unit, including composition, color, grain size, sorting, rounding, depositional structures, and trace fossils, were described, photographed, and sampled at georeferenced points for future detrital zircon dating.

Thicknesses and bedding attitudes were measured using a Jacob's staff and Brunton pocket transit, respectively. A stratigraphic column compiled from these observations (Fig. 3) illustrates the low-energy, meandering fluvial depositional sequence in which the BP/1/7811 sauropodomorph specimen is enclosed, shows its location within the sequence, and further serves as a basis for comparing the H5 section with other published Lower Elliot stratigraphic sections, to establish its regional context.

2.3 Specimen Excavation and Preparation

This specimen was collected in several separate jackets from the H5 quarry (Fig. 5) located on Driefontein Farm in the Eastern Cape of South Africa over the course of three years. The site was discovered in June of 2014 by Blair McPhee and Natasha Phillips and a thorough excavation began the following year. Excavation was conducted in two joint field seasons with crews from

the Universities of Oxford and the Witwatersrand in 2015 and 2016, after which excavation ceased.

All exposed bone at the quarry was coated with a diluted solution of Paraloid B-72 in acetone solvent. Once dry, the bone was coated with wet paper towels and capped with several layers of burlap coated in plaster of Paris. Hand-tools, rock-saws, and jackhammers were used to remove the subsequent plaster capped blocks and all material was brought to the ESI Collections.

The BP/1/7811 plaster blocks were opened in a preparation laboratory with an electric hand-saw and chisels. Photographs were taken at the time of opening and detailed notes were kept throughout the preparation process that could be used in the taphonomic section of this study (see *Taphonomic Methodology*). The matrix surrounding the bones was removed with handheld pneumatic airscribes and smaller hand-tools. Bones were consolidated with varying percentages of Paraloid B-72 in an acetone solvent.

2.4 Taxonomic and Anatomical Materials and Methodology

All fossil material from the H5 quarry pertains to a single associated individual, and was given the specimen number BP/1/7811, which consists of entirely original fossil material housed within the Evolutionary Studies Institute (ESI) Collections at the University of Witwatersrand. Axial elements include: two cervical vertebrae, seven dorsal vertebrae, and one caudal

vertebrae. Appendicular elements include: a left scapula, both humeri, a left proximal ulna, a right distal radius, a partial left manus, a left ilium, both pubes, a left femur, and left tibia, both fibulae, and a phalanx (Fig. 4).

Comparative data was collected from museums throughout South Africa (BPI, SAM, and NMQR), as well as from the United States of America (NHMU), Zimbabwe (QG), and China (IVPP) (See Inst. abbreviations). Permission was given by all institutions prior to accessing data collections and all rules and regulations stipulated by these institutions were strictly adhered to at all times.

2.5 Phylogenetic Systematics

Discrete character hypotheses were analyzed in the context of a larger phylogenetic data matrix designed to explore the interrelationships of basal sauropodomorph taxa. This was done with a matrix initially introduced by Yates (2007), and subsequently revised by Smith & Pol (2007), Yates et al. (2010), Yates (2010), Apaldetti et al. (2011), McPhee et al. (2014), and McPhee & Choiniere (2017). The matrix was collated in Mesquite v3.0 (Maddison & Maddison, 2014) and heuristically analyzed for shortest-length trees using the parsimony-based program TNT v. 1.1 (Goloboff et al., 2008).

For my analysis, I used the following settings: traditional search strategy, using 1000 Wagner trees and Tree Bisection and Reconnection (TBR) branch swapping saving 1 tree per replication.

Trees recovered from this round were submitted to an additional round of branch swapping, saving up to 10,000 most parsimonious topologies. Standard support analyses were also conducted for this morphological data (Bremer support and the Bootstrap).

The matrix consists of 368 discrete morphological characters and 61 terminal taxa. The following taxa/specimens were excluded from the final analysis: SAM-PK-3349/3350, SAM-PK-3532, *Meroktenos thabanensi, Agnosphytis,* and *Ignavusaurus.*

2.5.1 Selection of Problematic LEF Specimens for Cladistical Analysis Exclusion

The "*Melanorosaurus*" syntype (SAM-PK-3349 & SAM-PK-3350) and *Meroktenos thabanensis* (MNHN.F.LES16) are included within anatomical comparisons but were not included in my final phylogenetic analysis due to concerns over inter-association and issues pertaining to historical provenance (McPhee et al., 2017). The validity of the syntype specimens for the purpose of this dissertation is pending until further sampling can be done.

The "*Melanorosaurus*" operational taxonomic unit (OTU) introduced by Yates (2007) was based primarily on two referred assemblages (NMQR 1551 and NMQR 3314). This OTU was effectively employed unaltered in most subsequent analyses (e.g., McPhee et al., 2014). However, given the concerns pertaining to the validity of "*Melanorosaurus*" outlined above, and following McPhee et al. (2017), both NMQR 1551 and 3314 were treated as independent OTUs for the purpose of our analyses.

SAM 3532 was introduced by Houghton (1924) and referred to *"Melanorosaurus"* in the same paper where the *"Melanorosaurus"* syntype was established. SAM 3532 was found several kilometers from the SAM *Plateosauravus* material. The material includes an ilium, ulna, a partial humerus, a partial scapula, along with several indeterminate elements. Due to its uncertain provenance and the very limited diagnostic information it provides, SAM 3532 was not included.

Outside of the *"Melanorosaurus"* hypodigm, several other taxa were removed. *Agnosphytis,* from England, is known from an ilium, maxilla, astragalus, and humerus (Fraser et al., 2002) and was removed due to its diagnostic limitations generally and for the scope of this study. *Ignavusaurus* is from a young specimen and may not reflect adult morphology. It may also be a junior synonym of *Massospondylus* (Yates et al., 2011). For these reason, it too was excluded.

2.6 Institutional Abbreviations:

BPI, Evolutionary Studies Institute (formally Bernard Price Institute), Johannesburg, South Africa; **IVPP**, Institute of Vertebrate Paleontology and Paleoanthropology, Beijing, China; **MNHN**, Muséum National d'Histoire Naturelle, Paris, France; **NHMU**, Natural History Museum of Utah, Salt Lake City, Utah, USA; **QG**, Natural History Museum of Zimbabwe, Bulawayo, Zimbabwe; **NMQR**, Natural History Museum, Bloemfontein, South Africa; **SAM**; Iziko South African Museum, Cape Town, South Africa.

Chapter 3: Results

3.1 **H5 Lithofacies** (Fig. 3)

Unit 1: (1 m) Pale, yellow, fine-grained quartz arenite weathers to purple-brown. Grains are well sorted and rounded. Asymmetric current ripples with wavelength 3 cm, amplitude 0.7-0.8 cm, are indicative of northerly transport. At the base of this unit, *Planolites* burrows 0.5-1.0 cm wide and up to 10 cm long are abundant.

Unit 2: (1.8 m) Green-gray, silty, ripple-laminated quartz sandstone grades upward to mudstone. Mudstone is increasingly nodular-textured upward and mottled with patchy pale green reduced zones and purple-brown oxidized zones. *Planolites* burrows near top. Intruded by an igneous dike.

Unit 3: (0.25 m visible + 2.2 m unexposed between 3 & 4) Purple-brown weathering fine-grained sandstone with scoured, concave-upward basal contact indicating channel cut-and-fill origin. Also cut by igneous dike.

Unit 4: (2.5 m): Purple-weathering silty mudstone.

Unit 5: (0.5 m) Fine-grained pale yellow-green quartz sandstone. Grains well sorted and rounded, coarsening upward.

Unit 6: (1.3 m) Consolidated, olive-gray silty mudstone. Upper 0.3 m contains the basal sauropodomorph fossils described within this study (BP/1/7811). Small rip-up clasts found above vertebrate fossils. Intraformational rip-up clasts found (during preparation) directly above the bone layer.

Unit 7: (4.5 m) Interbedded purple- to red-weathering quartz sandstone and purple-weathering mudstone. Bed 1 (0.5 m) is purple, strongly weathered sandstone. Compact and featureless. Bed 2 (0.4 m) is an olive-gray silty mudstone. Bed 3 (2.8 m) is a brick-red sandy mudstone containing nodular sand concretions. Bed 4 (0.8 m) is a purple fine-grained mudstone.

Unit 8: (0.25 m) Medium-grained tan/white sandstone. Grains are moderately sorted and sub-rounded. No visible depositional structures.

Unit 9: (0.35) Brick-red-weathering mudstone. Nodular.

Unit 10: (0.2 m) Fine-grained, brick-red-weathering quartz sandstone. Contains *Planolites* burrows. Compact. Well-sorted, rounded.

Unit 11: (0.3 m) Brick-red-weathering mudstone.

3.2 Taphonomy

A detailed analysis of the components of the skeleton recovered for BP/1/7811 suggests that the specimen represents a single individual. Most bones are represented by the left side element only. In the three instances where two of the same element are preserved (humeri, pubes, fibulae), both a left and a right sided element are present. Moreover, the components are proportional in size and ontogenetic stage.

None of the preserved elements show indication of transportation abrasion, there is a lack of evidence for wet-rot and/or exfoliation, or root damage. There are no signs of predepositional cracking and no invertebrate borings were found on any of the material. The material does not bear any fractures indicative of trampling. There is some weathering that occurred predepositionally on the epiphyses of larger long bones.

The left pubis has three predation/scavenging tooth punctures (Fig. 11 A) and the right (Fig. 11 B) has a single tooth drag mark. The drag mark is approximately 80 mm long and shows signs of splintering. The bite mark scores are shallow and U-shaped, consistent with those made by crocodyliforms, differing from V-shaped score marks indicative of theropodan predation (Schwimmer, 2010; Drumheller et al., 2014; Hone & Tanke, 2015). Possible trace makers are explored in Taphonomic Discussion. These two elements were found not articulated but in close association (Fig. 5).

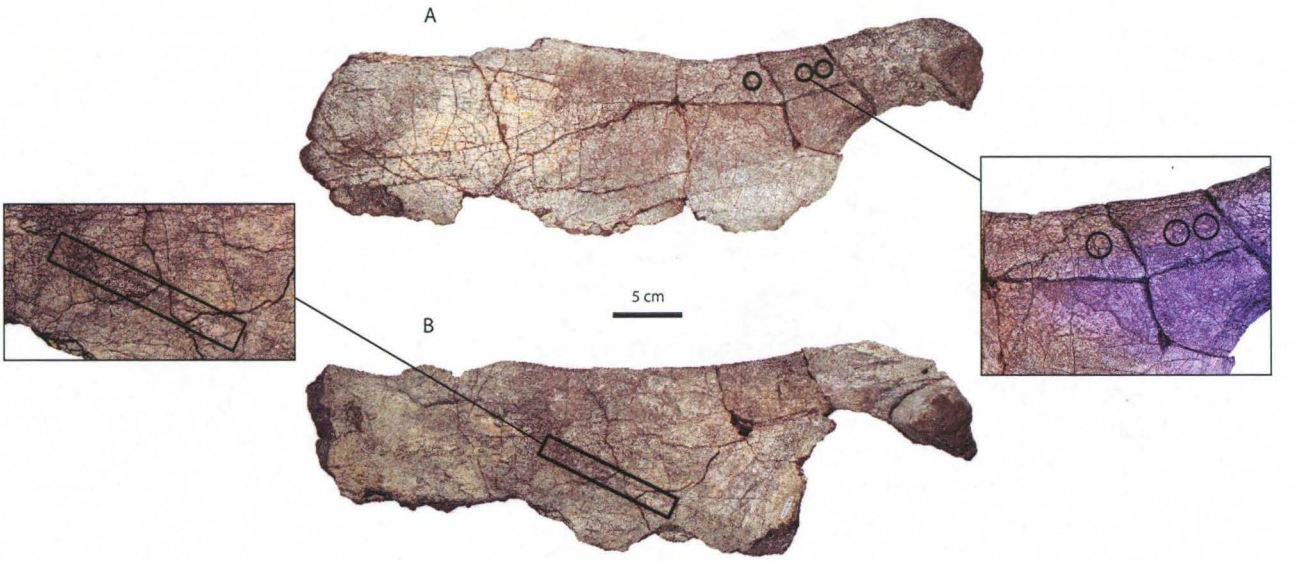

Figure 11: A) Left pubis showing tooth punctures B) Right pubis with drag marks. Circles show tooth punctures, rectangle shows tooth score. Scale bar = 5 cm.

BP/1/7811 is partially sorted according to body region (Fig. 7-9). Hindlimb bones, dorsal vertebrae, and dorsal ribs generally grouped with their respective anatomical regions. Forearm elements grouped with forearm elements as well as smaller manual elements, cervical vertebrae, and smaller rib fragments (Fig. 5). The orientation of individual bones were not strongly aligned, but some subsets of bones did have preferred orientations. Ribs (see rose diagram in Fig. 7) showed a fairly random distribution with a slightly greater northern/northeastern frequency. Large, elongate bones (the scapula, humeri, and hindlimb materal) have nonrandom orientation with a high northwestern frequency, and a secondary western trend (Fig. 8). When all elements excluding ribs (Fig. 9) are considered, however, there is a slight bias towards northwestern frequency but a more generally random distribution pattern overall.

3.3 Preparation Observations

During fossil preparation, small mud chips were found throughout the matrix surrounding the specimen, which I interpret as intraformational rip-up clasts. These mud chips are consistent with an ephemeral wet-dry system typically seen in monsoonal deposits and are evidence of nearby desiccated muds being present prior to deposition (Hounslow & Ruffell, 2006).

The matrix closest to the bone preserved a smattering of small, flattened, elongate bone flakes running parallel to the long axis of the bones with the largest flakes being preserved closest to the bone surface. These mm-scale bone flakes are consistent with having come from the bones that they are adjacent to. No evidence of biomaterial was found during this process.

The surface of most of the bones had a thin, oxidized, red-brown crust. Most of the long bones were found anterior side up, but the vertebrae were found in varying, arbitrary positions. Some of the bones appear to have undergone compaction postdepositionally, but the degree of postdepositional deformation is not extensive.

3.4 Facies Association Overview

A stratigraphic section of 15 meters was measured at the H5 quarry (Fig. 3). Based on correlations with Elliot Formation sections measured and described by (Bordy et al., 2004a, McPhee et al., 2017), these units are confidently placed within the Lower Elliot Formation.

Within the H5 section, 11 distinct units were identified that alternate between laterally continuous, thinly-bedded quartz-sandstones with gently scoured, concave upward basal contact, interbedded with silty mudstones. Volumetrically, mudstone accounts for approximately 60% of the section, and sandstone 40%. Sand is fine-to-medium grained and displays only unidirectional ripple cross bedding, indicative of lower flood regime traction transport in a shallow channel.

Owing to the preponderance of preserved mudstone over sandstone, and the presence of thin, channelized sand bodies preserving only ripple cross bedding, the H5 section is interpreted here to represent a low-energy fluvial meander plain. Cut-and-fill sand intervals likely represent shallow tributaries to a main trunk system. Some of the fine-grained quartz sandstone units contain *Planolites* burrows 0.5-1.0 cm wide, up to 10 cm long, but these burrows are not seen within the mudstones (Keighley & Pickerill, 2008; Metz, 2008; Gillette et al., 2010).

The upward-fining mudstones show a gradual infill of the channel into an oxbow lake environment. The mudstones in Units 4 and 6 preserve the presence of a floodplain where the intermediate sandstone constituting Unit 5 is interpreted as a crevasse-splay deposit. This is further supported but the mudstones which have a mottled texture and purple-red coloration that is indicative of paleosols and implies a highly vegetative floodplain. *Planolites* burrows in Unit 1 indicate a robust benthonic worm population.

Unit 6, a strongly consolidated, olive-gray silty overbank mudstone, persists for 0.3 meters and is the only vertebrate-fossil-yielding unit in the section. It contains no trace fossils, paleosols, or rooted horizons. The sandstone units above and below Unit 6 are both fine-grained, indicative of a low-energy, fluvial environment and possibly a distal source. While not observed while measuring this section, mud rip-up clasts were found during preparation just above the bone layer of Unit 6.

3.5 Anatomical Descriptions

3.5.1 Axial Skeleton

3.5.1.1 Cervical vertebrae

Two cervical vertebrae are preserved. The first is represented by only a neural arch but the second is complete. They are presumed to be C5 (Fig. 12) and C7 (Fig. 13), respectively based upon the location of the parapophyses. Both vertebrae have superficial cracking throughout but lack any serious deformation. The semi-open sutures on both elements, along with the lack of a centrum on C5?, suggest that this animal might not have been entirely fully grown (Irmis, 2007).

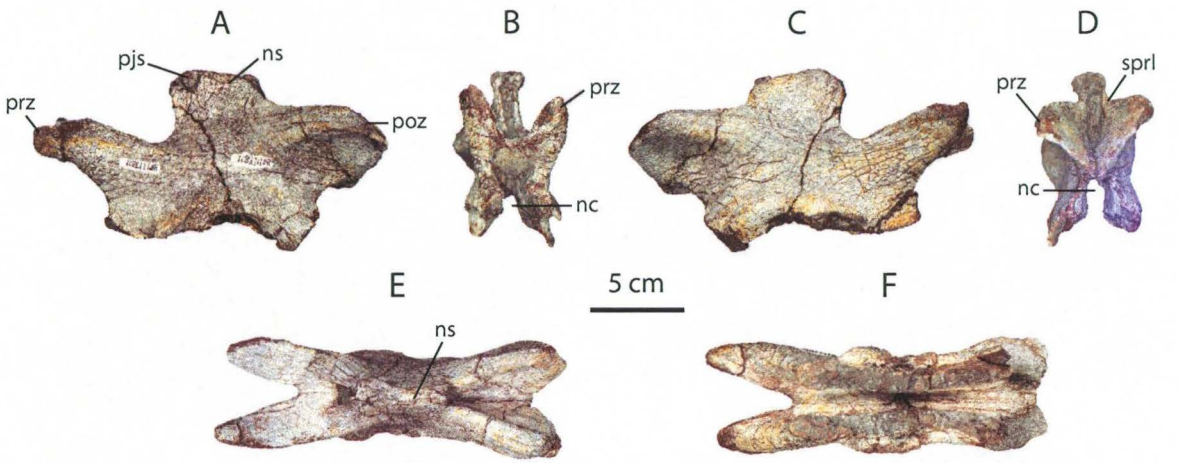

Figure 12: BP/1/7811, C5?. Left lateral (A) anterior (B) posterior (C) right lateral (D) dorsal (E) ventral (F). Abbreviations: di, diapophyses; nc, neural canal; ns, neural spine; pa, parapophyses; poz, postzygapophyses; prz, prezygapophyses; pjs; projecting spurs; sprl, spinoprezygapophyseal lamina. Scale bar = 5 cm

The presumptive C5, despite the lack of centra, has a complete and well-preserved neural arch. In dorsal view, C5? and C7? are quite similar in terms of general shape and elongation. Both have laterally projecting spurs coming off the proximal most tip of the neural spine, but these are more pronounced and more anteriorly placed in C5?. This is a feature seen scattered throughout sauropodomorpha (e.g., *Anchisaurus*, *Massospondylus*, *Sarahsaurus*) (Yates, 2007a; Yates, 2010; Rowe et al., 2011). The prezygapophyses are the same relative length and project anteriorly, but are wider on C7?. The postzygapophyses do not differ morphologically in this view, but are better preserved in C5? (Fig. 12 D). The only major difference observable dorsally between these two elements is the extension of the diapophyses. The diapophyses of C5? are minimal and directed distally where those seen in C7? in anteroposterior view (Fig. 13 B&D). While also distally directed, they flair out laterally and are more extensive than in C5?.

The anterior surfaces of C5? (Fig. 12 B) and C7? (Fig. 13 B) both have pronounced and excavated spinoprezygapophyseal fossae, bounded by long surrounding spinoprezygapophyseal laminae. The prezygapophyses open dorsolaterally, with C5? exhibiting a slightly more open and U-shaped infraprezygapophyseal laminae. Preserved on the transverse processes of C7? are centroprezygapophyseal fossae. Below these fossae, bounded by pronounced centroprezygapophyseal laminae, sharp prezygodiapopyseal lamina, and weak anterior centrodiapophyseal lamina are two shallow prezygocentrapophyseal fossae. Due to some compaction centralized on the left, only the right side shows the extension of these fossae. These features are not found on C5?.

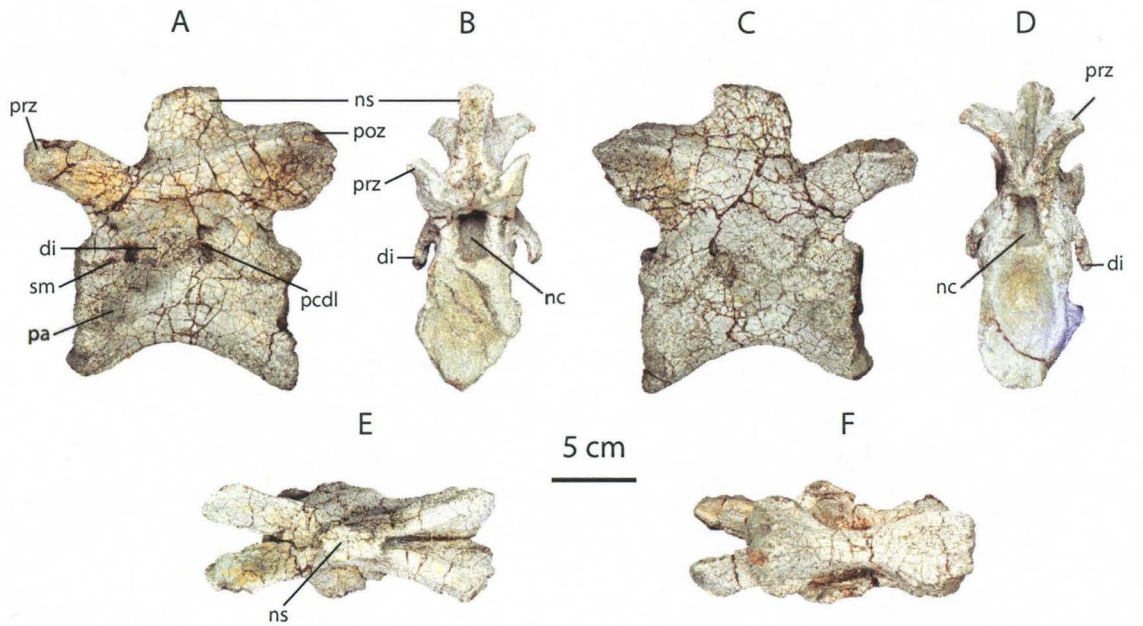

Figure 13: BP/1/7811, C7?. Left lateral (A) anterior (B) posterior (C) right lateral (D) dorsal (E) ventral (F). Abbreviations: di, diapophyses; epi, nc, neural canal; ns, neural spine; pa, parapophyses; poz, postzygapophyses; prz, prezygapophyses; sm, suture marks. Scale bar = 5

On the posterior surface, a deep spinopostzygapophyseal fossa is present in C5? and C7?. The spinopostzygapophyseal laminae are long and project posteriolaterally outwards along the tops of the postzygapophyses. The postzygapophyses in both elements project downwards.

The neural spine of C5? (Fig. 12 A&C) in lateral view is wider anteroposteriorly than it is dorsoventrally high, making it roughly rectangular, deflecting anteriorly in lateral view. The anteroposteriorly width and dorsoventrally height of C7? (Fig. 13 A&D) make more of a square shaped profile in lateral view (Table 2). The prezygapophyses in this view are positioned on the anterolateral surface of the neural arch and exhibit a slight dorsolateral curve upwards anteriorly. This positioning of this feature in both elements appears to be the common condition for all basal sauropodomorphs with the exception of *Pantydraco* where the prezygapophyses are strongly anterior projections (Yates, 2003; Galton et al., 2007). These prezygapophyses extend well past the anterior margin of the centrum.

The anteroposteriorly extending spinoprezygapophyseal laminae are sharp, steep features that dip downwards towards the posterior end of the element along the lateral surface of C5? and C7?. The postzygapophyses in lateral view are only minimally obliquely offset with respect to the prezygapophyses, without any obvious dorsal elevation from the coronal place as seen in *Leonerasaurus* and *Pulanesaura* (Pol et al., 2011; McPhee et al., 2015a). Situated below the prezygapophysis on the left lateral surface of C7? is a small cavity interpreted as a postzygocentrodiapophyseal fossae. It is not found on the right lateral surface or on any surface of C5?. On both cervicals, what might be the start of postzygodiapophyseal laminae do not

meet the edge of the transverse processes and are nothing like the tall and well-developed laminae present in later sauropods (Wilson, 1999 & Yates et al., 2012), which is the common condition for sauropodomorphs (Pol et al., 2011).

The diapophyses are present in both elements but are significantly more pronounced in C7?. They are situated below the medial end of the prezygapophyses and project laterally in lateral view. Running anteroposteriorly are a series of shallow depressions within of the centrodiapophyseal fossa, which may represent an autapomorphic feature for BP/1/7811. However, CT scans of the specimen (data not shown) indicate that these depressions do not continue internally, and thus do not represent pneumaticity (Yates et al. 2012).

Of the two cervical vertebrae preserved, C7? is the only one to preserve a centrum. In this vertebra, the neural arch and centrum are fused together but, as mentioned above, bear suture marks. The centrum, along with the arch, is tall and thin and the height of the neural arch is less than the height of the centrum (Table 2), which is the common condition for sauropodomorphs (Galton & Upchurch, 2004; Otero et al., 2015).

The articular faces of the centrum on the anterior and posterior surface (Fig. 13 B&D) are biconcave. This is the condition for all known non-sauropodan sauropodomorphs, but is convex in basal sauropods (Sues, 1997). The ventral surface of the centra displays a sagittal keel, which is a condition that is distributed widely amongst sauropodomorphs (e.g., *Anchisaurus*, *Lessemsaurus*, *Massospondylus*) (Bonaparte, 1999; Yates, 2004; Pol et al., 2011).

3.5.1.2 Dorsal vertebrae

There are eight dorsal vertebrae, along with several additional dorsal fragments. None of these elements were found in articulation. Based on the position of the parapophyses, the relative anteroposterior lengths of the neural spines, and the orientation of the diapophyses, the preserved elements are representative of all region of the dorsal series. They are identified here as D1? (Fig. 14), D2? (Fig. 15), D4? (Fig. 16) D5? (Fig. 17), D6? (Fig. 18), D8? (Fig. 19), D12? (Fig. 20), and D13? (Fig. 21).

All elements have undergone varying degrees of fracturing and compaction. The neurocentral sutures appear closed, although some still possess faint suture marks. This fusion suggests that BP/1/7811 was mostly grown at the time of death (Irmis, 2007; Hone et al., 2016) and should be considered as a subadult. The parapophyses in these elements are sub-ellipsoid in lateral view. Also in this view, weak pleurocoels are present within the neural arches, which is not seen in NMQR 1551 or NMQR 3314, but are present in a similar degree in taxa like *Aardonyx*, *Eucnemesaurus*, *Lessemsaurus*, and *Pulanesaura* (Bonaparte, 1999; Yates, 2007; Yates et al., 2010; McPhee et al., 2015b).

Another feature that is different from the NMQR specimens (1551 & 3314) is the appearance of accessory lamina that divide the posterior fossae from the postzygapophyses. All elements lack spinodiapophyseal laminae, the presence of which is only seen in transitional sauropods (Rauhut et al., 2011; Wilson et al., 2011; Fanti et al., 2013). These vertebrae are also lacking

well-developed suprapostzygapophyseal laminae. The spinopostzygapophyseal laminae are present, but appear only as singular features with no bifurcation distally.

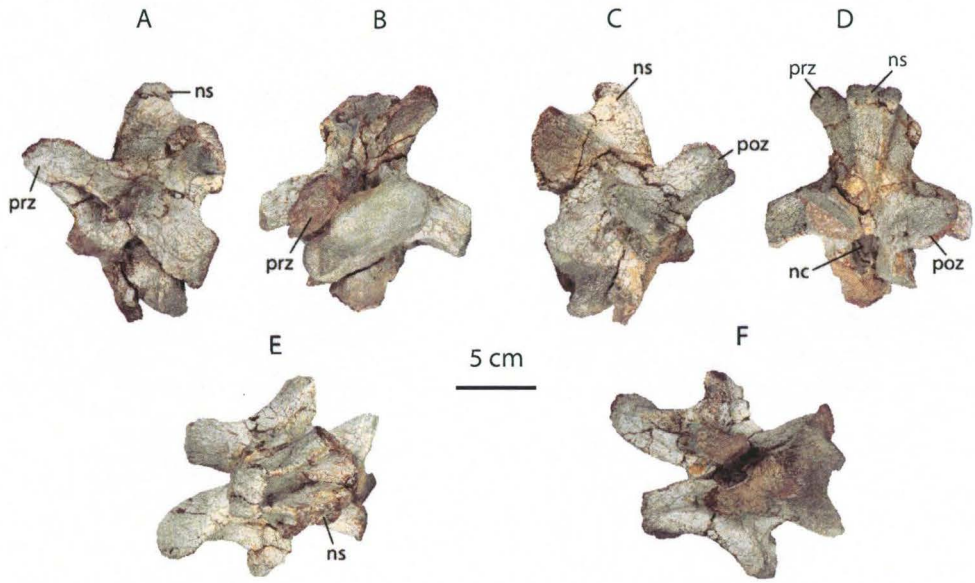

Figure 14: BP/1/7811, D1?. Left lateral (A) anterior(B) posterior (C) right lateral (D) dorsal (E) ventral (F). Abbreviations: epi, nc, neural canal; ns, neural spine; poz, postzygapophyses; prz, prezygapophyses. Scale bar = 5 cm

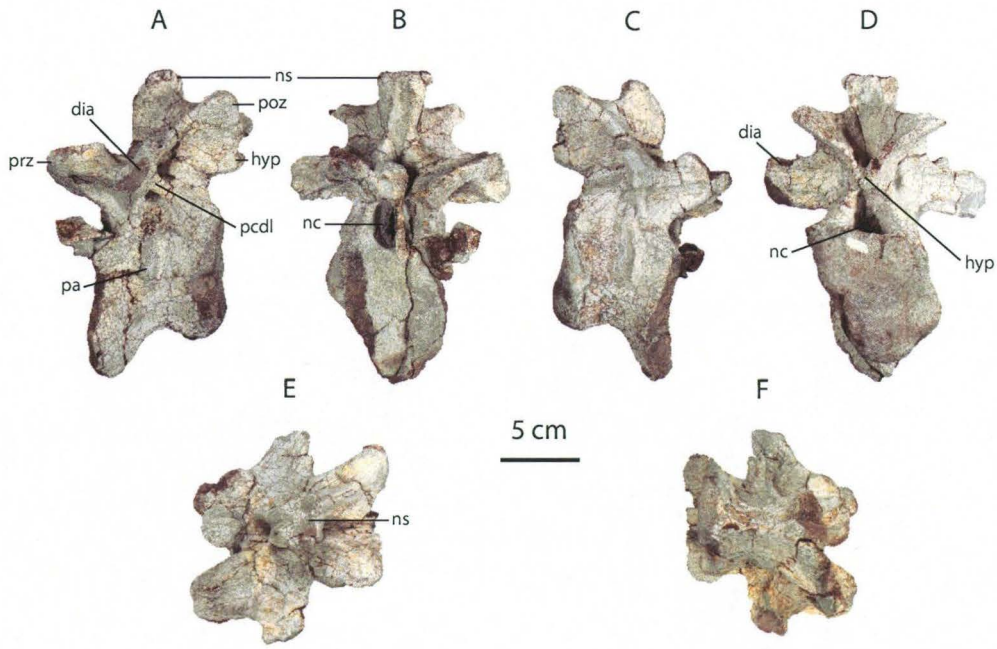

Figure 15: BP/1/7811, D2?. Left lateral (A) anterior (B) posterior (C) right lateral (D) dorsal (E) ventral (F). Abbreviations: di, diapophyses; hyp, hyposphene; nc, neural canal; ns, neural spine; pa, parapophyses; pcdl, posterior centrodiapophyseal lamina; poz, postzygapophyses; prz, prezygapophyses. Scale bar = 5 cm

All of the collected dorsal centra are completely amphicoelous, which is the expected condition for basal sauropodomorphs (e.g., *Leonerasaurus*, *Leyesaurus*, *Xingxiulong*) (Apaldetti et al., 2011; Pol et al., 2011; Wang et al., 2017). The orientation of the transverse processes on all dorsal vertebrae are horizontally directed, this is seen in all other non-eusauropodan sauropodomorphs (Pol et al., 2011; McPhee et al., 2014) with the exception of *Ignavusaurus* where the transverse processes are deflected upwards (Knoll, 2010). There is no sign of centroparapophyseal lamina or prezygoparapophyseal lamina in any of these elements.

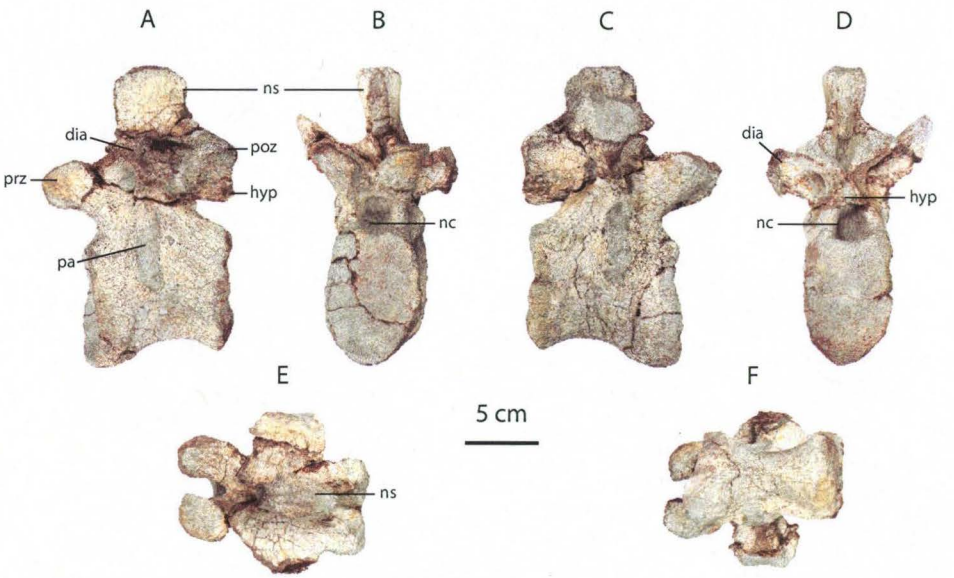

Figure 16: BP/1/7811, D4?. Left lateral (A) anterior (B) posterior (C) right lateral (D) dorsal (E) ventral (F). Abbreviations: di, diapophyses; hyp, hyposphene; nc, neural canal; ns, neural spine; pa, parapophyses; poz, postzygapophyses; prz, prezygapophyses. Scale bar = 5 cm

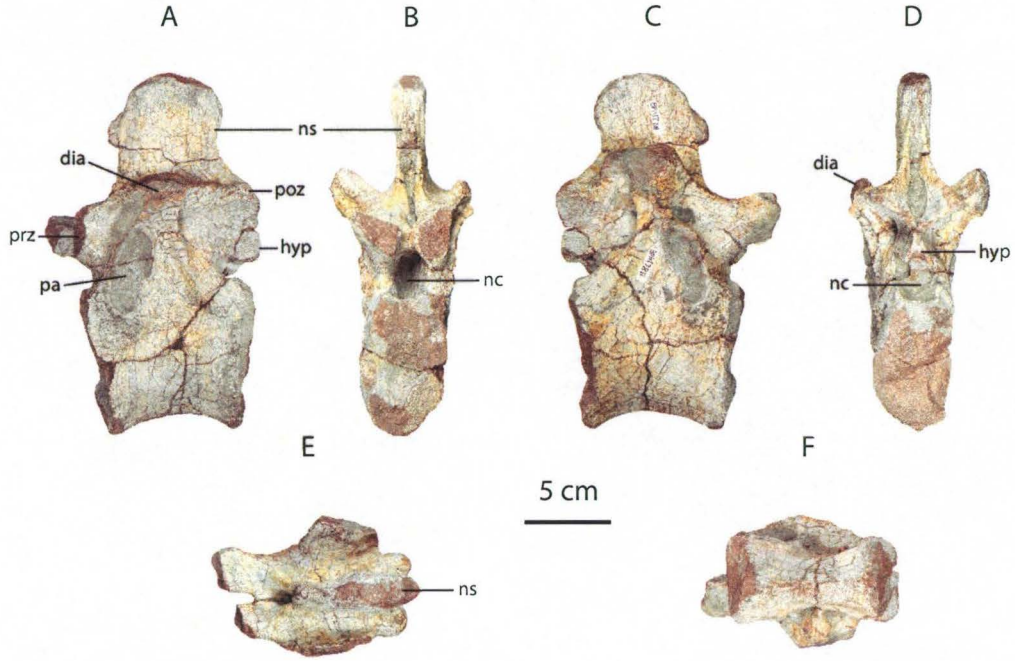

Figure 17: BP/1/7811, D5?. Left lateral (A) anterior (B) posterior (C) right lateral (D) dorsal (E) ventral (F). Abbreviations: di, diapophyses; hyp, hyposphene; nc, neural canal; ns, neural spine; pa, parapophyses; poz, postzygapophyses; prz, prezygapophyses. Scale bar = 5 cm

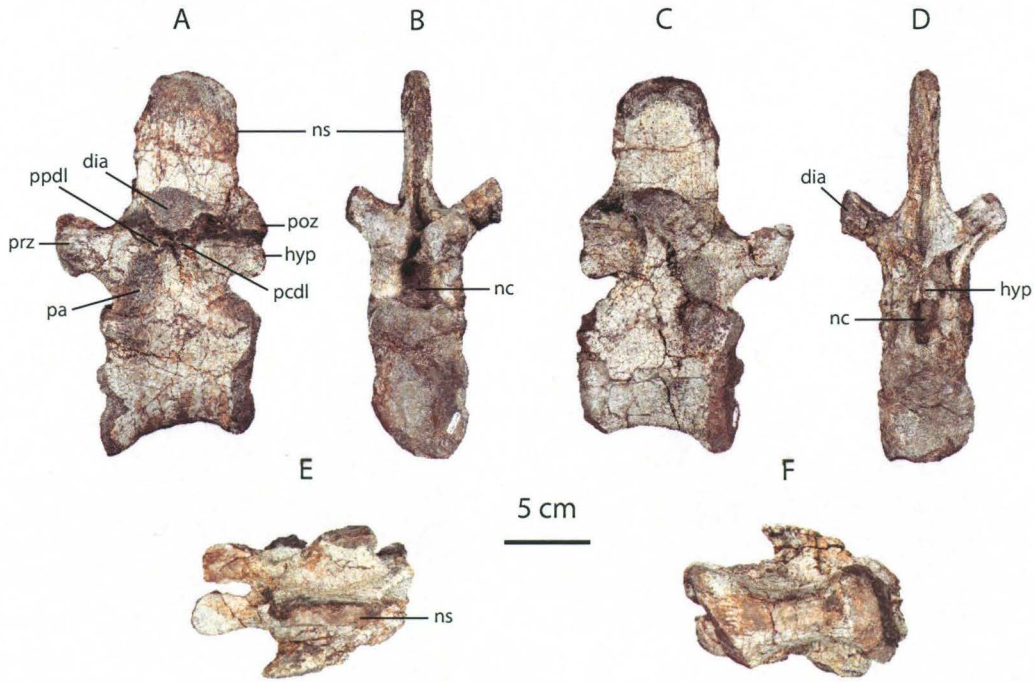

Figure 18: BP/1/7811, D6?. Left lateral (A) anterior (B) posterior (C) right lateral (D) dorsal (E) ventral (F). Abbreviations: di, diapophyses; hyp, hyposphene; nc, neural canal; ns, neural spine; pa, parapophyses; pcdl, posterior centrodiapophyseal lamina; poz, postzygapophyses; ppdl, posterior infradiapophyseal subfossa; prz, prezygapophyses. Scale bar = 5 cm

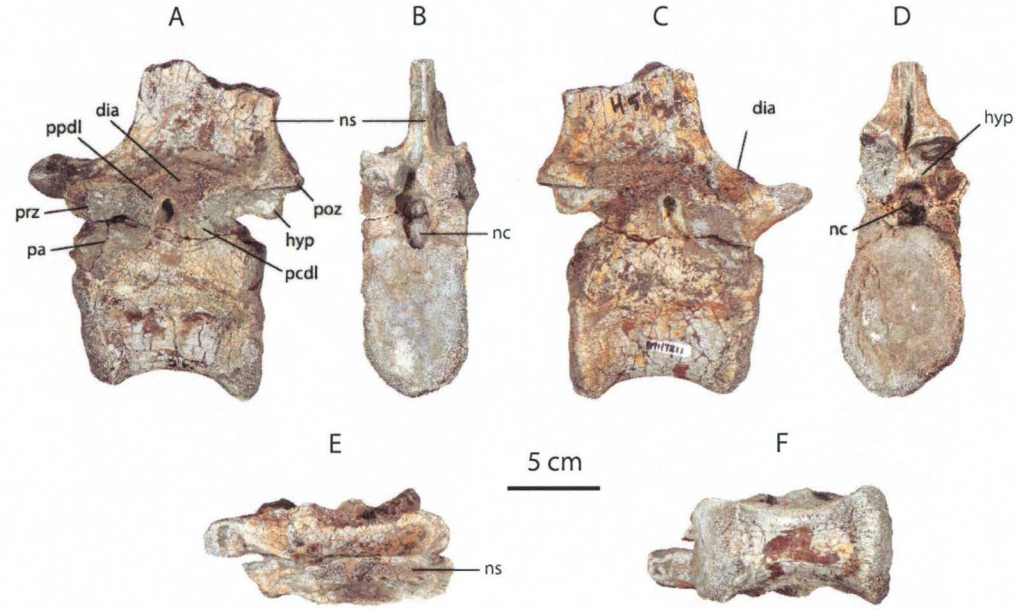

Figure 19: BP/1/7811, D8?. Left lateral (A) anterior(B) posterior (C) right lateral (D) dorsal (E) ventral (F). Abbreviations: di, diapophyses; hyp, hyposphene; nc, neural canal; ns, neural spine; pa, parapophyses; pcdl, posterior centrodiapophyseal lamina; poz, postzygapophyses; ppdl, posterior infradiapophyseal subfossa; prz, prezygapophyses. Scale bar = 5 cm

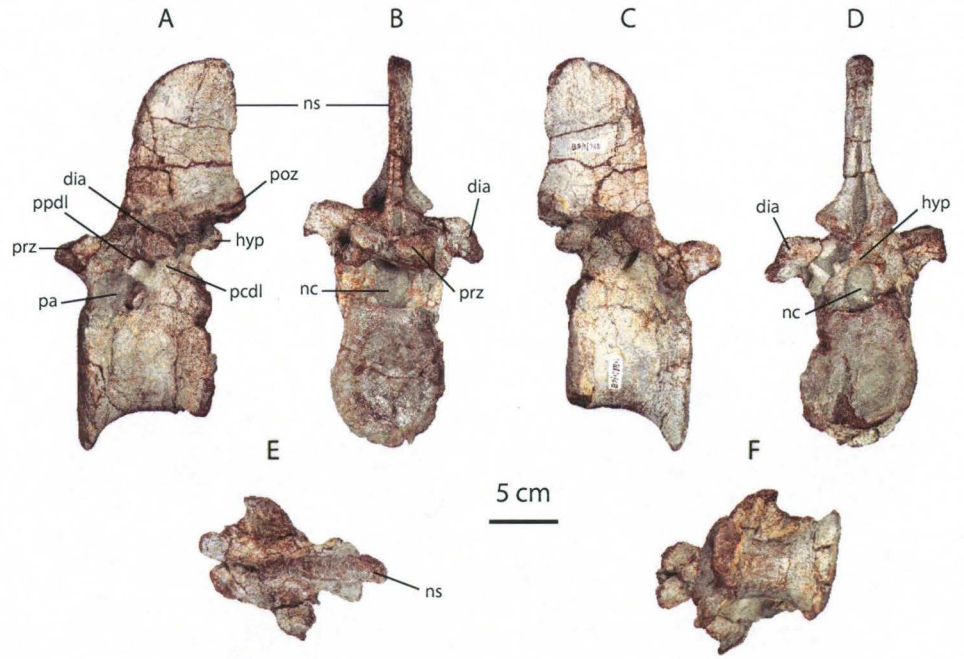

Figure 20: BP/1/7811, D12?. Left lateral (A) anterior(B) posterior (C) right lateral (D) dorsal (E) ventral (F). Abbreviations: di, diapophyses; hyp, hyposphene; nc, neural canal; ns, neural spine; pa, parapophyses; pcdl, posterior centrodiapophyseal lamina; poz, postzygapophyses; ppdl, posterior infradiapophyseal subfossa; prz, prezygapophyses. Scale bar = 5 cm

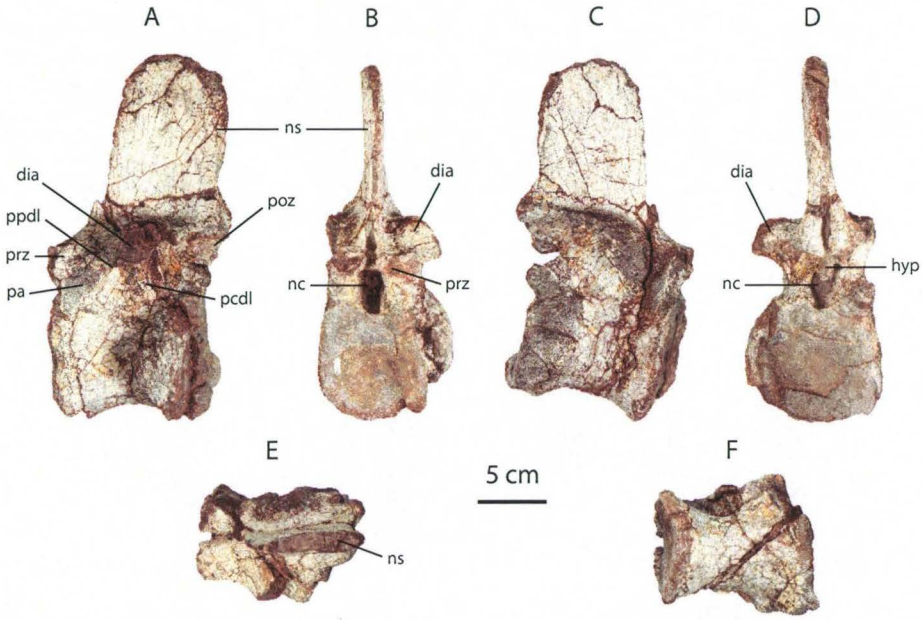

Figure 21: BP/1/7811, D13?. Left lateral (A) anterior(B) posterior (C) right lateral (D) dorsal (E) ventral (F). Abbreviations: di, diapophyses; hyp, hypo-sphene; nc, neural canal; ns, neural spine; pa, parapophyses; pcdl, posterior centrodiapophyseal lamina; poz, postzygapophyses; ppdl, posterior infra-diapophyseal subfossa; prz, prezygapophyses. Scale bar = 5 cm

D1? (Fig. 14) and D2? (Fig. 15) have much shorter neural arches than the rest in the series and have well developed diapophyses, located back from the anterior margin on the lateral surface of the centrum. In anterior views, the lateral margins of the neural spines are sub-parallel. As seen in taxa like *Aardonyx*, *Plateosaurus*, and *Yunnanosaurus* (von Meyer, 1837; Lü et al., 2007; Yates et al., 2010), there is a longitudinal keel that runs across the ventral surface of the centra in these two vertebrae.

The mid-posterior dorsal vertebrae have much higher neural arches than those seen in the anterior-most dorsal elements of BP/1/7811. In the most posterior vertebrae, the neural spine makes up almost half of the element and is more extensive broader anteroposteriorly than dorsoventrally. There is an absence of prezygodiapophyseal lamina in these vertebrae.

3.5.1.3 Caudal vertebra

One partially complete posterior caudal vertebra was preserved (Fig. 22) along with two caudal fragments (not figured). The posterior position is assumed from the size and location of the transverse processes. The anterior-posterior caudal was collected near the femur in the same depositional level (Fig. 5). Based on element size and location within the quarry, it is reasonable to assume they are from the individual.

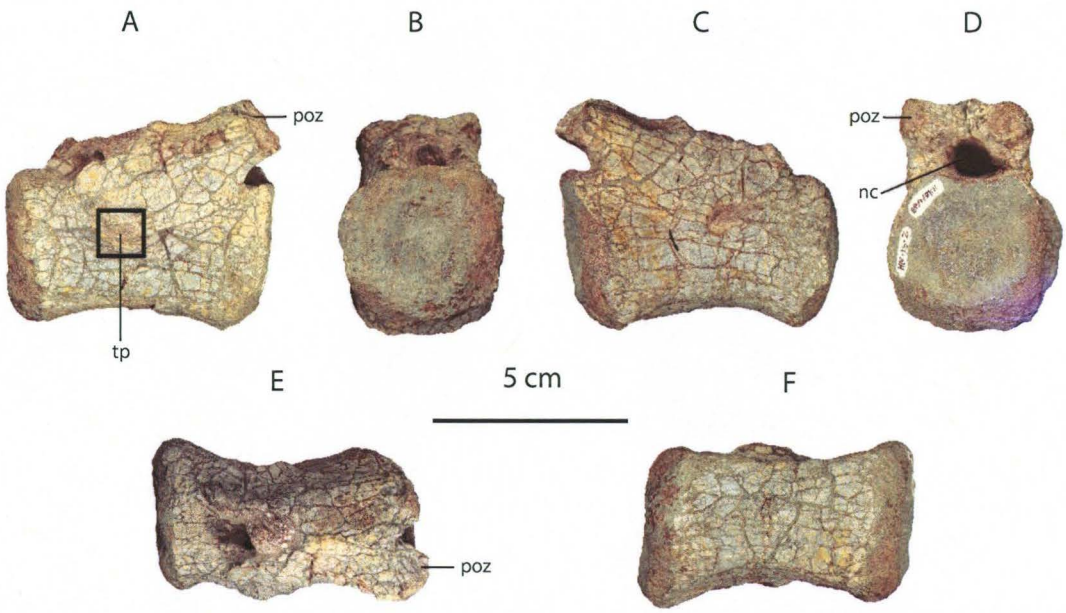

Figure 22: BP/1/7811, Posterior caudal. Left lateral (A) anterior (B) posterior (C) right lateral (D) dorsal (E) ventral (F). Abbreviations: di, diapophyses; epi, nc, neural canal; tp, transverse process; poz, postzygapophyses. Scale bar = 5 cm

The posterior caudal in lateral views (Fig. 22 A&C) shows the placement of an anteriorly positioned neural spine, but most of the spine was not preserved. In these views, the partially preserved postzygapophyses can be observed. These features are positioned anteroposteriorly

with no lateral deflection. Their placement steeply backwards makes an acute angle of approximately 30 degrees. The prezygapophyses were not preserved on this element.

The cross-section of the centrum is sub-rectangular, with flattened laterally, which is a feature observable in some transitional sauropodomorphs (i.e., *Aardonyx, Anchisaurus,* NMQR 3314*, Mussaurus,* and *Sefepanosaurus*) (McPhee et al., 2014; Otero et al., 2015).

3.5.2 Appendicular Skeleton

3.5.2.1 Scapula

The left scapula (Fig. 23) is heavily fractured throughout and is missing the lateral most ends of the scapular blade, as well as the scapular-coracoid facet and the acromion facet. Despite these damages, the element appears undistorted. Due to the condition of the fossil, the occurrence or absence of a closed scapulocoracoid suture cannot be determined. There are not obvious markings or tubercles on the scapula.

The dorsal end of the scapular blade expands anteriorly and posteriorly, in a similar fashion to Lessemsaurus (PVL 4822/51). This differs from most basal sauropodomorphs where there is significantly less dorsal expansion (e.g., *Coloradisaurus*, *Lufengosaurus*, *Massospondylus*) (Owen, 1854; Young, 1942; Pol & Powell, 2007; Yates, 2007a). The blade remains consistently anteroposteriorly thin until it terminates in a dorsally convex margin, so that the distal end is

sub-ellipsoid in lateral view. The blade, while thin throughout, is thinnest at is dorsal-most end. Sections of the anterior and posterior margins of the dorsal end of the scapula are missing but the anterior and posterior margins suggest an outline similar to *Antetonitrus* (BP/1/4952c) (McPhee et al., 2014), but slightly longer dorsoventrally in comparison to anteroposterior width.

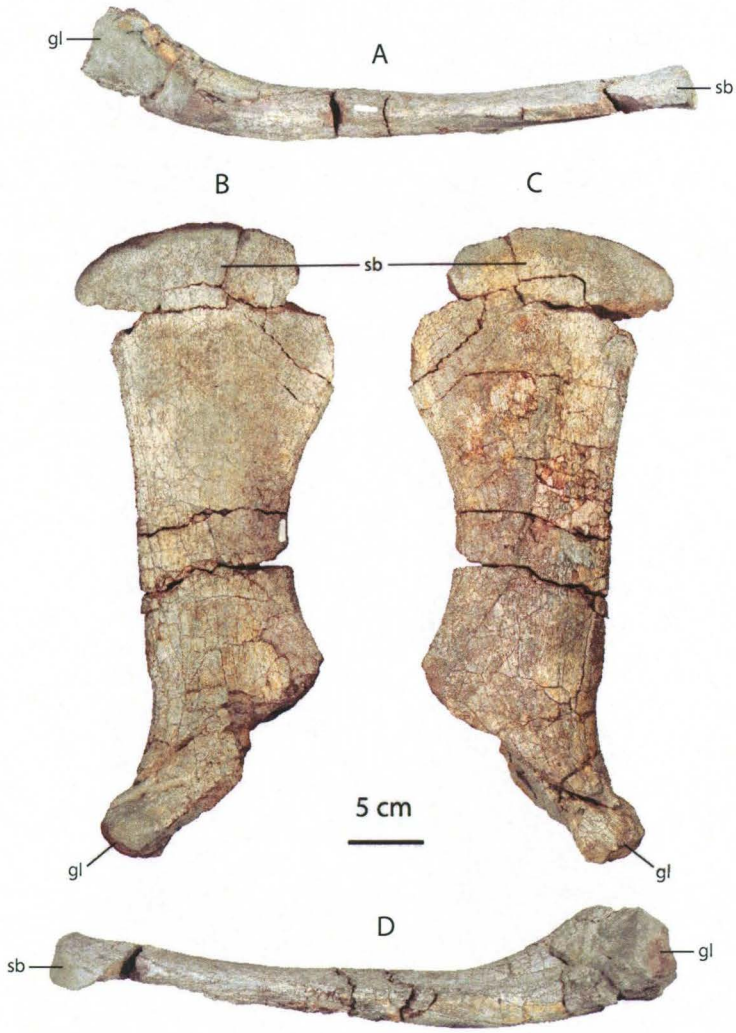

Figure 23: BP/1/7811, left scapula. Anterior (A) medial (B) lateral (C) posterior (D). Abbreviations: gl, glenoid; sb, scapular blade. Scale bar = 5 cm

The scapular blade is long and narrow, similar to taxa like NMQR 1551, *Isanosaurus*, and *Shunosaurus* (Pol & Powell, 2007; McPhee et al., 2014). The scapula displays minor lateral concavity in the ventromedial third of the element in anterior view, but straightens out for the remaining 65% of the element. According to Remes (2007), this concavity defines the boundary of the facet for the m. subscapularis anteriorly, as well as for the facet for the m. serratus superficialis in posteriorly (McPhee et al., 2014). The glenoid is the only feature preserved on the ventral end of the element, and is heavily damaged.

3.5.2.2 Humerus

Both the left and right humeri are well preserved and mostly complete (Fig. 24). Several small fragments of bone are missing from the distal end of the medial margin of the left humerus, appearing to have been lost through surface erosion. There are small cracks and several major fractures that interrupt the cortical surfaces but do not interfere with anatomical interpretation.

Both elements have a strong hourglass shape in anterior (Fig. 24 A) and posterior (Fig. 24 B) views with greater expansion proximally than distally, which is the noted condition for non-sauropodan sauropodomorphs (Bonnan & Yates, 2007; Remes, 2007), and has a sigmoid outline in lateral view (Fig. 24 D). The humeral circumference (Table 3) in relation to the overall humeral length is similarly observed in other melanorosaurid type animals (e.g. NMQR 1551, NMQR 3314).

In proximal view (Fig. 24 E), the humerus of BP/1/7811 is lenticular in outline, with a sinuate curve connecting the deltopectoral crest and medial tuberosity via the humeral head. The proximal surface of the humeral head is strongly rounded and convex anteriorly and posteriorly which is characteristic of most non-sauropodan sauropodomorphs with the exception of some specimens of *Plateosaurus* and *Unaysaurus* (UFSM 11069) (Leal et al., 2004; Remes, 2007; McPhee et al., 2014). The convexity of the humeral head can also be seen strongly on the anterior and lateral surfaces of the element, where posteriorly and laterally there is a shift to concavity. The apex of the head is positioned slightly more laterally relative to the transverse midpoint of the proximal surface.

Although the proximal surface of the medial tuberosity is imperfectly preserved in both elements, it is clear that the process deflects posteriorly from the humeral head. In contract, the medial tuberosity of many other basal sauropodomorphs (e.g., *Antetonitrus*, *Lessemsaurus*) deflects at a much sharper angle (Bonaparte, 1999; Pol & Powell, 2007; McPhee et al., 2014) The condition in BP/1/7811 is thus more similar to that observed in sauropod dinosaurs, which present a reduced medial tuberosity (Remes, 2007).

In the concavity made on the anteromedial face of the proximal half of the humerus between the margins of the deltopectoral crest and the medial tuberosity, there is a well-developed fossa preserved that is presumed to be the insertion of the *m. coracobrachialis* (Remes, 2007).

In lateral view the deltopectoral crest is subrectangular in general outline, which is the typical condition for Sauropodomorpha (e.g., *Seitaad*, *Vulcanodon*, *Yunnanosaurus*) (Raath, 1984; Sertich & Loewen, 2010; Wang et al, 2017). The length of the deltopectoral crest is almost half of the length of the humerus which is similarly seen in NMQR 3314 and SAM 3342. The crest curves medially and is relatively straight along the anteromedial margin, which is similar to the condition seen in derived, non-sauropodan sauropoodiforms like *Leonerasaurus*, *Coloradisaurus*, and *Antetonitrus*.

The posterior surface of the left humerus (and to a lesser degree the right) is close the proximal end of the deltopectoral crest. On the medial surface of the humerus, at the same level as the base of the deltopectoral crest, large nutrient foramina are visible (Fig. 24 D). These notable features deflect proximally and have been hypothesized to related to blood flow, body size increase, and/or high activity (Seymour et al., 2012; Allan et al., 2014).

The humeral diaphysis is proximodistally short and has an ovoid cross-section with the major axis of the oval oriented mediolaterally, similar to other non-sauropodan sauropodomorphs (Remes, 2007). The humeral diaphysis becomes narrower as it extends distally.

The radial and ulnar condyles are separated by a deep cuboid fossa, which is the similar condition seen in the majority of non-sauropodan sauropodomorphs (e.g., NMQR 3314, *Plateosaurus,* and *Lufengosaurus* (Young, 1942; Mallison et al., 2009). The ulnar condyle is slightly larger in anterior view (Fig. 24 A) than the radial condyle, which shifts the center of the

fossa closer to the ulnar condyle. The distal condyles are rotated about 25 degrees relative to the transverse plane of the proximal end. This differs from taxa like *Plateosaurus, Lufengosaurus,* and *Massospondylus* that are typically offset approximately 45 degrees (McPhee et al., 2014).

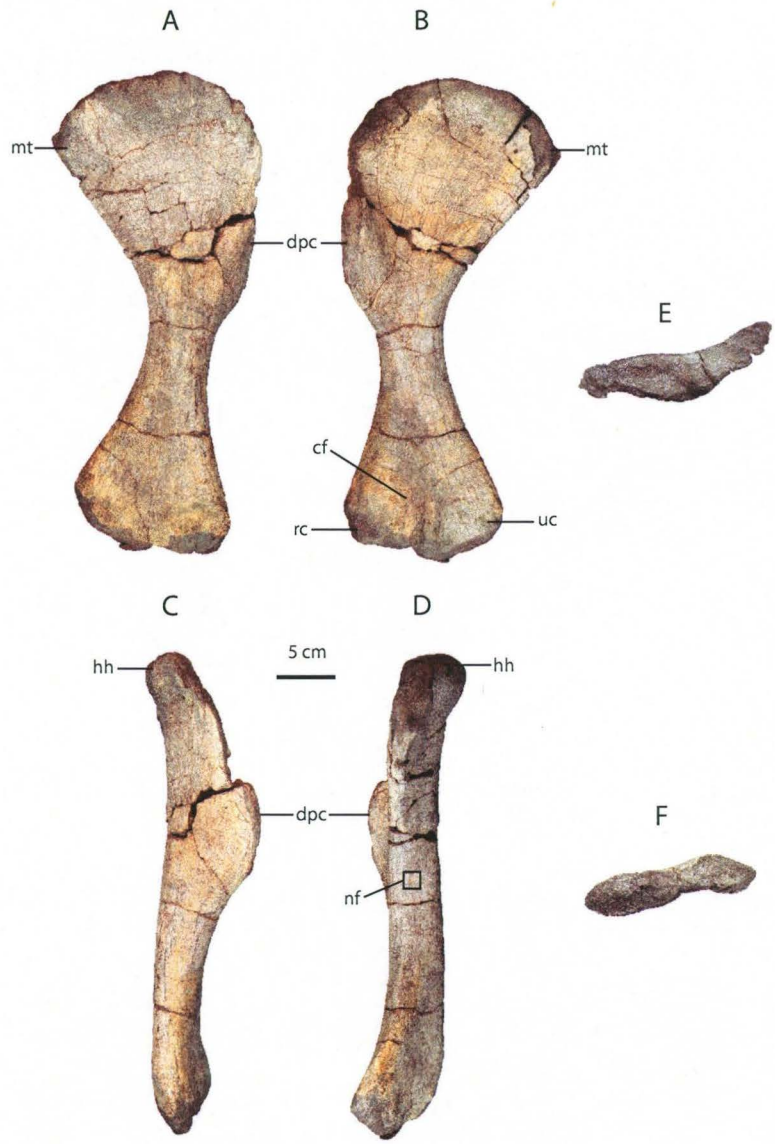

Figure 24: BP/1/7811, right humerus. Anterior (A) posterior (B) medial (C) lateral (D) proximal (E) distal (F). Abbreviations: cf, cuboid fossa; dpc, deltopectoral crest; hh, humeral head; mt, medial tuberosity, nf, nutrient foramina; rc, radial condyle; uc, ulnar condyle. Scale bar = 5 cm

In distal view (Fig. 24 F) the radial and ulnar condyle are both rounded and ovoid. The transverse width of the condyles (Table 3) is approximately 30% of the total length of the humerus, a metric that is comparable most basal sauropodomorphs excluding *Coloradisaurus* (Bonaparte, 1978; Novas et al., 2011), *Yunnanosaurus* (Young, 1942; Lu et al., 2007), *Riojasaurus* (Bonaparte & Pumares, 1995), *Sarahsaurus* (Rowe et al., 2011), and *Lessemsaurus* (Bonaparte, 1999), which exhibit a proportionally greater distal expansion (Pol et al., 2011).

3.5.2.3 Radius

The distal half of the right radius is preserved (Fig. 25). The bone is straight in anterior and posterior views (Fig. 25 C&D), which is common in most basal sauropodomorphs (Otero et al., 2015). In medial and lateral views (Fig. 25 A&B), the bone flares outwards along the medial margin, where the ulnar ligament scar sits but not to the extent observed in *Antetonitrus* by McPhee et al. (2014).

The shaft of the radius is subovoid in cross-section. In lateral and anterior view, a biceps tubercle can be observed, which is interpreted as the insertion point for the tendon of the m. biceps brachii (Gray, 1918). In medial view (Fig. 25 B), below the ulnar ligament, there is a small fossa observed which Yates at al. (2010) have described as a muscle scar, which is also present in *Sefapanosaurus*, *Mussaurus*, *Aardonyx*, and *Antetonitrus* (Otero & Pol, 2013; McPhee et al., 2014; Otero et al., 2015).

The distal end of the radius (Fig. 25 E) is mostly flattened, although this could be slightly exaggerated by predepositional damages. Despite this compaction, the distal outline is subovoid and expands laterally.

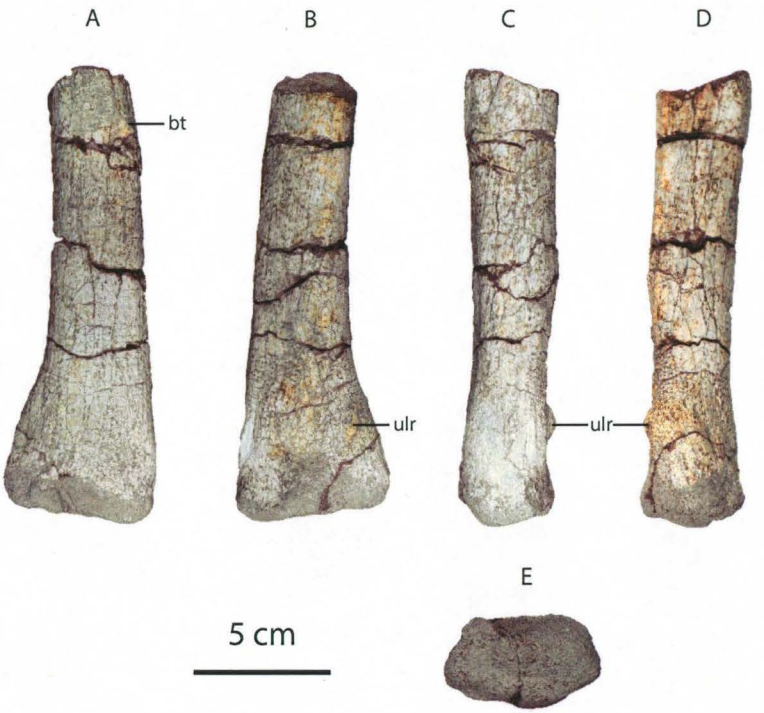

Figure 25: BP/1/7811, distal right radius. Lateral (A) medial (B) anterior (C) posterior (D) distal (E). Abbreviations: bt, biceps tubercle; ul, ulnar ligament of the radius. Scale bar = 5 cm

3.5.2.4 Ulna

The single left ulna is poorly preserved and missing the distal end including more of the shaft (Fig. 26). The proximal end is also badly eroded, missing most of the coronoid process. The features that did preserve fully in this element are the olecranon process, the craniolateral process, and the radial fossa.

The proximal surface of the ulna (Fig. 26 E) shows is sub-triangular in outline. This differs from the triradiate shape seen in other sauropodomorphs more derived than *Aardonyx* (e.g., *Sefepanosaurus,* NMQR 3314) (Galton & Upchurch, 2004; Bonnan & Yates, 2007), but due to the severe erosional damages on this element, it is difficult to make proper comparison with other Elliot sauropodomorph taxa.

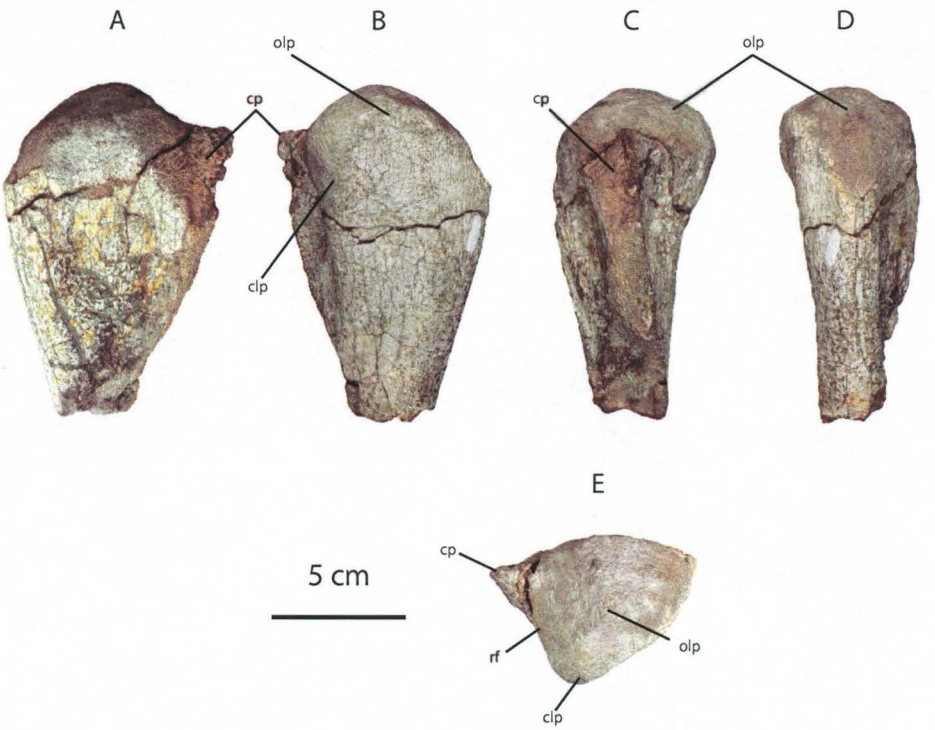

Figure 26: BP/1/7811, left proximal ulna. Medial (A) lateral (B) anterior (C) posterior (D) proximal (E). Abbreviations: clp, craniolateral process; cp, coronoid process; olp, olecranon process; rf, radial fossa. Scale bar = 5 cm

The radial fossa, which is situated between the lateral process and the coronoid process, is shallowly concave. This fossa provides support for the corresponding radius (Bonnan & Yates, 2007). It is similarly developed to that of NMQR 3314, but is not as exaggerated as the fossa present in *Sefepanosaurus* (BP/1/7437). However, these observations may be hyperbolized due to a degree of diagenetic distortion.

The olecranon process is strongly convex, as in NMQR 3314 and other closely related non-sauropodan sauropodomorphs (e.g., NMQR 1551, *Sefepanosaurus*, *Aardonyx*). The lateral process is a rounded protuberance that extends laterally to a similar degree seen in the ulnae of *Antetonitrus* and *Aardonyx* (Yates et al., 2010; McPhee at al., 2015a).

3.5.2.5 Manus

Six manual elements are preserved for BP/1/7811, none of which were found in articulation. These elements include metacarpal I (Fig. 27), metacarpal 2 (Fig. 28), three non-terminal ?manual phalanges (Fig. 29), and one ?manual ungual phalanx (Fig. 30).

3.5.2.5.1 Metacarpal 1

One left metacarpal 1 (MC 1) has been preserved (Fig. 27) and is good condition throughout. As is seen in most sauropodomorphs (e.g., *Jingshanosaurus*, *Massospondylus*, *Seitaad*) the proximal width of MC 1 is greater than the proximal width of metacarpal 2 (MC 2) (Apaldetti et al., 2011). However, unlike in taxa like *Jingshanosaurus* (Zhang & Yang, 1995), *Massospondylus* (all), and *Seitaad* (UMNH VP 18040), the minimum transverse shaft width of MC 1 is less than twice the minimum transverse shaft of MC 2 in BP/1/7811.

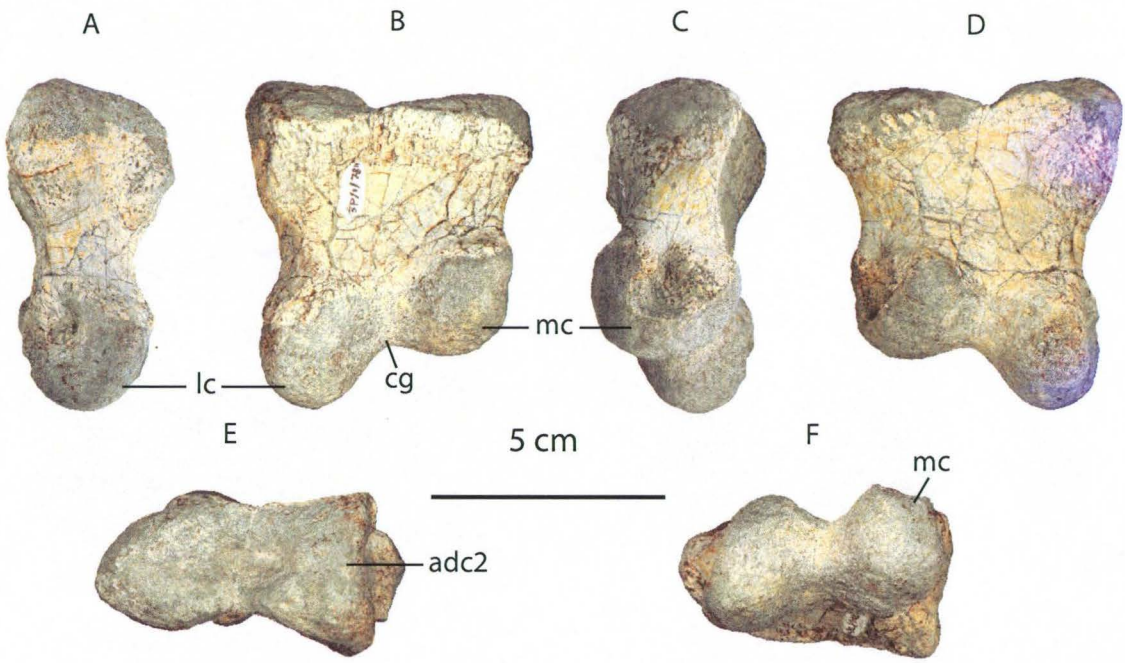

Figure 27: BP/1/7811, left MC1. Lateral (A) anterior (B) medial (C) posterior (D) proximal (E) distal (F). Abbreviations: adc2, articular surface for distal carpal; cg, central ginglymus; lc, lateral condyle; mc, medial condyle. Scale bar = 5 cm

In proximal view (Fig. 27 E), the outline of MC 1 is keyhole-shaped, is transversely elongate, and bears central, shallow pitting and a proximolateral fossa. The mediolateral width of MC 1 is 88% of its overall proximodistal length (Table 3). This percentage is similar to taxa like *Aardonyx*, *Antetontirus* (BP/1/4952), and *Lessemsaurus* which all have proximodistally short MC 1s (Bonnan & Yates, 2007; Yates et al., 2010; McPhee et al., 2014).

Similarly seen in NMQR 3314 (personal observation), the proximolateral edge of MC 1 has some overlap with the proximal articular surface of the corresponding MC2. This observation, along with the presence of a proximolateral fossa on MC1, was theorized to have enabled articulation for these two elements by Bonnan & Yates (2007). On the anterior surface of MC 1 (Fig. 27 B), the articular surface for distal carpal 2 is visible on the lateral margin. In this view, the mid-shaft

is mediolaterally constricted, which is the similar condition for taxa like *Antetonitrus, Lessemsaurus,* and *Sefapanosaurus* (McPhee et al., 2014; Otero et al., 2015).

The posterior surface of MC 1 (Fig. 27 D) has a slight concavity at its center and lacks the mild striations seen on the anterior surface. In this view, the medial condyle deflects slightly dorsomedially and the articular surface for distal carpal 2 is obstructed by the lateral margin. The distal condyles are the same general size and shape and a both strongly asymmetrical, which is consistent with the condition of all non-sauropodan sauropodomorphs (Bonnan, 2003; McPhee et al., 2014). They differ significantly in anteroposterior height, with the lateral condyle being heavily descended in comparison to the medial. These condyles are separated by a U-shaped distal ginglymus.

3.5.2.5.2 Metacarpal 2

A single MC 2 (Fig. 28) was preserved and is longer than the corresponding MC1 (Fig. 27). This element has a substantially narrower mediolateral width and overall circumference (Table 3). The proximal outline (Fig. 28 E) is weathered slightly but is clearly trapezoidal. The proximal articular surface is slightly convex, but not to the degree noted in *Antetonitrus* (BP/1/4952) (McPhee et al., 2014) In this view, the proximolateral flange extends out laterally. This proximolateral flange may have been the buttress for metacarpal 3 proximomedially and is commonly found in most non-eusauropodan sauropodomorphs (e.g., *Antetonitrus, Lessemsaurus*, *Plateosaurus*) (McPhee at al., 2014).

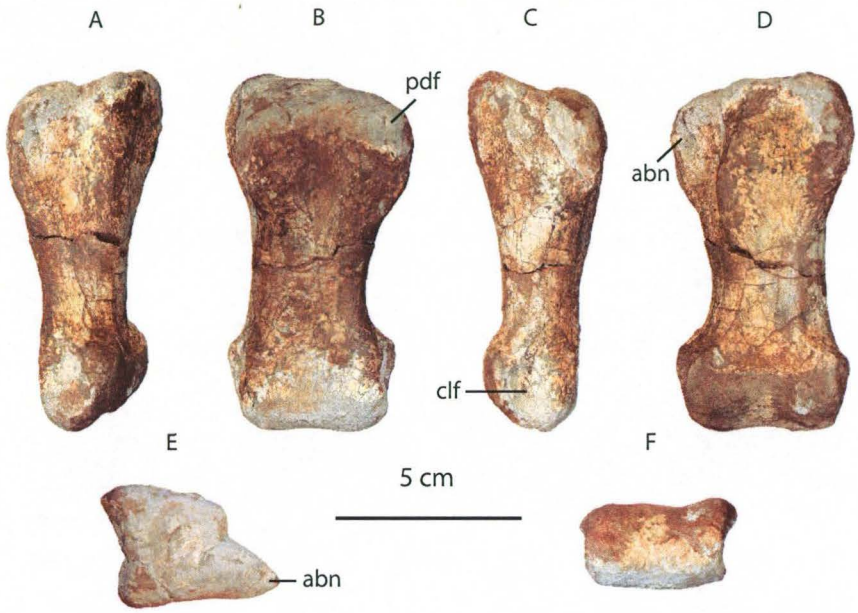

Figure 28: BP/1/7811, left MC2. Lateral (A) anterior (B) medial (C) posterior (D) proximal (E) distal (F). Abbreviations: abn, anterior bifurcated notch; clf, collateral fossa; pmf, proximodistal flange. Scale bar = 5 cm

The anterior surface of MC 2 (Fig. 28 B) has a medial trending anterior bifurcated notch on the proximal end of the element. This degree of pronouncement appears to be relatively rare, but is unmistakably present in *Antetonitrus* (BP/1/4952), *Sefapanosaurus* (BP/1/7438), and BP/1/7120. In this view as well as in posterior view, the bone is mildly expansive proximally and distally but not as flared out as in *Antetonitrus* (BP/1/4952) and *Sefapanosaurus* (BP/1/7438).

On the posterior surface (Fig. 28 D), the proximolateral flange is visible proximomedially. The shaft has a rhomboidal cross-section. It is straight proximodistally with no twisting. The distal condyles are similarly shaped to those seen in MC 1 but sit at the same level and are not separated by a ginglymus joint.

3.5.2.5.3 Non-terminal ?manual phalanges

There are three non-terminal ?manual phalanges that preserved for BP/1/7811 (Fig. 29). All of these phalanges share similar style of well-preservation. These elements were found in close proximity to one-another but not in a state of articulation. In the two larger elements, the lateral condyle sits substantially lower than the medial condyle but in the smallest phalange that condyles sit at relatively the same level. In proximal view these phalanges are all subcirular in profile and are similarly distally deflecting.

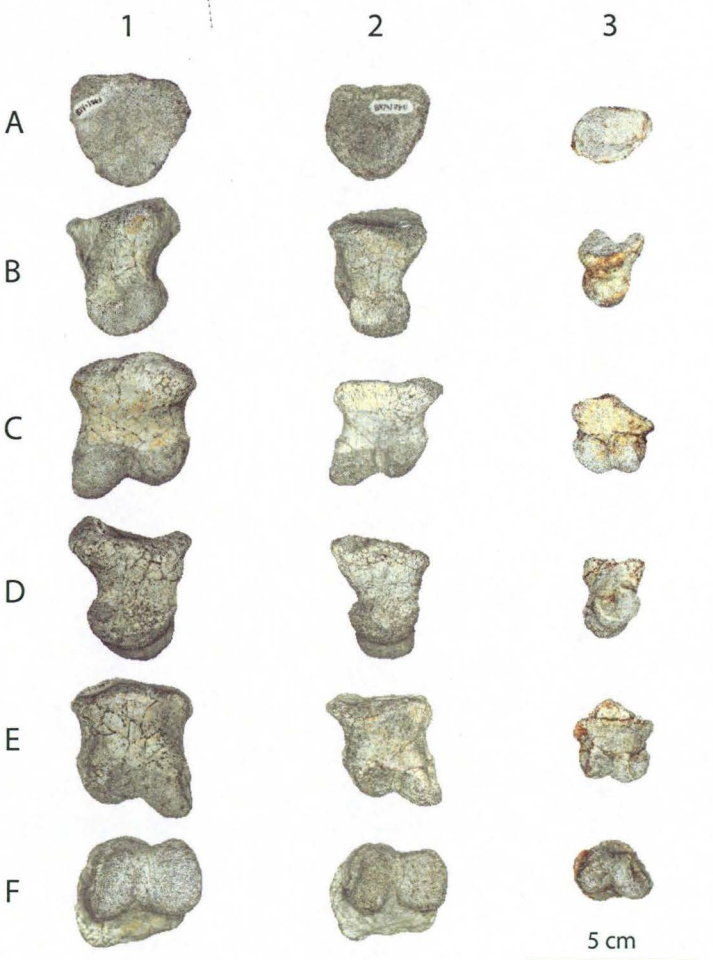

Figure 29: BP/1/7811 non-terminal ?manual phalanges. Proximal (A) lateral (B) anterior (C) medial (D) posterior (E) distal (F). Scale bar = 5cm.

3.5.2.5.4 ?manual ungual phalanx

One partial ?manual ungual phalanx was preserved (Fig. 30). Out of all the six preserved manual elements, this has the highest degree of damage and is missing the distal end. It preserves slight flexor tubercles on the lateral and medial surfaces.

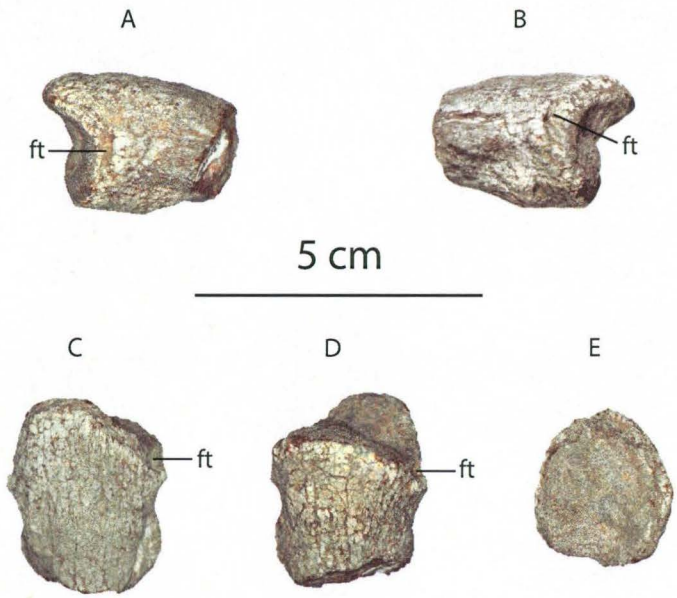

Figure 30: BP/1/7811 ?manual ungual phalanx. Lateral (A) medial (B) posterior (C) anterior (D) posterior (E). Abbreviations: ft, flexor tubercle. Scale bar = 5 cm.

3.5.2.6 Ilium

The single left ilium (Fig. 31) has undergone severe pre- and post-depositional damage on all surfaces, although the majority of the damage is restricted to the medial surface. The element is heavily fractured and is missing most of the preacetabular process as well as a portion of the dorsal iliac blade.

The lateral surface of the ilium (Fig. 31 B) is slightly concave, primarily due to the strong mediolateral thinning of the iliac blade above the laterally projecting supracetabular process. What remains of the preacetabular process indicates that this feature pointed anteriorly, lacking the dorsoventral expansion seen in more derived sauropods (e.g., *Tazoudasaurus*, *Mamenchisaurus*, *Shunosaurus*) (Allain et al., 2004; Young, 1954, Dong et al., 1983).

The anterior iliac blade (Fig. 31 A) connecting the preacetabular process to the postacetabular process is mediolaterally thin with a slight bulge at the midpoint between the two processes that may be associated with the *m. iliofibularis* (Ezcurra, 2010). The blade runs roughly at same height as the preacetabular process and the dorsal margin of the blade is slightly concave in lateral view, with most of the concavity restricted to the anterior portion. Consistent to the plesiomorphic condition of most nonsauropodan sauropodomorphs, this blade sits low and is anteroposteriorly elongate, but not quite to the extent seen in NMQR 4125 (McPhee & Choiniere, 2016).

Despite some minor erosion, the postacetabular process is quite complete, being sub-rectangularly shaped, though not to the degree seen in *Efraasia* (Galton, 1973). In lateral and medial views with the posteroventral corner is sharper than the posterodorsal corner. This process extends posteriorly for approximately 40% of the distance between the pubic and ischial peduncles (Table 3).

The posterior surface of the postacetabular process (Fig. 31 D) does not possess a distinct brevis fossa. However, there is a slight brevis crest extending from the mediolateral edge of the element connecting the postacetabular process to the proximal end of the posterior surface of the ischial peduncle.

The pubic peduncle is a robust strut of bone that curves anteriorly and forms the anterior portion of the acetabulum, bearing a lacriform outline in posterior view (Fig. 31 C). The medial surface extends posteriorly and creates a thin acetabular wall.

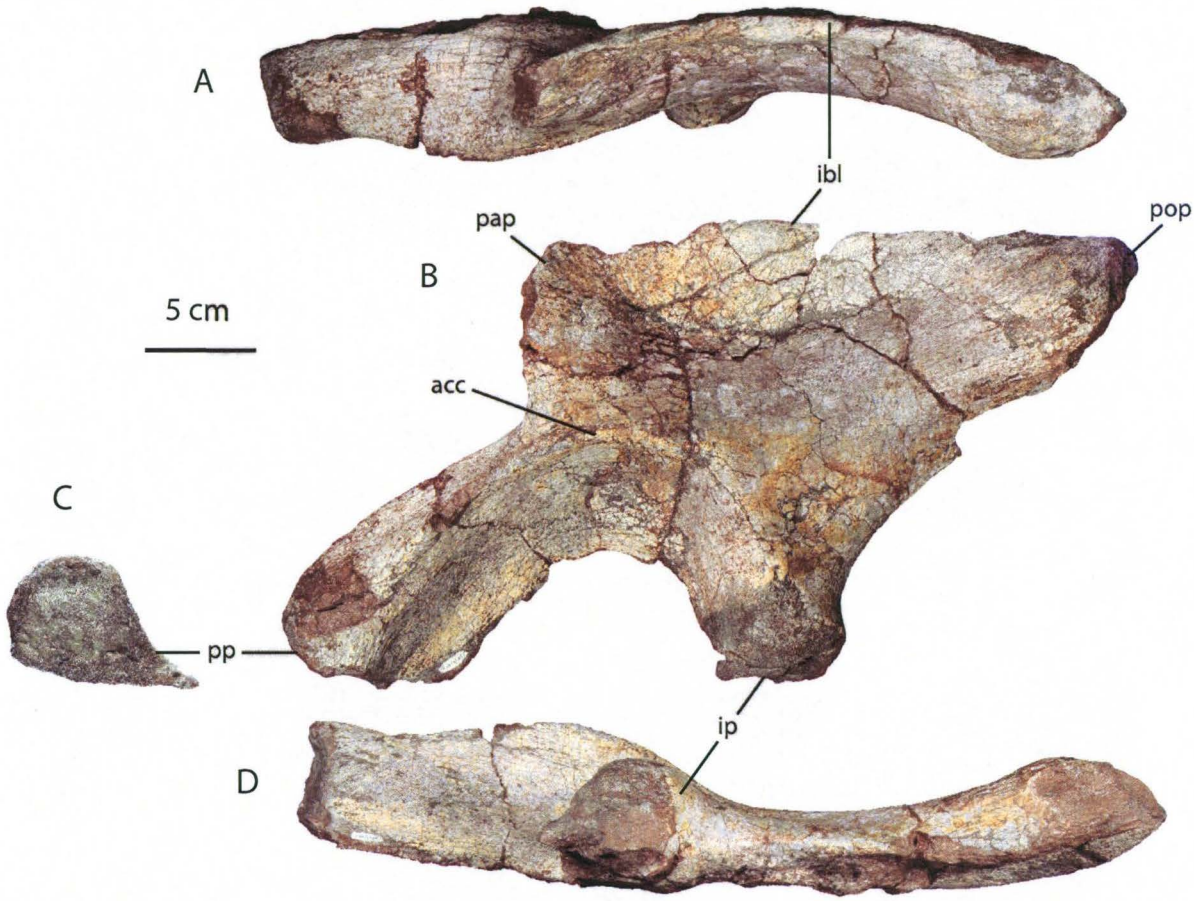

Figure 31: BP/1/7811, left ilium. Anterior (A) lateral (B) posterior pubic peduncle (C) posterior (D). Abbreviations: acc, acetabular crest; ip, ischial peduncle; ibl, iliac blade; pap, preacetabular process; pop, postacetabular process; pp, pubic peduncle. Scale bar = 5 cm

The ischial peduncle is mediolaterally thinner and less anteriorly extensive as well as having a subrectangular distal outline. It is slightly shorter than the pubic peduncle, which is the common condition for nonsauropod sauropodomorphs (Apaldetti et al., 2012). Both peduncles lack the extreme dorsoventral reduction seen in true sauropods where the pubic peduncle is highly extensive (Lü at al., 2007; Peyre de Fabregues & Allain, 2016).

The acetabular crest sits high leaving room for a strongly projected sloping acetabulum. This feature extends all the way to the pubic peduncle. The morphology of this crest is shared with all basal sauropodomorphs (e.g., *Plateosaurus*, *Plateosauravus*, *Riojasaurus*) (Bonaparte, 1969; Bittencourt et al., 2012), excluding the basal most members of the group.

3.5.2.7 Pubis

The left and right pubes were preserved in BP/1/7811 (Fig. 32). Both elements are heavily fractured and have undergone a similar degree of erosional damage. Most features were preserved, but neither bone preserved the ischial peduncle. The medial margin of the pubic apron is also partially damaged/lost.

Similarly seen in most basal sauropodomorphs, the pubis is elongate and slender (Martínez & Alcober, 2009). The pubes were not found conjoined (Fig. 5), but there is enough of the two elements preserved to show that the combined mediolateral width of the two elements would have been less than their individual proximodistal lengths (Table 3). This is the expected condition for more basal sauropodomorphs (*Antetonitrus* [BP.1.4952] *Coloradisaurus*, NMQR 1551) (McPhee et al., 2014; Fabrègues & Allain, 2016).

The proximal outline of the pubis (Fig. 32 D) is sub-rectangular with rounded edges and a flat iliac peduncle. The proximal length is greatest mediolaterally on this surface. In this view, the medial symphysis flairs out posteromedially.

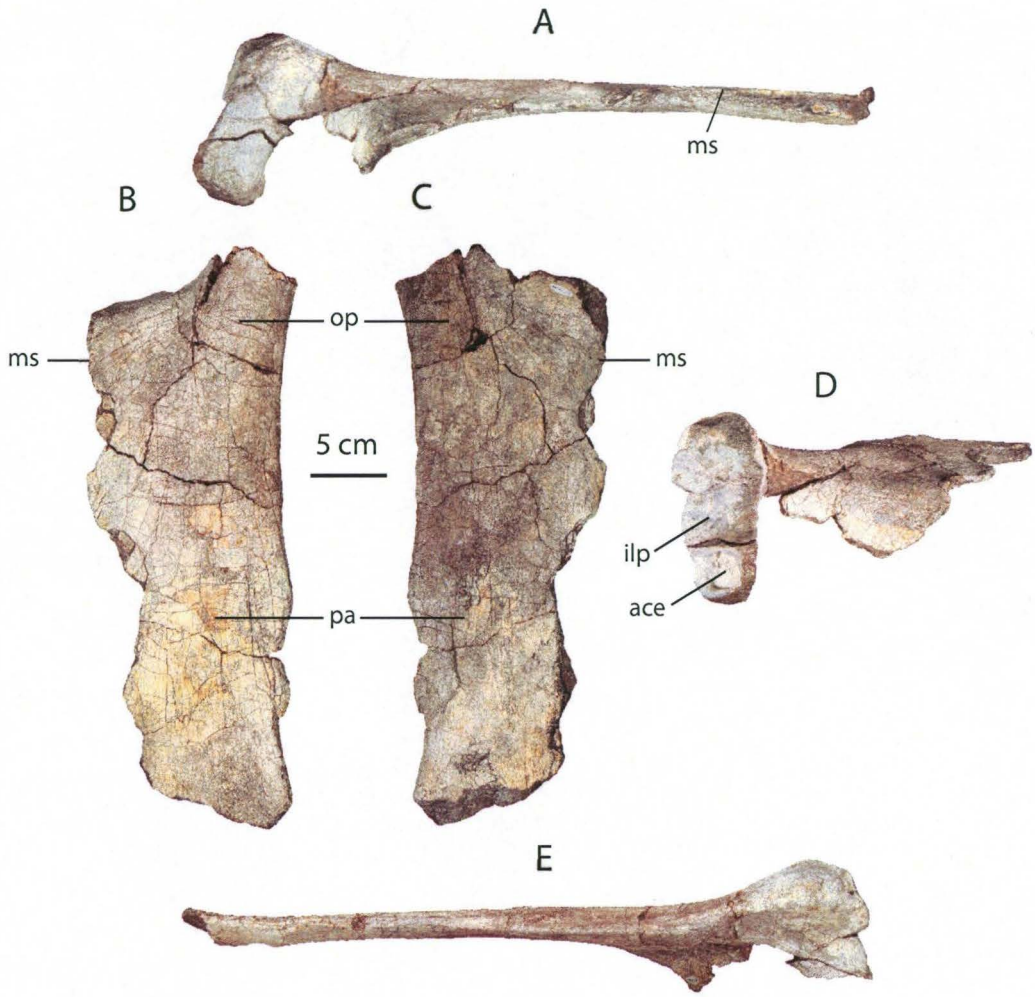

Figure 32: BP/1/7811, left pubis. Posterior (A) medial (B) lateral (C) proximal (D) anterior (E). Abbreviations: ace, acetabulum; ilp, iliac peduncle; ms, medial symphysis; op, obturator plate; pa, pubic apron. Scale bar = 5 cm

Overall, the pubic plate is relatively thick in comparison to the pubic apron in anterior and posterior views (Fig. 32 A&E) where it progressively thins distally. The large obturator foramina, which extends proximodistally and is sub-ovular in shape, is partially preserved and visible on the medial and anterior surfaces. The acetabular process is visible on the posteromedial surface but is not well defined. The ischial peduncle would have been visible on all surfaces but this feature did not preserve in BP/1/7811.

Below the obturator foramina lies a mostly flat, transversely oriented pubic apron that runs proximodistally straight and anteroposteriorly wide, which is the noted plesiomorphic condition for basal sauropodomorphs (McPhee et al, 2014). The overall medial surface of the pubis is convex proximally with the pubic apron flaring out anteromedially. This convexity tapers out into flatness as it progresses distally along the apron. The triangular outline of the iliac peduncle is visible in this view and is set medially to the pubic apron, which in turn makes a strong inflection both proximally and medially.

The lateral surface of the pubis is also convex. The proximal section on this surface has been compressed and damaged. Also on the lateral surface bears a long, shallow, U-shaped line running proximomedially to mediodistally, which is possibly indicative of predation (Fig. 11 B).

The posterior surface is heavily damaged along the proximodistal length of the pubic apron but a slight lateral twist can be observed in this view. Despite this twist, the proximodistal length is fairly straight and lacking concavity, the presence of which is seen as a primarily Massospondylidae trait (Galton & Upchurch, 2004). In anterior view the pubic apron significantly less damaged than the posterior surface.

3.5.2.8 Femur

A single left femur (Fig. 33) was found in situ. The femur is nearly complete and undistorted, but the distal ends have some pre-diagenetic erosion and some abrasion due to excavation.

The femur is robust and elongate, with measurements similar to those observed in NMQR 3314 and NMQR 1551 (Table 3). Consistent with the majority of sauropodiform taxa, the element is relatively straight in lateral view (e.g., *Camelotia, Antetonitrus*) (Galton, 1984; McPhee et al., 2014). Along the lateral margin of the anterior surface, the element in entirely straight. The humeral/femoral ratio for BP/1/7811 is consistent with taxa like *Antetonitrus* and *Lessemsaurus.*

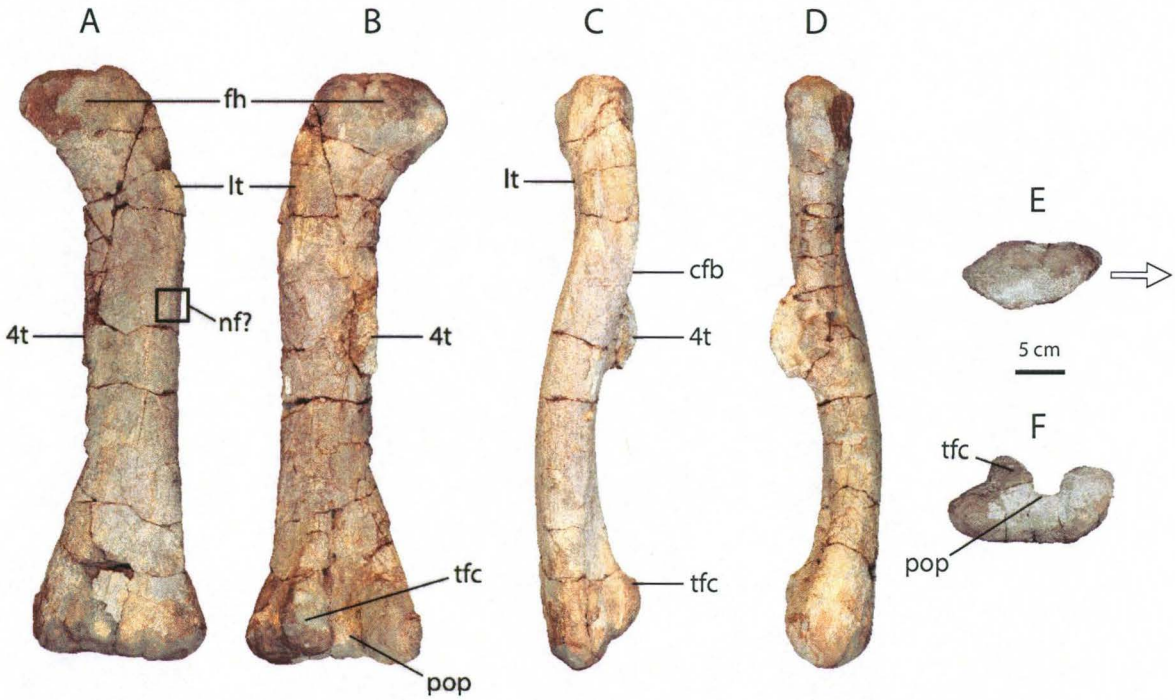

Figure 33: BP/1/7811, left femur. Anterior (A) posterior (B) lateral (C) medial (D) proximal (E) distal (F). Abbreviations: 4t, fourth trochanter; cfb, M. caudofemoralis; fh, femoral head; lt, lesser trochanter; nf, nutrient foramina; pop, poplitral fossa; tfc, tibiofibular crest. Arrow points medially. Scale bar = 5 cm

The proximal surface of the femoral head (Fig. 33 E) is well-rounded and convex, similar to other basal sauropods as well as basal eusauropods (Galton & Upchurch, 2004; Otero et al., 2015). In proximal and anterior views (Fig. 33 A), the head is medially oriented. This is the condition for all sauropodomorphs with the exclusion of basal most sauropodomorphs (e.g.,

Saturnalia, Thecodontosaurus, Efraasia) (Langer et al., 1999; Benton et al., 2000; Yates, 2003; Otero & Pol, 2013).

The lesser trochanter is positioned on the anterior surface (Fig. 33 A) of the femur is distal to the greater trochanter and very close to the lateral margin of this surface. It is an augen-shaped feature that has a proximodistally oriented long axis. Similar to *Eucnemesaurus*, *Riojasaurus*, and NMQR 3314 this feature is higher as it extends out laterally than it is proximodistally wide (Table 3) (Galton & van Heerden, 1985; McPhee et al., 2015b). Laterally, situated below the lesser trochanter and above the fourth trochanter is a large, proximal deflecting nutrient foramen (Fig. 33 A). Similar foramina are also found on the humeri of BP/1/7811 (Fig. 24) (Seymour et al., 2012; Allan et al., 2014).

The fourth trochanter straddles the midpoint of the shaft and is visible in all views excluding anterior. In general outline on the lateral and medial surfaces, the fourth trochanter is asymmetrically sub-crescentic and is straight proximodistally, with its distal margin forming a steeper right angle with the femoral shaft than is seen along the proximal margin. This morphology is similar to other non-sauropodan sauropodomorphs (e.g., *Lessemsaurus*, *Plateosaurus*) (Galton, 1998; Bonaparte, 1999). The poor preservation of the fourth trochanter in NMQR 3314 and NMQR 1551 prohibits comparison with these specimens. In medial view at the anterodorsal base of the forth trochanter the attachment for the m. caudofemoralis longus is visible as a small fossa (Langer, 2003; Ezcurra, 2010).

The femoral shaft is sub-ovoid in cross-section and is much flatter anteroposteriorly, which is similar to taxa like *Aardonyx*, *Camelotia*, and *Vulcanodon* (Raath, 1984; Galton & van Heerden, 1985; Yates et al., 2010). This condition differs in taxa like *Plateosaurus*, *Yunnanosaurus*, and *Massospondylus* where the cross-sectional shape is more sub-circular (Young, 1942; Yates & Kitching, 2003).

Both distal condyles are mediolaterally expanded and slightly anteroposteriorly flattened. The tibiofibular crest is an oval feature that projects strongly, which differs from taxa like *Antetonitrus* and other more derived taxa where the crest is more reduced (McPhee et al., 2014; Fabrègues & Allain, 2016). This crest makes a right angle with the posterior surface as it extends outwards. The lateral condyle projects slightly more from the margin of the distal end than in the medial condyle. The medial condyle is a bulbous feature, especially in medial view. The popliteal fossa cuts in a deep U-shaped valley and trends laterally towards the tibial condyle.

3.5.2.9 Tibia

The left tibia (Fig. 34) is weathered but is well-preserved and lacking obvious distortion. The weathering is primarily centralized around the proximal (Fig. 34 E) and distal (Fig. 34 F) ends of the elements. The tibia is approximately 75% the proximodostal length of the femur (Table 3), which is the pleisomorphic condition exhibited by earlier branching taxa (Martínez & Alcober,

2009). The element is proximodistally straight in lateral and medial views, but bows laterally slightly in anterior view.

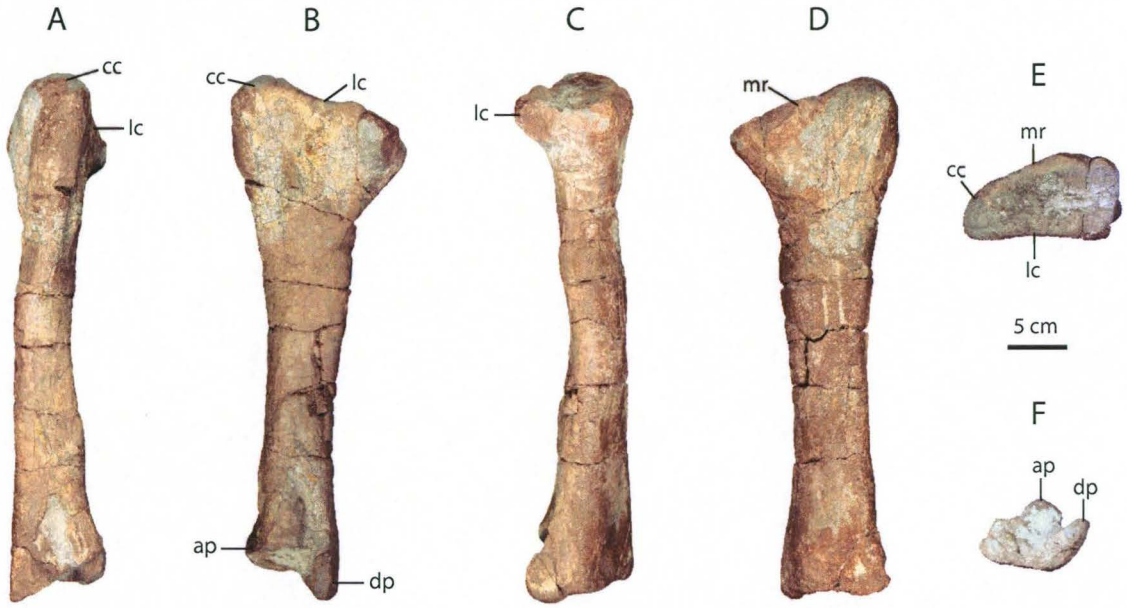

Figure 34: BP/1/7811, left tibia. Anterior (A) lateral (B) posterior (C) medial (D) proximal (E) distal (F). Abbreviations: ap, ascending process; cc, cnemial crest; dp, descending process; lc, lateral condyle; mr, medial ridge. Scale bar = 5 cm

The proximal surface (Fig. 34 E) of is sub-ovoid in outline. The fibular condyle is a bulbous feature in this view, and its posterior margin is anterior to the level of the posterior margin of the medial condyle. This differs strongly from the more symmetrically developed, typically triangular proximal outline of the tibiae of massospondylids (Galton, 1990; Bonaparte, 1978).

The region of the lateral surface between the cnemial crest and the fibular condyle is shallowly concave laterally, but much less so than the condition in *Antetonitrus* (McPhee et al., 2014). Visible on the proximal surface, the cnemial crest projects laterally. The anteroposterior length (Table 3) of the proximal surface is almost twice as long as it is wide, which is a typically derived

ratio within the tibiae of sauropodomorphs (e.g., *Blikanasaurus*, *Pulanesaura*, *Tazoudasaurus*) (Galton & van Heerden, 1985; Allain et al., 2004; Ezcurra & Apaldetti, 2011; McPhee et al., 2015b).

The tallest point of the cnemial crest sits close to the proximal end of the crest where it projects proximally above the level of the rest of the proximal surface and slopes laterally in anterior view. In contrast, the tallest point of the cnemial crest in taxa like *Vulcanodon* is located closer to the proximodistal midpoint of the crest (Raath, 1972). There is no paramarginal ridge present, as in most other sauropodomorphs except for several Chinese genera: *Jingshanosaurus*, *Lufengosaurus*, and *Yunnanosaurus*.

The tibial shaft in ovoid in cross-section, being slightly mediolaterally compressed. At the midpoint of the shaft, the element is at its smallest circumference (Table 3) but is gradually expansive as it progresses proximally and distally.

In anterior view (Fig. 34 A), the anterolateral process is steeply raised. Although this portion of the bone suffered the most damage overall, it is clear that the anterolateral process did not extend laterally beyond the lateral margin of the posterolateral process. The lateral notch between the anterolateral process and posterolateral process has been heavily eroded. Despite the damages, the lateral notch is observable as a U-shaped feature with a similar degree of depth to taxa like *Adeopapposaurus*, *Coloradisaurus*, and *Riojasaurus* (Martínez & Alcober,

2009; Ezcurra & Apaldetti, 2011). The distal outline is sub-rectangular, with a strong lateral projection of the posterolateral process.

3.5.2.10 Fibula

Two fibulae are present in the assemblage (Fig. 35). The right was found associated with the ilium, pubes, femur, tibia, and several dorsal vertebrae. The left was collected half a meter away but still from the same unit of deposition as the rest of the hindlimb (see Taphonomy and Fig. 5). Based upon agreement in size, preservation, and association, it is presumed that both fibulae come from the same individual.

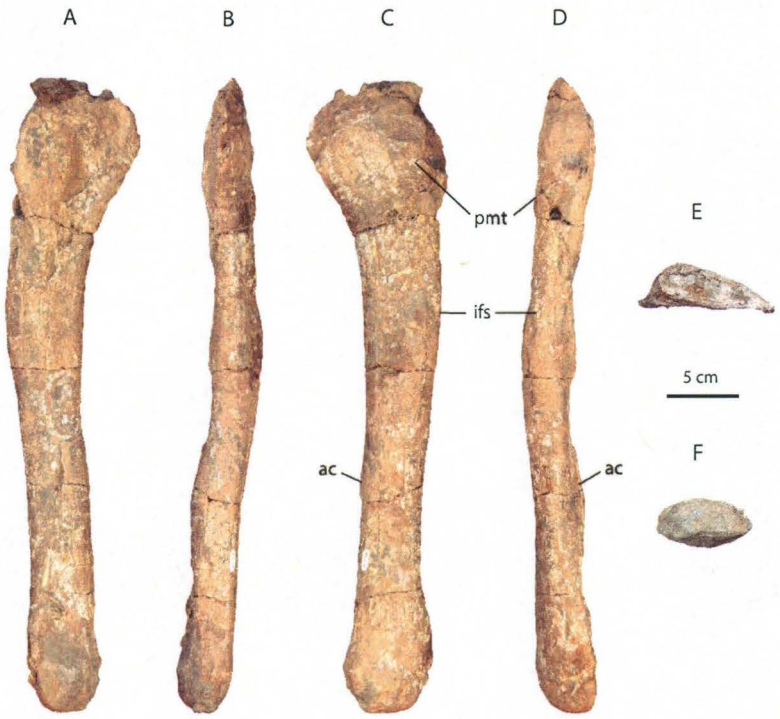

Figure 35: BP/1/7811, right fibula. Lateral (A) medial (B) anterior (C) proximal (D) distal (E). Abbreviations: ac, anterior crest; ifs, iliofibularis scar; mpt, proximomedial tubercle. Scale bar = 5 cm

The proximal surface (Fig. 35 E) of both fibulae is heavily eroded but would have been laterally convex as that is the plesiomorphic state. The medial surface of the proximal end bears a small proximomedial tubercle that would have touched the fibular notch of the tibia (Gray, 1918). This feature is only slightly raised from the medial surface and positioned slightly posterior to the midline. Like other non-sauropodan sauropodomorphs (e.g., *Coloradisaurus*, *Lufengosaurus*, Massospondylus) the medial surface is smooth and lacks rugose pitting (Young, 1942; Bonaparte, 1978; Botha-Brink et al., 2012). The lateral surface bears a low, U-shaped ridge the borders the concave medial region.

The sub-ovoid shaft of the fibula is bowed both anteroposteriorly and mediolaterally. The anterior margin of the shaft is shallowly convex (which could be in part a product of crushing), particularly towards the proximal end in the region of the raised and pronounced *m. iliofibularis* scar. The insertion point of the *m. iliofibularis* does not have rugose pitting. This feature is probably homologous with the trochanters seen in the fibulae of *Vucanodon* and *Tazoudasaurus* (Raath, 1984; Allain et al., 2004; McPhee et al., 2014).

The lateral surface (Fig. 35 A) of the fibular shaft is shallowly concave, bowing away from the shaft of the tibia, which is plesiomorphic for basal sauropodomorphs. While the bowing doesn't appear to be artificial, the degree of curvature could be a result of postdepositional compaction.

The medial margin of the proximal end of the fibula scribes a sigmoidal line in proximal view (Fig. 35 E). The mediolaterally broadest portion of this shape is located close to the posterior margin of the proximal end, and the more anterior portion of the medial margin tapers sharply in breadth. The medial surface of the distal end is displaced towards the anterior side of fibula and grades gradually into the distal end. It is bounded anteriorly by a low ridge of bone that eventually reaches and forms an anteriorly projecting feature, which appears to extend to the distal end of the element.

The distal end (Fig. 35 F) of the fibula has an ovoid outline in distal view. It is subtly expanded from the shaft both anteroposteriorly and mediolaterlly. It possesses the flattened, teardrop shape and prominent medial projection that is shared by other basal sauropodomorphs (Galton & van Heerden, 1998; Otero et al., 2015). There is a shallow anteromedial fossa on the distal articular surface. Due to weathering, it cannot be determined how hollowed out this feature would have been.

3.5.2.11 Pes

A right pedal ungual (Fig. 36) was the only element preserved from the pes. It is heavily fractured and missing the distal tip. The overall shape of this element is shallow and pointed, completely lacking the sickle shape and recurving observed in *Vulcanodon* (Cooper, 1984; Bonnan, 2005; McPhee et al., 2014), the absence of which is characteristic of sauropodomorphs more basal than *Vulcanodon* and *Tazoudasaurus* (Pol et al., 2011).

The element has slightly convex anterior sides as well as a broad anterior surface, which is a condition seen in more derived nonsauropodan sauropodomorphs (e.g., *Antetonitrus*, *Blikanasaurus*, NMQR 3314). The proximal articular surface of the ungual has a medially deflecting intercondylar groove. The outline of the proximal surface (Fig. 36 E) is sub-ovoid and is mediolaterally compressed with the mediolateral width decreasing dorsally. The wider posterior end (Fig. 36 C) has a small flexor tubercle towards its anterior edge.

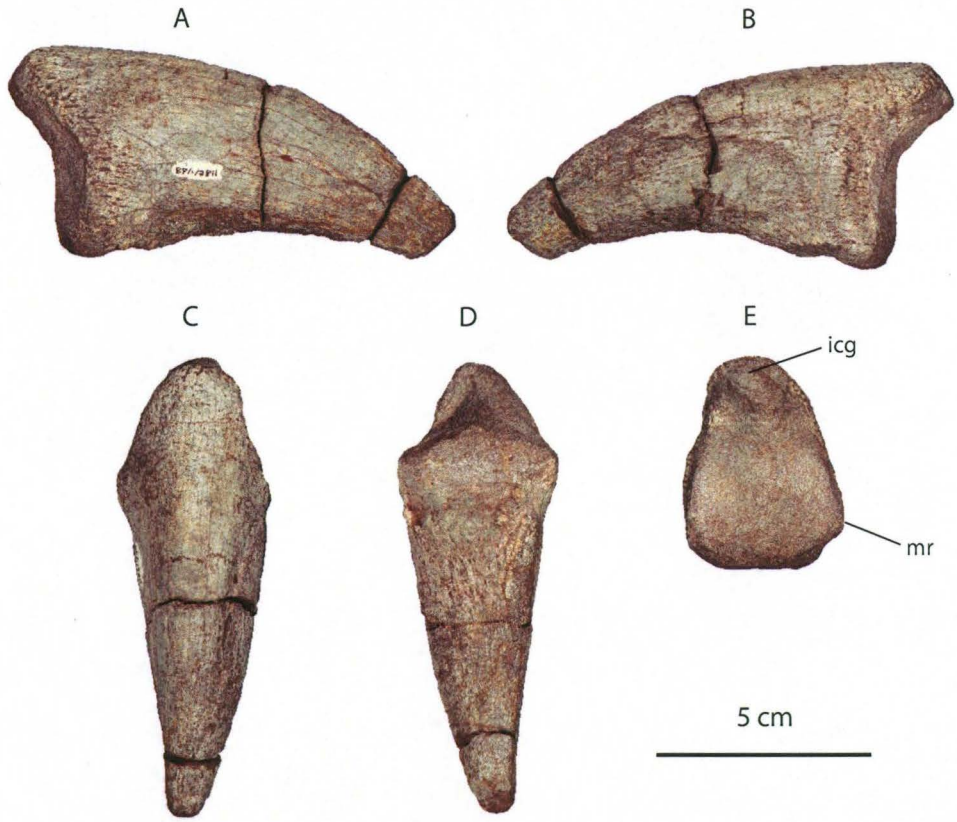

Figure 36: BP/1/7811, right pedal ungual. Lateral (A) medial (B) posterior (C) anterior (D) posterior (E). Abbreviations: icg, intercondylar groove; mr, medial ridge. Scale bar = 5 cm

In lateral and medial view, the intercondylar groove extends past the ventral edge, further than seen in taxa like *Leonerasaurus* (MPEF-PV 1663). Also visible on these surfaces is a proximodistal medial line, interrupted intermittently by shallow cavities, situated at the midpoint between the anterior and posterior margins.

Lateral deflection is seen on the dorsal and ventral surfaces of the ungual proximodistally, opposite to the medial deflection of the intercondylar groove. This deflection becomes more developed in eusauropods (Bonnan, 2005; McPhee et al., 2014).

3.6 Taxonomy

The newly discovered BP/1/7811, based upon a number of features, may have once been referred to the genus, *"Melanorosaurus"* (e.g., a high humerus-femur ratio, derived femoral morphology). However, due to the possible *nomen dubium* status of *"Melanorosaurus"*, such a referral is not possible.

Within the specimens currently assigned to *"Melanorosaurus"*, there is the syntype series (SAM-PK 3449-3450, SAM-PK 3532 referred) and the Bloemfontein pair (NMQR 1551, NMQR 3314). *"Melanorosaurus" (Meroktenos) thabanensi* (MNHN.F.LES16) has recently been removed (de Fabrègues & Allain, 2016). A detailed history for each can be found in Ch. 1 (*Lower Elliot Taxa Taxonomy and Legitimacy*).

The syntype series is problematic because the primary material comes from two separate localities and might contain other disassociated material (Galton et al., 2005, McPhee et al., 2015a; de Fabrègues & Allain, 2016). It is likely that material is chimaeric, and it was excluded from the phylogenetic analyses (although still used in anatomical comparisons) and I recommend that it be omitted from all future analyses seeking to understand sauropodomorph relationships. The referred "*Melanorosaurus*" assemblage SAM-PK-3532 (Haughton, 1924), has a limited amount of dissociated material with poor provenance data. For these reasons, it was also excluded from phylogenetic analysis.

These problems with the syntype and older referred material have led more recent authors to use newer, more complete referred material as their exemplar for "*Melanorosaurus*". In the most recent analysis (McPhee et al., 2017), this was restricted to the referred specimens: NMQR 1551 and NMQR 3314. These two assemblages are considered to be monospecific but have been revealed to have some character conflicts as well as being stratigraphically incongruent (McPhee et al., 2017).

The referral of NMQR 1551 and NMQR 3314 to "*Melanorosaurus*" is anatomically problematic anatomically. A monograph on the postcranial anatomy of "*Melanorosaurus*" has never been produced and instead is based off of observed features informally mentioned within the literature: deep and thin hyposphenes on dorsal vertebrae, a sacrum composed of four vertebrae, anterior caudal centra with a ventral longitudinal sulcus (SAM-PK-3349/3350), a shallow radial fossa, the position of the lesser trochanter on the anterior femoral surface, and a

relatively straight femur in mediolateral views (Yates, 2003; Yates et al., 2007 a&b; McPhee et al., 2015b, 2017).

Differing from "*Melanorosaurus*", NMQR 1551 possesses more dorsoventral vertebrae, a highly compressed first caudal centrum, a sub-rounded caudal margin of the postacetabular process of the illium, and a relatively flat distal articular surface of the astragalus. It is lacking a hyposphenal ridge on any of the caudal vertebrae observable in the syntype.

NMQR 3314 differs from "*Melanorosaurus*" by possessing a minimally-developed, rounded humeral head, having a deltopectoral crest between 30-50% of the length of the humerus, the medial deflection of the proximal ulna, a smaller transverse tibial width, and a smaller third metatarsal. On these grounds, NMQR 1551 and NMQR 3314 cannot be assumed to be *"Melanorosaurus"*.

BP/1/8711 and NMQR 1551 have precise, definitive provenance data showing that they are from the LEF, and thus likely Rhaetian in age. Despite being near-contemporaries (their exact positions within LEF stratigraphy have yet to be worked out), the two specimens differ in several key ways. Most of these differences are found within the dorsal vertebrae, where BP/1/7811 shows signs of incipient skeletal pneumaticity (Wedel, 2003), but also relate to BP/1/7811's robusticity of the scapula and the sub-crescent shape of the femoral 4th trochanter. For the purpose of this study, they are included in the analysis but they are not considered to be their own, separate entities and not as referred "*Melanorosaurus*" specimens.

All MPTs (summarized as a strict consensus in Fig. 37) posit a position for BP/1/7811 as a member of a monophyletic clade formed with NMQR 1551 and NMQR 3314 that is in turn nested outside of Sauropoda but within Anchisauria (Galton & Upchurch, 2004; Yates, 2010). The exact nature of the relationships between these three specimens is unresolved.

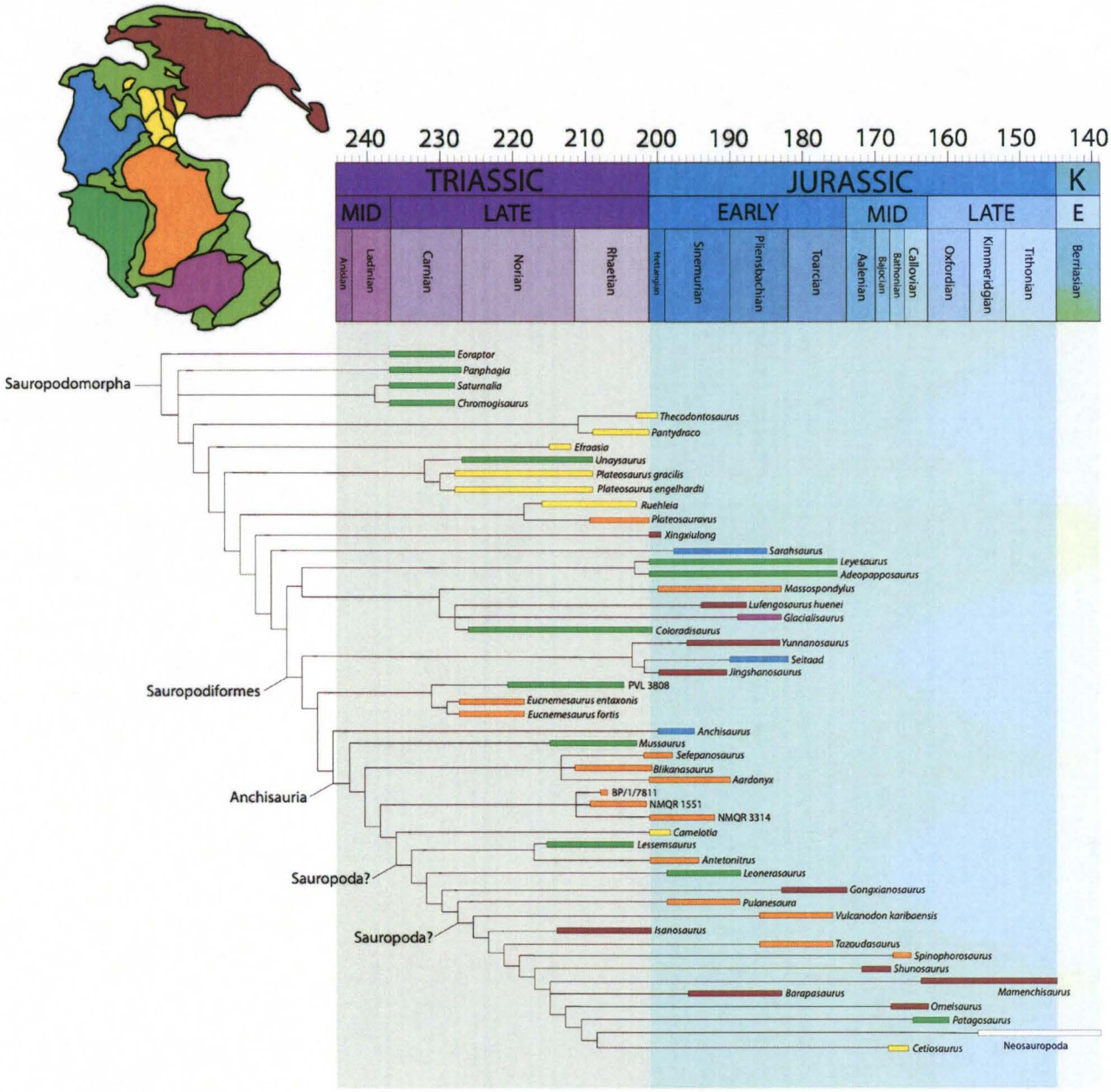

Figure 37: Time-calibrated strict consensus including the position of BP/1/7811. Colors from Triassic world map show modern continents and correlate with each bar adjacent to taxa.

3.7 Phylogenetics

The analysis resulted in the recovery of 12 most parsimonious trees (MPTs) with a CI of 0.330 and an RI of 0.693) (Fig. 37) with BP/1/7811 forming a clade with NMQR 1551 and NMQR 3314. This relationship is supported by Character 180 (0 →1): Shape of the iliac articular facets of the first primordial sacral rib, Character 255 (0 → 1): Length of the preacetabular process of the ilium, and Character 305 (0 → 1): Well-developed tibiofibular crest on distal femur.

3.8 BP/1/7811 Differentiation

3.8.1 BP/1/7811 vs. NMQR 1551

While quite similar, BP/1/7811 and NMQR 1551 differ in some key features. The height of the hyposphenes in the dorsal vertebrae are slightly shorter in BP/1/7811 (158), NMQR 1551 does not possess an accessory lamina (162) nor does it show potential excavation within the dorsal neural arches (163), the scapula is more robust in BP/1/7811 (203) than in NMQR 1551 (and NMQR 3314), and the shape of the 4th trochanter differs slightly between the two with NMQR 1551s being more symmetrical (300).

3.8.2 BP/1/7811 vs NMQR 3314

As to expected of two animals living in separate time periods, there are several key differences between NMQR 3314 (UEF) and BP/1/7811 (LEF). NMQR 3314 lacks the anterior spur-like projections seen on the neural spines of the two preserved cervical vertebrae of BP/1/7811 (139) and has a proportionally shorter humerus than BP/1/7811. The shape of the anterior centrum face is also more flattened in NMQR 3314. NMQR 3314 has a slightly larger humerus/femur ratio than BP/1/7811 (208) and also has the faint presence of a brevis fossa on the ilium (262).

3.8.3 BP/1/7811 vs *Plateosauravus*

Plateosauravus (SAM 3341-45, 3345, 3348. 3350, 3356, 3602, 3603) differs from BP/1/7811 and NMQR 1551 slightly in the height of the hyposphenes within the dorsal vertebrae, being less the height of the neural canal (158). Like NMQR 1551, *Plateosauravus* lacks accessory lamina dividing the posterior fossae from the postzygapophyses (162) as well as an absence of potential excavation within dorsal neural arches (163). Also different from BP/1/7811 is the absence of a longitudinal ventral sulcus on the middle caudal vertebrae (192). NMQR 1551 has a sub-square shaped caudal margin on the postacetabular process of the ilium, which is more pointed ventrally in NMQR 3314 (264). In the first and third metatarsals, the two taxa differ in size with NMQR 3314 exhibiting a more robust condition (341, 349).

3.8.4 BP/1/7811 vs. *Sefapanosaurus*

Unlike BP/1/7811, *Sefapanosaurus* has epipophyses overhanging the rear margin of the postzygapophyses (138), the presence of which is fairly rare in basal sauropodomorphs. *Sefapanosaurus* has dorsal vertebrae hyposphenes, but they are shorter than those seen in BP/1/7811 (158). The presence of accessory lamina (162) and potential dorsal excavation are not found in *Sefapanosaurus* - these features are relatively specific to BP/1/7811 within this grade of animals. The shape of the posterior dorsal neural canal in *Sefapanosaurus* is slit-shaped, which is an unusual shape for Sauropodiforms (167). Most notably, *Sefapanosaurus* differs from BP/1/7811 (and other similar animals) in the metacarpals. The shape of the first metacarpal in *Sefapanosaurus* is more of a square shaped element with BP/1/7811 having a less robust structure (232). The two also differ in the shape of the second and third metacarpal of *Sefapanosaurus* is trapezoidal (236).

The femur of *Sefapanosaurus* is dissimilar to BP/1/7811. *Sefapanosaurus* has a subcircular femoral cross-section, contrasting with the more elliptical cross-section seen in BP/1/7811 (287). It also differs in the position of the lesser trochanter, with *Sefapanosaurus*'s being located anteriorly (296) and obscured entirely in posterior view (297). In addition, distinctive of *Sefapanosaurus* is the shape of the proximal articular surface of the tibia, having a transverse width subequal to its anteroposterior length (313).

3.8.5 BP/1/7811 vs. *Eucnemesaurus*

Eucnemesaurus fortis and *Eucnemesaurus entaxonis* have a much larger suit of character differences than any of the other taxa discussed above. *Eucnemesaurus entaxonis* does not have the laterally expanded spine tables seen in BP/1/7811 (150). It does, along with *Eucnemesaurus fortis* have hyposphenes present in dorsal vertebrae, but these are taller in BP/1/7811. BP/1/7811's distinctive accessory lamina (162) are partially seen in *Eucnemesaurus fortis,* as is a degree of pneumatic excavation (163). *"Eucnemesaurus"* does not have the longitudinal ventral sulcus seen in the caudal of BP/1/7811 (192). The shape of the distal caudal centra in *Eucnemesaurus fortis* is more oval shaped than the condition observed within *"Melanorosaurus"* and in BP/1/7811 which appear as more square-shaped features (194). *Eucnemesaurus entaxonis* has a well-developed brevis fossa that is absent in NMQR 1551 and BP/1/7811 (262). This feature is partially present in NMQR 3314.

The femoral characters of *"Eucnemesaurus"* differ greatly from BP/1/7811. *Eucnemesaurus fortis* has a subcircular cross-section (287), and both *Eucnemesaurus* genera have a well-developed swelling on the posterior margin of the femoral head, which is much more reduced in BP/1/7811 (290). *"Eucnemesaurus"* has a more robust lesser trochanter than BP/1/7811 (295) and the lesser trochanter is placed more anteriorly (296), being invisible in posterior view (297). The forth trochanter of *"Eucnemesaurus"* is rounded (301), unlike the subrectangular shape seen in NMQR 1551, *Plateosauravus*, *Sefapanosaurus*, and BP/1/7811. *"Eucnemesaurus"* also has extensor depressions on the anterior surfaces of the distal femora (303). *Eucnemesaurus entaxonis* does not have the wider tibiofibular crest of NMQR 1551, NMQR

3314, or BP/1/7811 (306). Out of the taxa discussed above, "*Eucnemesaurus*" is the most dissimilar to BP/1/7811.

Chapter 4: Systematics

4.1 Systematic paleontology

Dinosauria: Owen, 1842

Saurischia: Seeley, 1887

Sauropodomorpha: von Huene, 1932 *sensu* Galton & Upchurch, 2004

Massopoda: Yates, 2007

Sauropodiformes: Sereno, 2007

4.2 *Gen. et. Spec. nov.*

TO BE NAMED LATER

4.3 Holotype:

BP/1/7811; associated partial postcranial skeleton (individual animal): 2 cervical vertebrae, 7 dorsal vertebrae, 1 caudal vertebra, 1 left scapula, both humeri, 1 distal right radius, 1 proximal left radius, portion of a left manus, both pubes, 1 left femur, 1 left tibia, both fibulae, and a left? pedal ungual.

4.4 Type Locality:

BP/1/7811 was collected from an outcrop of LEF in a quarry designated "H5" on the Dreifontein Farm near the town of Roussouw in the Eastern Cape Province of South Africa (Fig. 5). Regionally, the LEF records perennial meandering channels and point bar sandstones embedded in mudstones of a broad alluvial plain (Visser & Botha, 1980; Eriksson, 1985; Smith et al., 1993; Bordy et al., 2004a, b; Bordy & Eriksson, 2015; Viglietti & Dinter, 2016).

4.5 Horizon and Age:

BP/1/7811 was preserved in gray silty overbank mudstone between two sandstone units within the Lower Elliot Formation (Fig. 3). The Elliot Formation covers the Norian to Sinemurian stages of the Triassic and Jurassic as represented in South Africa and Lesotho (Bordy et al., 2004c). The Elliot Formation is a member of the sedimentary Stormberg Group, which is part of the larger Karoo Supergroup (Smith et al., 1993).

4.6 Diagnosis:

BP/1/7811 is a large, intermediate non-eusauropod sauropodomorph (=Sauropodiform) dinosaur specifically diagnosed by the following unique combination of features: the presence of accessory lamina dividing the posterior fossae from the postzygapophyses, the concave shape of the anterior centrum face, the presence of hyposphenes in the dorsal vertebrae – specifically being less than the height of the neural canals, the presence of accessory lamina

dividing the posterior fossae from the postzygapophyses, the equivocal pneumatic excavation of the dorsal neural arches, the increased width of the scapula, the pronounced tubercle on the anterolateral corner of shaft of the second metacarpal just below the proximal surface, and the absence of an extensor depression on the anterior surface of the distal end of the femur.

Chapter 5: Discussion

5.1 Taphonomy

The blunt gnawing bite marks found on the pubes (Fig. 11) are consistent with predation or scavenging (Schwimmer, 2010). Known carnivores at the time of deposition limit the predator or scavenger to a crocodyliform or theropodan trace maker (e.g., Bonaparte, 1969; Jacobsen, 1998; Bristowe & Raath, 2004; Weishampel et al., 2004; Drumheller et al., 2014). The U-shaped score mark in lieu of a V-shaped score found on the right pubis is more indicative of a crocodyliform trace maker, but due to the faintness of the marks, does not entirely rule out a different predator (Schwimmer, 2010; Sahle et al., 2017).

There are currently no crocodylomorph body fossils known from the lower Elliot Formation (Dollman et al., 2017). However, globally there have been large bodied sphenosuchians from the Late Triassic (*Redondavenator* and *Carnufex*), so it is possible that crocodylomorphs did exist in South Africa during the Late Triassic but that the remains of these animals have not yet been recovered (Nesbitt et al., 2005; Zanno et al., 2015).

Based upon the provided evidence, predation or scavenging is presumed to have been early on the biostratinomic timeline. The lack of predation or scavenging marks on the other material suggests that predation was minimal after the remaining material came to its final resting site.

While BP/1/7811 has these traces, the cause of death cannot be said with certainty. However, senescence can be ruled out upon the suture scars observable in the vertebral sequence.

The remaining material stayed on the surface after predation or scavenging and ultimately would have lost most surrounding tissue, but likely retained enough soft material to sufficiently hold anatomically proximate elements in close association as it continued to rot on the floodplain. However, it is not likely that material remained on the surface for an extended period of time due to an almost complete absence of surface damage (e.g., wet-rot, root damage, predepositional cracking). The ends of the long bones have a rough texture which is consistent with very minor bone surface weathering and exfoliation. This mild surface weathering is consistent with a single season or less of weathering (Behrensmeyer, 1978), placing it somewhere within Stage 0-1 on the Behrensmeyer Weather Stage chart (Fig. 10). It is possible that the minor bone degradation at proximal and distal ends is due to interfacing between cartilage that rotted around the ends of the bones (Trueta, 1968), which could change this timeline slightly.

Warm temperatures were globally experienced in the Late Triassic (Sellwood & Valdes, 2006). A now fragmenting Pangea experienced polarized wet-dry seasonality due in part to low-pressure systems from the Tethys Ocean (Hounslow & Ruffell, 2006) which was likely associated with monsoons and regular seasonal flooding. However, following the Carnian Pluvial Event (CPE), the Norian experienced an increase in global aridity (Simms & Ruffell, 1989) which can be observed in Late Triassic lower Elliot Formation deposits (Bordy & Eriksson, 2015). This is

supported by the presence of intraformational rip-up clasts in Unit 6 (Fig. 3), the presence of which show intermittent aridity (Glennie, 1998). For rip-up clasts to form, there must be desiccated or partially consolidated mud (possibly mud cracks) near to a river or stream that repetitiously dries and floods but the floods cannot be too high energy to destroy the scoured mud-cracks before deposition (Kindle, 1917; Jackson, 1997).

From the interpreted low-energy depositional environment of H5 (see *H5 depositional environment*), specifically Unit 6 (Fig. 3), along with the nearly random distribution of skeletal remains observed in the rose charts (Fig. 7-9), BP/1/7811 probably died locally rather than having been transported to the quarry by a tributary stream. The overall lack of significant orientation of elements in the H5 Quarry argues against significant transport in a fluvial system, although the northwesterly orientation of the long bones (Fig. 8) may suggest some local reworking and is consistent with an articulated animal falling apart on a floodplain (Behrensmeyer, 1978). The depositional pattern in the H5 Quarry is also consistent with a sudden disaster amplified by predation or current on account of association, the predation/scavenging traces, and the minimal hydraulic sorting (Badgley, 1986).

The mudstone deposit constituting Unit 6 suggests that currents were mostly weak (Aplin et al., 1995), but the upward fining mudstones below the fossil layer could mean that currents were strong at some point, prior to deposition. These small elements are more likely to be preserved within mudstone units in an ephemeral wet-dry system (Levick et al., 2008). From the

experiments conducted on mammalian bones by Voorhies (1969), if substantial transport occurred over a long period of time, these smaller elements are expected to be washed away.

The association, despite the disarticulation, shows that very little transport must have occurred prior to final deposition (Aslan & Behrensmeyer, 1996). The intraformational rip-up clasts surrounding the bones point towards rapid, medium energy deposition of encasing sediments, large enough to reach the floodplain environment, causing rapid burial of the remaining bones but not rapid enough to wash away smaller elements (Voorhies, 1969). This burial would have prevented further winnowing, allowing for fossilization to begin (Schwartz & Gillette, 1994).

5.2 Taxonomic and Phylogenetic Analysis

BP/1/7811 is the most associated and best-preserved non-sauropodan sauropodomorph collected from the LEF to date. However, there is relatively limited overlap between South African LEF non-sauropodan sauropodomorphs, making comparison and phylogenetic analysis more difficult. NMQR 1551, which is penecontemporaneous with BP/1/7811, shares many morphological similarities BP/1/7811, but does not preserve all overlapping elements. Despite the concerns listed above, the grouping of NMQR 1551 and NMQR 3314 with BP/1/7811 in a clade is not unexpected given the anatomical similarities between the three specimens.

Distinguishing BP/1/7811 from the NMQR specimens are the following character states: the presence of accessory lamina dividing the posterior fossae from the postzygapophyses, the

equivocal pneumatic excavation of the dorsal neural arches, the presence of a longitudinal ventral sulcus on proximal and middle caudal vertebrae, the width of the scapula, and the symmetry of the profile of the 4th trochanter of the femur being asymmetrical with a steeper distal slope than the proximal slope and a distinct distal corner. BP/1/7811 is markedly different from other LEF taxa, meriting the erection of a new genus and species.

BP/1/7811 is grouped within Anchisauria primarily due to the anterior visibility of the partially preserved obturator foramen on the pubes (Fig. 32), the humeral/femoral ratio (Table 3), the straightness of the femoral shaft in mediolateral views (Fig. 33 C&D), and the placement of the 4th trochanter on the posteromedial margin of the femoral shaft (Fig. 33) (Galton, 2005). Galton (2005) also included the hourglass-shaped proximal metatarsal II as indicative of Anchisauria, but this element is not preserved in BP/1/7811.

The grouping of Anchisauria is similar to Yate's 2010 cladistic analysis but excludes *Yunnanosaurus* from the clade, placing *Anchisaurus* with Sauropoda. This result is consistent with other recent analyses in that it recovers several monophyletic clades (Plateosauridae and Massospondylidae) within non-sauropodan Sauropodomorpha along the stem leading to Sauropoda (e.g., Yates, 2007b; McPhee et al., 2014; Otero et al., 2015).

The character states that affirm BP/1/7811's non-sauropodan condition include the relatively large humeral deltopectoral crest (Fig. 24), the subtriangular shape of the proximal ulna (Fig.

26), the reduction of the ulnar olecranon process (Fig. 26), an extensive ischial peduncle (Fig. 31), and a relatively large 4th trochanter (Fig. 33).

The character states that place BP/1/7811 within "Melanorosauridae" are seen primarily through femoral apomorphies: the prominent lesser trochanter on the femur (Fig. 33), the projection of which is visible on the posterior surface of the femur (Fig. 33 B), the central placement of the 4th trochanter (Fig. 33), and the ovular profile of the femoral shaft (being anteroposteriorly compressed). Another apomorphy includes the sigmoidal profile of the ilium in lateral view (Fig 31) (Galton, 2005).

In the future, there might be a resolution of the trichotemy of NMQR 1551, NMQR 3314, and BP/1/7811 if more skeletal material is found. Despite this lack of resolution, this new BP/1/7811 fossil does provide new insight on the interrelationships of the NMQR specimens and to the relationships of other LEF sauropodomorphs, due to its proven association and the precision of its stratigraphic placement within the formation. The features supporting the clade containing these three animals is the presence of a deep, medially-directed pit excavation the surface of the non-articulation gap of the first primordial sacral rib (181: 0 → 1), the absence of the buttress between the preacetabular process and the supraacetabular crest of the ilium (256: 0 → 1), the mediolaterally wide distal surface of the tibiofibular crest (306: 0 → 1), and the position of the lateral margin of the descending caudoventral process of the distal end of the tibia protruding laterally (319: 1 → 0). The grouping of these animals will aid in future works aiming to untangle the remaining basal sauropodomorphs ascribed to "Melanorosauridae" and

will assist in the identification and classification of discoveries yet to come from the Elliot Formation of South Africa.

An interesting aspect of this new clade is the inclusion of NMQR 3314, in that this animal shows a lineage of large Triassic animals that were seemingly relatively unphased by a massive extinction event. The survival of this clade provides additional evidence to the hypothesis that the end-Triassic extinction and the subsequent available niche space left by species unable to survive was what allowed dinosaurs to become the largest land animals Earth has ever seen.

5.2.1 Functional Morphology

The work of Remes (2007) pointed to certain forelimb characteristics that are linked to an abducted forelimb posture in archosaurs. Of these, BP/1/7811 has a both a humeral cuboid fossa (Fig. 24) as well as an enlarged ulnar olecranon process (Fig. 26). The humeral cuboid fossa is suggested by Bonnan and Yates (2007) to be indicative of a well-developed flexural capacity in forearm. The ratios used in Bonnan and Yates (2007) for cannot be repeated in this study due to the incomplete preservation of BP/1/7811, but the measurements of the manal elements that did preserve are similar to those of the significantly more complete NMQR 3314. Their work points to NMQR 3314's manus being one that was designed for occasional bipedality.

The humeral length divided by the femoral length gives a ratio of approximately 73%, which is similar to, though at the higher end, most other contemporary sauropodomorphs (e.g., *Plateosaurus*, *Anchisaurus*, *Lufengosaurus*) who have ratios ranging between 53% and 78% (McPhee et al., 2014). As some elements were not preserved, a ratio from the total lengths of the forelimb vs. the hindlimb could not be obtained.

The minimal femoral circumference divided by the total femoral length of BP/1/7811 gave a ratio of approximately 43%. From the measurements provided in Benson et al. (2014), this ratio is consistent with those seen in the larger, quadrupedal basal non-sauropodan taxa. The femur of BP/1/7811 is entirely straight along the lateral margin of the anterior surface and bears a prominent lesser trochanter, which shows a move towards columnar limb posture (Carrano, 2005).

Based upon these observations and ratios, it does not appear that BP/1/7811 would have been an obligate quadruped. More likely from the evidence above, BP/1/7811 would have been primarily quadrupedal, but with the ability to stand on two legs when the need arose. This animal would have also had the ability to abduct its forelimb, and would have possessed some degree of dexterity in its hands. These adaptions suggest that BP/1/7811 would have been a bulk-browser, rather than a grazer.

Chapter 6: Conclusion

BP/1/7811 is the most complete, associated basal sauropodomorph from the lower Elliot Formation that has been recovered to date. Of particular usefulness within this deposit is the relative stratigraphic preciseness. From this phylogenetic analysis, this specimen likely belongs within the family currently dubbed "Melanorosauridae". However, the name-sake for this family, "*Melanorosaurus*", is in need of fundamental revision. The character inconsistencies within valid "*Melanorosaurus*" taxa (valid within this study) do not suggest that BP/1/7811 fits within "*Melanorosaurus*" and is instead a new genus.

The dissimilarities between BP/1/7811 and other similar taxa further reinforces the LEF's status as an important deposit for understanding the diversity of transitional basal sauropodomorphs in the Triassic and, based upon the close affinities with NMQR 1551 and NMQR 3314, provides new incite on the "Melanorosaurid" clade and how it endeavored across the Triassic-Jurassic Boundary extinction event. While this deposit is dissimilar in completeness and provincial data to other lower Elliot Formation specimens, the taphonomic implications are quite similar, in that BP/1/7811 was preserved in a low-energy, fluvial floodplain ecosystem.

REFERENCES

AgiSoft PhotoScan Professional (Version 1.2.6) (Software), (2016), Retrieved from http://www.agisoft.com/downloads/installer/.

Allain R, Aquesbi N, Dejax J, Meyer C, Monbaron M, Montenet C, Richir P, Rochdy M, Taquet P. 2004. A basal sauropod dinosaur from the Early Jurassic of Morocco. *Comptes Rendus Palevol* 3(3): 199-208.

Allan GH, Cassey P, Snelling, EP, Maloney SK, Seymour RS. 2014. Blood flow for bone remodeling correlates with locomotion in living and extinct birds. *The Journal of Experimental Biology* 217: 2956-2962.

Apaldetti C, Martinez RN, Alcober OA, Pol D. 2011. A new basal sauropodomorph (Dinosauria: Saurischia) from Quebrada del Barro Foration (Marayes-El Carrizal Basin) northwestern Argentina. *PLoS One* 6(11): e26964.

Apaldetti C, Pol D, Yates A. 2012. The postcranial anatomy of *Coloradisaurus brevis* (Dinosauria: Sauropodomorpha) from the Late Triassic of Argentina and its phylogenetic implications. *Paleontology* 56(2): 1-25.

Apaldetti C, Martinez RN, Pol D, Souter T. 2014. Redescription of the skull of the *Coloradisaurus brevis* (Dinosauria: Sauropodomorpha) from the Late Triassic Los Colorados Formation of the Ischigualasto - Villa Union Basin, northwestern Argentina. *Journal of Vertebrate Paleontology* 34(5): 1113-1132.

Aplin AC, Yang A, Hansen S. 1995. Assessment of B, the compression coefficient of mudstones and its relationship with detailed lithology. *Mar Petrol Geology* 12(8): 955-963.

Aslan A, Behrensmeyer AK. 1996. Taphonomy and time resolution of bone assemblages in a contemporary fluvial system: The East Fork River, Wyoming. *Palaios* 11(5): 411-421.

Badgley CE. 1986. Taphonomy of mammalian fossil remains from Siwalik rocks of Pakistan. *Paleobiology* 12: 119-142.

Baron MG, Norman DB, Barrett PM. 2017. A new hypothesis of dinosaur relationships and early dinosaur evolution. *Nature* 543, 501-506

Barrett PM. 2009. A new basal sauropodomorph dinosaur from the upper Elliot Formation (Lower Jurassic) of South Africa. *Journal of Vertebrate Paleontology* 29:1032-1045.

Barrett PM, Upchurch P. 2005. Sauropodomorph diversity through time: Paleoecological and macroevolutionary implications, IN: Currie Rogers, K.A. & Wilson, J.A. (eds.), *The Sauropods: Evolution and Paleobiology*: University of California Press, Berkeley, 125-126,

Behrensmeyer AK. 1978. Taphonomic and ecologic information from bone weathering. *Paleobiology*. 4(2): 150-162.

Benson RBJ, Campione NE, Carrano MT, Mannion PD, Sullivan C, Upchurch P, Evans DC. 2014. Rates of dinosaur body mass evolution indicate 170 million years of sustained ecological innovation of the avian stem lineage. *PLoS Biol.* 12(5): e1001853.

Benton MJ. 2004. Origin and relationships of Dinosauria. *In: The Dinosauria, second edition (eds. D.B. Weishampel, P. Dodson and H. Osmolska) University of California Press, Berkley* 7-19.

Benton MJ, Jull L, Storrs GW, Galton PM. 2000. Anatomy and systematics of the prosauropod dinosaur *Thecodontosaurus antiquus* from the upper Triassic of southwest England. *Journal of Vertebrate Paleontology* 20: 77-108.

Bittencourt JS, Leal LA, Langer MC, Azevedo SAK. 2012. An additional basal sauropodomorph specimen from the Upper Triassic Caturrita Formation, southern Brazil, with comments on the biogeography of plateosaurids. *Alcheringa: An Australian Journal of Palaeontology* 1-10.

Blackburn TJ, Olsen PE, Bowring SA, McLean NM, Kent DV, Puffer J, McHone G, Rasbury ET, Et-Touhami M. 2013. Zircon U-Pb geochronology links the end-Triassic extinction with the Central Atlantic Magmatic Province. *Science* 340: 941-945.

Bonaparte JF. 1969. Dos nuevas 'faunas' de reptiles Triasicos de Argentina. *Gondwana Stratigraphy (IUGS Symposium, Buenos Aires)* 2: 283-306.

Bonaparte JF. 1978. *Coloradia brevis*, n. g. et n. sp. (Saurischia-Prosauropoda), dinosaurio Plateosauridae de la Formacion Los Colorados, Triasico Superior de La Rioja, "Argentina" *Ameghiniana* 15(3-4): 327-332.

Bonaparte JF, Pumares JA. 1995. Notas sobre el primer craneo de *Riojasaurus incertus* (Dinosauria, Prosauropoda, Melanorosauridae) del Triasico Superio de La Rioja, Argentina. *Ameghiniana* 32(4): 341-349.

Bonaparte JF. 1999. Evolución de las vertebras presacras en sauropodomorpha. *Ameghiniana* 36: 115-187.

Bonaparte JF, Coria R. 1993. Un nuevo y gigantesco sauropodo titanosaurio de la Formacion Rio Limay (Albiano-Cenomaniano) de la Provincia del Neuguen, Argentina. *Ameghiniana* 30(3): 271-282.

Bonnan MF. 2003. The evolution of the manus shape in sauropod dinosaurs: implications for functional morphology, forelimb orientation, and phylogeny. *Journal of Vertebrate Paleontology* 23(3): 595-613.

Bonnan, M.F., 2005, Pes anatomy in sauropod dinosaurs: implications for functional morphology, evolution, and phylogeny, IN: Thunder-Lizards: The Sauropodomorph Dinosaurs, Indiana University Press, Bloomington, p. 346-380.

Bonnan MF, Yates AM. 2007. A new description of the forelimb of the basal sauropodomorph *Melanorosaurus*: implications for the evolution of pronation, manus shape, and quadrupedalism in sauropod dinosaurs. *The Paleontological Association: Special Papers in Paleontology* 77: 157-168.

Bordy EM, Hancox PJ, Rubidge BS. 2004a. Fluvial variations in the Late Triassic-Early Jurassic Elliot Formation, main Karoo Basin, South Africa. *Journal of African Earth Sciences* 38: 383-400.

Bordy EM, Hancox PJ, Rubidge BS. 2004b. Basin development during the deposition of the Elliot Formation (Late Triassic-Early Jurassic), Karoo Supergroup, South Africa. *South African Journal of Geology* 107: 397-412.

Bordy EM, Hancox PJ, Rubidge BS. 2004c. A description of the sedimentology and palaeontology of the Late Triassic-Early Jurassic Elliot Formation in Lesotho. *Palaeont. Afr.* 40: 43-58.

Bordy EM, Hancox PJ, Rubidge BS. 2005. The contact of the Molteno and Elliot formations through the main Karoo Basin, South Africa: a second-order sequence boundary. *South African Journal of Geology* 108: 351-364.

Bordy EM, Sciscio L, Abdala F, McPhee BW, Choiniere JN. 2017. First Lower Jurassic vertebrate burrow from southern Africa (upper Elliot Formation, Karoo Basin, South Africa). *Palaeogeography, Palaeoclimatology, Palaeoecology* 468: 362-372.

Bordy EM, Catuneanu O. 2001. Sedimentology of the upper Karoo fluvial strata in the Tuli Basin, South Africa. *Journal of African Earth Sciences* 33: 605-629.

Bordy EM. Eriksson P. 2015. Lithostratigraphy of the Elliot Formation (Karoo Supergroup), South Africa. *South African Journal of Geology* 118(3): 311-316.

Botha-Brink J, Abdala F, Chinsamy-Turan A. 2012. The radiation and osteohistology of nonmammaliaform cynodonts. IN: *Forerunner of Mammals*, Indiana: Indiana University Press, 223-248.

Bristowe A, Raath MA. 2004. A juvenile coelophysoid skull from the Early Jurassic of Zimbabwe, and the synonymy of *Coelophysis* and *Syntarsus*. *Palaeontologia Africana* 40: 31-41.

Brusatte SL, Benton MJ, Ruta M, Lloyd GT. 2008. Superiority, competition, and opportunism in the evolutionary radiation of dinosaurs. *Science* 321 (5895): 1485-1488.

Buffetaut E, Suteethorn V, Cuny G, Tong H, Le Loeuff J, Khansubha S, Jongautchariyakul S. 2000. The earliest known sauropod dinosaur. *Nature* 407: 72-74.

Butler RJ. 2005. The 'fabrosaurid' ornithischian dinosaurs from the upper Elliot Formation (Lower Jurassic) of South Africa and Lesotho. *Zooligical Journal of the Linnean Society* 145(2): 175-218.

Carpenter K, Currie PJ (edited by). 1990. *Dinosaur systematics, approaches, and perspectives*, Cambridge: Cambridge University Press, 218.

Carrano M. 2005. The evolution of sauropod locomotion: morphological diversity of a secondary quadrupedal radiation, IN: *The sauropods: Evolution and paleobiology* (ed. Curry Rodgers KA, Wilson JA), Berkeley: University of California Press, 229-251.

Catuneanu O, Wopfner H, Eriksson PG, Cairncross B, Rubidge BS, Smith RMH, Hancox PJ. 2005. The Karoo basins of south-central Africa. *Journal of African Earth Sciences* 43: 211-253.

Charig AJ, Attridge J, Crompton AW. 1965. On the origin of the sauropods and the classification of the Saurischia. *Proceedings of the Linnean Society of London* 176: 197-221.

Collins AS, Windley BF. 2002. The tectonic evolution of central and northern Madagascar and its place in the final assembly of Gondwana. *The Journal of Geology* 110: 325-339.

Cooper MR. 1984. A reassessment of *Vulcanodon karibaensis*, Raath (Dinosauria: Saurischia) and the origin of the Sauropoda. *Palaeontologia Africana* 25: 203-205, 211-213, 223, 230-231.

Dong Z, Zhou S, Zhang Y. 1983. Dinosaurs from the Jurassic. *Palaeontologica Sinica* 162(23): 1-136.

du Fabrègues CP, Allain R. 2016. New material and revision of *Melanorosaurus thabanensis*, a basal sauropodomorph from the Upper Triassic of Lesotho. *Peer J* 4: e1639.

Drumheller SK, Stocker MR, Nesbitt SJ. 2014. Direct evidence of trophic interactions among apex predators in the Late Triassic of western North America. Naturwissenschaften 101(11): 975-987.

Ellenberger P. 1970. Establissement de Zones Straigraphiques Détaillées dans le Stromberg du Lesotho (Afrique du Sud) (Trias Supérieur à Jurassique). In: S.H. Haughton (ed.). *Proceedings and Papers of the Second Gondwanaland Symposium* 343–370.

Ellenberger F, Ellenberger P. 1956. Le gisement de dinosauriens de Maphutseng (Basutoland, Afrique du sud). *Comptes Rendus Sommaires de la Societe Geologique de France* 8: 99–101.

Eriksson PG. 1985. A palaeoenvironmental study of the Molteno, Elliot, and Clarens Formations in the Natal Drakensberg of northeastern Orange Free State. *Trans. Geological Society of South Africa* 88: 19-26.

Ezcurra MD. 2010. A new dinosaur (Saurischia: Sauropodomorph) from the Late Triassic of Argentina: a reassessment of dinosaur origin and phylogeny. *Journal of Systematic Palaeontology* 8(3): 371-425.

Ezcurra MD, Apaldetti C. 2012. A robust sauropodomorph specimen from the Upper Triassic of Argentina and insights on the diversity of the Los Colorados Formation. *Proceedings of the Geologists Association* 123: 155-164.

Fanti F, Cau A, Hassine M, Contessi M. 2013. A new sauropod dinosaur from the Early Cretaceous of Tunisia with extreme avian-like pneumatization. *Nature Communications* 4:79-95.

Fraser NC, Padian K, Walkden GM, Davis ALM. 2002. Basal dinosauriform remains from Britain and the diagnosis of the Dinosauria. *Palaeontology* 45(1): 79-95.

Galton PM. 1973. On the anatomy and relationships of *Efraasia diagnostica* (von Huene) n. gen., a prosauropod dinosaur (Reptilla: Saurischia) from the Upper Triassic of Germany. *Paläontologische Zeitschrift* 47(3/4): 229-255.

Galton PM. 1976. Prosauropod dinosaurs (Reptilia: Saurischia) of North America. *Postilla* 169: 1-98.

Galton PM. 1984. Cranial anatomy of the prosauropod dinosaur *Plateosaurus* from the Knollenmergel (Middle Keuper, Upper Triassic) of Germany, Two complete skulls from Trossingen/Württ – with comments on the diet. *Geologica et Palaeontologica* 18: 139-171.

Galton PM. 1990. Basal Sauropodomorpha-Prosauropoda, IN: Weishampel DB, Dodson P, Osmólska H (eds.): The Dinosauria, University of California Press, Berkeley, p.320-344.

Galton PM. 1998. Saurischian dinosaurs from the Upper Triassic of England: *Camelotia* (Prosauropoda, Melanorosauridae) and *Avalonianus* (Theropoda?, Carnosauria). *Palaentograpgica Abteilung* 250: 155-172.

Galton PM. 2005. Basal sauropodomorph dinosaur taxa *Thecodontosaurus* Riley & Stutchbury, 1836, *T. antiquus* Morris, 1843 and *T. caducus* Yates, 2003: their status re: humeral morphs from the 1834 fissure fill (Upper Triassic) in Clifton, Bristol, UK. Journal of Vertebrate Paleontology 25(3, suppl.): 61A.

Galton PM, van Heerden J, Yates AM. 2005. Postcranial anatomy of referred specimens of the sauropodomorph dinosaur *Melanorosaurus* from the Upper Triassic of South Africa, IN: Thunder-Lizards: The Sauropodomorph Dinosaurs, Indiana University Press, Bloomington 1-37.

Galton PM, Yates AM, Kermack D. 2007. *Pantydraco* n. gen. for *Thecodontosaurus caducus* Yates 2003, a basal sauropodomorph dinosaur from the Upper Triassic or Lower Jurassic of South Wales, UK. *Neues Jahrbuch für Geologie und Paläontologie* 243: 119-125.

Galton PM, van Heerden J. 1985. Partial hindlimb of *Blikanasaurus cromptoni* n. gen. and n. sp., representing a new family of prosauropod dinosaurs from the Upper Triassic of South Africa. *Geobios* 18: 509-516.

Galton PM, van Heerden J. 1998. Anatomy of the prosauropod dinosaur *Blikanasaurus cromptoni* (Upper Triassic, South Africa), with notes on the other tetrapods from the lower Elliot Formation. *Paläontologische Zeitschrift* 72: 163-177.

Galton PM, Upchurch P. 2004. Prosauropoda, IN: Weishampel, D.B., Dodson, P., & Osmólska, H. (eds.): The Dinosauria: 2nd Edition, Berkeley: University of California Press, 232-258.

Gauffre FX. 1993a. Biochronostratigraphy of the Lower Elliot Formation (Southern Africa) and preliminary results on the Maphutseng dinosaur (Saurischia: Prosauropoda) from the same formation of Lesotho. *New Mexico Museum of Natural History and Science Bulletin* 3: 147-149.

Gauffre FX. 1993b. The most recent Melanorosauridae (Saurischia, Prosauropoda), Lower Jurassic of Lesotho, with remarks on the prosauropod phylogeny. *Neues Jahrbuch für Geologie und Paläontologie* 11: 648-654.

Gauffre FX. 1996. Phylogénie des dinosaurs prosauropodes et étude d'un prosauropode du Trias supérieur d'Afrique australe Dissertation. *Muséum National d'Histoire Naturelle*.

Gauthier JA. 1986. Saurischian monophyly and the origin of birds, IN: Padian, K, The Origin of Birds and Evolution of Flight, Memoirs of the California Academy of Sciences, California Academy of Sciences, San Francisco, 8: 1-55.

GeoRose 0.5.0. 2014. Yong Technology. Edmonton, Canada http://www.yongtechnology.com/download/georose.

Gillette L, Pemberton SG, Sarjeant W. 2010. A Late Triassic invertebrate ichnofauna from Ghost Ranch, New Mexico. *Ichnos* 10: 141-151.

Glennie KW. 1998. *Petroleum Geology of the North Sea: Basic Concepts and Recent Advances*, Blackwell Science: Oxford, 356.

Goloboff PA, Farris JS, Nixon K. 2008. TNT: a free program for phylogenetic analysis cladistics 24: 774-786.

Gray H. 1918. *Anatomy of the Human Body*, Philadelphia: Lea & Febiger, 307.

Haines T, Chambers P. 2007. *The Complete Guide to Prehistoric Life*, Buffalo, New York: Firefly Books.

Hallam A. 1990. The end-Triassic mass extinction event. *Geological Society of America: Special Papers* 247: 577-584.

Haughton SH. 1924. The fauna and stratigraphy of the Stormberg. *Series Annals of South African Museum* 12: 323–497.

Hennig W. 1966. Dixidae aus dem Baltischen Bernstein, mit Bemerkungen über einige andere fossile Arten aus der Gruppe Culicoidea, *Beitr Naturkde* 153: 1-16.

Hone DWE, Tanke DH. 2015. Pre- and postmortem tyrannosaurid bite marks on the remains of *Daspletosaurus* (Tyrannosaurinae: Theropoda) from Dinosaur Provincial Park, Alberta, Canada. *Peer J* 3:e885.

Hone DWE, Farke AA, Wedel MI. 2016. Ontogeny and the fossil record: What if anything is an adult dinosaur? *Biol. Letters* 12: 20150947.

Hounslow MW, Ruffell A. 2006. Triassic: seasonal rivers, dusty deserts, and saline lakes. IN: Rawson PF, Brenchley P (Eds.). *The Geology of England and Wales*. Geological Society of London 295-325.

Huxley TH. 1867. On some remains of large dinosaurian reptiles from the Stormberg Mountains, South Africa. *Quarterly Journal of the Geological Society* 23: 1-6.

Irmis RB. 2007. Axial skeleton ontogeny in the parasuchia (archosauria: pseudosuchia) and its implications for ontogenetic determination in archosaurs. *Journal of Vertebrate Paleontology* 27(2): 350-361

Irmis RB. 2010. Evaluation hypotheses for the early diversification of dinosaurs. *Earth and Environmental Science Transactions of the Royal Society of Edinburgh* 101: 397-426.

Jackson JA. 1997. *Glossary of Geology (4th ed.),* American Geological Institute, Alexandria, VA, 769.

Jacobsen AR. 1998. Feeding behavior of carnivorous dinosaurs as determined by tooth marks on dinosaur bones. *Historical Biology* 13: 17-26.

Keighley DG, Pickerill RK. 2008. The ichnotaxa Palarophycus and Planolites: Historical perspectives and recommendations. *Ichnos* 3: 301-309.

Kent DV, Olsen PE, White WK. 1995. Late Triassic-Early Jurassic geomagnetic polarity sequence and paleolatitudes from drill cores in the Newark rift basin (Eastern North America). *Journal of Geophysical Research* 100: 14965-14998.

Kindle EM. 1917. Some factors affecting the development of mud-cracks. *Journal of Geology* 25(2): 135-144.

Kitching JW, Raath MA. 1984. Fossils from the Elliot and Clarens formations (Karoo sequence) of the northeastern Cape, Orange Free State and Lesotho, and a suggested biozonation based on tetrapods. *Palaeontologia Africana* 25: 111-125.

Knoll F. 2010. A primitive sauropodomorph from the upper Elliot Formation of Lesotho. *Geological Magazine* 147(6): 814-829.

Langer MC. 2003. The pelvic and hindlimb anatomy of the stem-sauropodomorph *Saturnalia* tupiniquim (Late Triassic, Brazil). *PaleoBios* 23(2): 1-30.

Langer MC, Abdala F, Richter M, Benton M. 1999. A sauropodomorph dinosaur from the Upper Triassic (Carnian) of southern Brazil. *Comptes Rendus de l'Académie des Sciences* 329: 511-517.

Langer MC, Ezcurra MD, Bittencourt JS, Novas FE. 2010. The origin and early evolution of dinosaurs. *Biological Reviews* 85: 55-110.

Langer MC, Ezcurra MD, Rauhut, OWM, Benton, MJ, Knoll F, McPhee BW, Novas FE, Pol D, Brusatte SL. 2017. Untangling the dinosaur family tree, *Nature* 551(7678).

Leal LA, Azevoda SAK, Kellner AAW, de Rosa AAS. 2004. A new early dinosaur (Sauropodomorph) from the Caturrita Formation (Late Triassic), Paraná Basin, Brazil. *Zootaxa* 690: 1-24.

Letourneau PM, Olsen PE (editors). 2003. The great rift valleys of Pangea in Eastern North America, Vol. 2: Sedimentology, Stratigraphy, and Paleontology, Columbia University Press, New York, p. 273-292.

Levick L, Fonseca J, Goodrich D, Hernandez M, Semmens D, Stormberg J, Leidy R, Scianni M. Guertin DP, Tlucezek M, Kepner W, 2008. The ecological and hydrological significance of ephemeral and intermittent steams in the arid and semi-arid American southwest. *U.S. Environmental Protection Agency and USDA/ARA Southwest Watershed Research Center* EPA/600/R-08/134, ARS/233046: 116.

Lü J, Li T, Zhong S, Azuma Y, Fujita M, Dong Z, Ji Q. 2007. New yunnanosaurid dinosaur (Dinosauria, Prosauropoda) from the Middle Jurassic Zhanghe Formation of Yuanmou, Yunnan Province of China. *Memoir of the Fukui Prefectural Dinosaur Museum* 6: 1-15.

Lucas SJ, Hancox PJ. 2001. Tetrapod-based correlation of the nonmarine upper Triassic of southern Africa. *Albertiana* 25: 5-9.

Maddison WP, Maddison DR. 2014. Mesquite: a modular system for evolutionary analysis, http://mesquiteproject.org.

Mallison H, Pfretzschner H, Hohlock A. 2009. Mechanical digitizing for paleontology – new and improved techniques. *Palaeontologia Electronica* 12:2.

Marsh OC. 1882. Classification of Dinosauria. *American Journal of Science* 3(23): 81-86.

Marsh OC. 1898. On the Families of Sauropodous Dinosauria, Report of the British Association for the Advancement of Science, 68th.

Martínez RN, Alcober OA. 2009. A basal sauropodomorph (Dinosauria: Saurischia) from the Ischigualasto Formation (Triassic, Carnian) and the early evolution of sauropodomorpha. *PLoS ONE* 4(2): 1-12.

McPhee BW, Yates AM, Choiniere JN, Abdala F. 2014. The complete anatomy and phylogenetic of Antetonitrus ingenipes (Sauropodiformes, Dinosauria): implications for the origins of sauropoda. *Zoological Journal of the Linnean Society* 171: 151-205.

McPhee BW, Bonnan MF, Yates AM, Neveling J, Choiniere JN. 2015a. A new a basal sauropod from the pre-Toarcian Jurassic of South Africa: evidence of niche-partitioning at the sauropodomorph-sauropod boundary? *Scientific Reports* 5:13224.

McPhee BW, Choiniere JN, Yates AM, Viglietti PA. 2015b. A second species of *Eucnemesaurus* van Hoepen, 1920 (Dinosauria, Sauropodomorpha): new information on the diversity and evolution of the sauropodomorph fauna of South Africa's lower Elliot Formation (latest Triassic). *Journal of Vertebrate Paleontology* 35(5): 1-24.

McPhee BW, Bordy EM, Sciscio L, Choiniere JN. 2017. The sauropodomorph biostratigraphy of the Elliot Formation of southern Africa: Tracking the evolution of sauropodomorpha across the Triassic-Jurassic boundary. *Acta Palaeontologica Polonica* 62(3): 441-465.

McPhee BW, Choiniere JN. 2016. A hyper-robust sauropodomorph dinosaur ilium from the Upper Triassic-Lower Jurassic Elliot Formation of South Africa: Implications for the functional diversity of basal sauropodomorpha. *Journal of African Earth Sciences* 123: 177-184.

Metz R. 2008. Ichnologic stuy of the lockatong formation (Late Triassic) Newark basin, southeastern Pennsylvania. *Ichnos* 4: 43-51.

Müller RT, Silva SD. 2017. Taxon sample and character coding deeply impact unstable branches in phylogenetic trees of dinosaurs. *Historical Biology* 1-4.

Nesbitt SJ, Barrett P, Werning S, Sidor CA, Charig A. 2012. The oldest dinosaur? A Middle Triassic dinosauriform from Tanzania. *Biology Letters* 9:20120949.

Novas FE. 2009. *The Age of Dinosaurs in South America*, Indiana: Indiana University Press, 452.

Novas FE, Ezcurra MD, Chatterjee S, Kutty TS. 2011. New dinosaur species from the Upper Triassic upper Malerj and lower Dharmaram formations of central India. *Earth and Environmental Science Transactions of the Royal Society of Edinburgh* 101(3-4): 333-349.

Olsen PE, Kent DV, Sues HD, Koeberl C, Huber H, Montanari A, Rainforth EC, Szaina MJ, Hartline BW. 2002. Ascent of dinosaurs linked to an iridium anomaly at the Triassic-Jurassic boundary. *Science* 296: 1305-1307.

Olsen PE, Galton PM. 1977. Triassic-Jurassic tetrapod extinctions: are they real?. *Science* 197: 983-986.

Otero A, Krupandan E, Pol D, Chinsamy A, Choiniere JN. 2015. A new basal sauropodiform from South Africa and the phylogenetic relationships of basal sauropodomorphs. *Zoological Journal of the Linnean Society* 174: 589-634.

Otero A, Pol D. 2013. Postcranial anatomy and phylogenetic relationships of *Mussaurus patagonicus* (Dinosauria, Sauropodomorpha), *Journal of Vertebrate Paleontology* 33: 1138-1168.

Owen R. 1842. Report on British Fossil Reptiles, Part II: Report of the 11th Meeting of the British Association for the Advancement of Science, London: John Murray, 60-204.

Owen R. 1854. Descriptive catalogue of the fossil organic remains of Reptilia and Pisces contained in the Museum of the Royal College of Surgeons of England. London, 80, 97.

Pol D, Garrido A, Cerda IA. 2011. A new sauropodomorph dinosaur from the Early Jurassic of Patagonia and the origin and evolution of the sauropod-type sacrum. *PLoS ONE* 6(1).

Pol D, Powell JE. 2007. New information on *Lessemsaurus sauropoides* (Dinosauria: Sauropodomorpha) from the Upper Triassic of Argentina. *Special Papers in Palaeontology*. 77: 223-243.

Quan TM, van de Schootbrugge B, Field P, Rosenthal Y, Falkowski PG. 2008. Nitrogen isotope and trace metal analyses from the Mingolsheim core (Germany): Evidence for redox variations across the Triassic-Jurassic boundary. *Global Biogeochemical Cycles* 22(2): GB2014.

Raath MA. 1972. Fossil vertebrate studies in Rhodesia: a new dinosaur (Reptilia, Saurischia) from near the Triassic-Jurassic boundary. *Arnoldia* 5: 1-2, 4

Rauhut OWM, Fechner R, Remes, K, Reis K. 2011. How to get big in the Mesozoic: The evolution of the sauropodomorph body plan, IN: *Biology of the Sauropod Dinosaurs: Understanding the Life of Giants (eds.),* Klein N, Gee CT, Sander PM, Bloomfield: Indiana University Press, 119-149.

Remes L. 2007. Evolution of the pectoral girdle and forelimb in sauropodomorpha (Dinosauria, Saurischia): Osteology, myology, and function, Ludwig-Maximilians-Universität, Muchen zur Erlangung des Doktorgrades (Dr. rer. nat.)

Roff S. 2011. Dark days of the Triassic: Lost World. *Nature* 479(7373): 287-289.

Rowe TB, Sues HD, Reisz RR. 2011. Dispersal and diversity in the earliest North American sauropodomorph dinosaurs, with a description of the new taxon. *Proceedings of the Royal Society: Biological Sciences* 278(1708): 1044-1053.

Ryder G, Fastovsky DE, Gartner S. 1996. The Cretaceous-Tertiary event and other catastrophes in Earth History. *Geological Society of America* 19.

Sahle Y, Zaatari SE, White TD. 2017. Hominid butcher and biting crocodiles in the African Plio-Pleistocene. PNAS 114(50): 13164-13169.

Sahney S, Benton MJ, 2008. Recovery from the most profound mass extinction of all time. *Proceedings of the Royal Society: Biological Sciences* 275(1636): 759-165.

Sander PM, Christian A, Clauss M, Fechner R, Gee CT, Griebeler E, Gunga H, Hummel J, Mallison H, Perry ST, Preuschoft H, Rauhut OW, Remes K, Tütken T, Wings O, Witzel U. 2011. Biology of the sauropod dinosaurs: the evolution of gigantism. *Boil. Rev. Camb. Philos. Soc.* 86(1): 117-115.

Schwartz HL, Gillette DD. 1994. Geology and taphonomy of the *Coelophysis* Quarry, Upper Triassic Chinle Formation, Ghost Ranch, New Mexico. *Journal of Paleontology* 68(5): 1118-1130.

Sciscio L, Bordy EM. 2016. Palaeoclimatic conditions in the Late Triassic-Early Jurassic of southern Africa: A geochemical assessment of the Elliot Formation. *Journal of African Earth Sciences* 119: 102-119.

Sciscio L, du Kock M, Bordy EM, Knoll F. 2017. Magnetostratigraphy across the Triassic-Jurassic boundary in the main Karoo Basin. *Elsevier B.V.* 51: 177-192.

Schwimmer DR. 2010. Bite marks of the giant crocodilian Deinosuchus on Late Cretaceous (Campanian) bones. *Faculty Bibliography* 115.

Seeley HG. 1887. On the classification of the fossil animals commonly named Dinosauria. *Proceedings of the Royal Society of London.*

Sellwood BW Valdes PJ. 2006. Mesozoic climates: General circulation models and the rock record. *Sedimentary Geology* 190: 269-287.

Sereno PC. 1998. A rationale for phylogenetic definitions, with applications to the higher-level taxonomy of Dinosauria. *Neues Jahrbuch für Geologie und Paläontologie, Abhandlungen* 210: 41-83.

Sereno PC. 1999. The Evolution of Dinosaurs. *Science* 284: 2137-2147.

Sereno PC. 2007. Basal sauropodomorpha: historical and recent phylogenetic hypotheses, with comments on *Ammosaurus major* (Marsh, 1889) IN: Evolution and Palaeobiology of Early Sauropodomorph Dinosaurs, (eds.) Barrett PM, Batten DJ. *Special Papers in Palaeontology* 77: 261-289.

Sereno PC, Forster CA, Rogers RR, Monetta AM. 1993. Primitive dinosaur skeleton from Argentina and the early evolution of dinosaurian. *Nature* 361(19): 64-66.

Sertich JJW, Loewen MA. 2010. A new basal sauropodomorph dinosaur from the Lower Jurassic Navajo sandstone of southern Utah. *PLoS ONE* 5(3): e9789.

Seymour RS, Smith SL, White CR, Henderson DM, Wings D. 2012. Blood flow to long bones indicate activity metabolism in mammals, reptiles, and dinosaurs. *Proceedings of the Royal Society* 279: 451-456.

Simms MJ, Ruffell AH. 1989. Synchroneity of climatic change in the Late Triassic. *Geology* 17: 265-268.

Smith RMH, Eriksson PG, Botha WJ. 1993. A review of the stratigraphy and sedimentary environments of the Karoo-aged basins of Southern Africa. *Journal of African Earth Science* 16: 143-169.

Smith RMH, Kitching J. 1997. Sedimentology and vertebrate taphonomy of the Tritylodon Aceme ZoneL a reworked palaeosol in the Lower Jurassic Elliot Formation, Karoo Supergroup, South Africa, Palaeogeography, Palaeoclimatology. *Palaeoecology* 131: 29-50.

Smith ND, Pol D. 2007. Anatomy of a basal sauropodomorph dinosaur from the Early Jurassic Hanson Formation of Antarctica. *Acta Palaeontologica* Polonica 52(4): 657-674.

Sues HD. 1997. "Sauropods" IN: Farlow JO, Brett-Surman MK. *The Complete Dinosaur.* Bloomington: Indiana University Press, 318.

Tanner LH, Hubert JF, Coffrey BP, McInerney DP. 2001. Stability of atmosphere CO2 levels across the Triassic/Jurassic boundary. *Nature* 411: 3-139.

Tidwell V, Carpenter K. 2005. Thunder Lizards: The Sauropodomorph Dinosaurs. Bloomington: Indiana University Press, Xi + 495 pp.

Toots H. 1965a. Random orientation of fossils and its significance. *Rocky Mountain Geology* 4: 59-62.

Toots H. 1965b. Orientation and distribution of fossils as environmental indicators. *Wyoming Geological Association* Guidebook 19: 219-229.

Trueta J. 1968. Studies of the Development and Decay of the Human Frame, William Heineman, London.

Upchurch P. 1995. The evolutionary history of sauropod dinosaur. *Biol. Sci.* 349: 365-390.

Upchurch P. 1998. The phylogenetic relationships of sauropod dinosaurs. *Zoological Journal of the Lennean Society* 124: 43-103.

Upchurch P, Barrett PM, Dodson P. 2004. *Sauropoda, The Dinosauria: 2nd Edition,* 259-322.

Upchurch P, Barrett PM, Galton P. 2007. A phylogenetic analysis of basal sauropodomorph relationships: implications for the origin of sauropod dinosaurs. *Special Papers in Palaeontology* 77: 57-90.

Upchurch P, Barrett PM. 2005. A phylogenetic perspective on sauropod diversity, IN: Curry-Rogers KA, Wilson JA. (eds.) *The Dinosauria (2nd edition)*, Berkeley: University of California Press, 259-322.

van Heerden J. 1979. The morphology and taxonomy of Euskelosaurus (Reptilia: Saurischia) Late Triassic from South Africa. *Navorsinge can die Nasionale Museum* 4: 21-84.

van Hoepen EC, 1920. Contributions to the knowledge of the reptiles of the Karoo Formation: Further dinosaurian material in the Transvaal Museum. *Annals of the Transvaal Museum* 7: 93-140.

von Huene F. 1920. Bemerkunge zur Systematik und Stammesgeschichte einiger Reptilien, *Zeitschrift fur Induktive Abstammungslehre und Verebungslehre* 24: 162-166.

Visser JNJ, Botha BJV. 1980. Meander channel, point bar, crevasse splay, and aeolian deposits from the Elliot Formations in Barkly Pass, northeastern Cape. *Transactions of the Geological Society of South Africa* 83: 55-62.

Visser JNJ, Botha BJV. 1984. A review of the Stormberg Group and Drakensberg volcanics in southern Africa. *Palaentologia Africana* 25: 5-27.

von Huene F. 1932. Die fossile Reptil-Ordnung, Saurischia, ihre Entwick-lung und Geschichte. *Monographien zur Geologie und Paläontologie* 4: 1-361.

von Meyer H. 1845. System der fossilen Saurier. *Neues Jahrbuch für Mineralogie, Geognosie, Geologie, und Petrfakten-Kunde* 278-285.

Voorhies MR. 1969. Taphonomy and population dynamics of an Early Pliocene vertebrate fauna - Knox County, Nebraska. *Contributions to Geology, University of Wyoming Special Paper* 1: 1-69.

Wang Y, You H, Wang T. 2017. A new basal sauropodiform dinosaur from the Lower Jurassic of Yunnan Province, China. *Scientific Reports* 7: 41881.

Wedel MJ. 2003. Vertebral pneumaticity, air sacs, and the physiology of sauropod dinosaurs. *Paleobiology* 29(2): 243.

Weishampel DB, Dodson P, Osmólska H. 2004. Dinosaur distribution (Late Triassic, Africa), IN: (eds) *The Dinosauria, 2nd edition*, Berkeley: University of California Press, 528-529.

Whiteside JH, Olsen PE, Eglinton T, Brookfield ME, Sambrotto RN. 2010. Compound-specific carbon isotopes from Earth's largest flood basalt province directly link eruptions to the end-Triassic mass extinction, *Proc. Natl. Acad. Sci., USA* 107: 6721-6725.

Wilson JA. 1999. A nomenclature for vertebrate laminae in sauropods and other saurischian dinosaurs. *Journal of Vertebrate Paleontology* 19(4): 639-653.

Wilson JA. 2002. Sauropod dinosaur phylogeny: critique and cladistics analysis. *Zoological Journal of the Linnean Society* 136: 217-276.

Wilson JA, D'Emic MD, Ikeiiri T, Moacdiah EM, Whitlock JA. 2011. A nomenclature for vertebral fossae in sauropods and other saurischian dinosaurs. *PLoS ONE* 6(2): e17114.

Wilson JA, Sereno PC. 1998. Early evolution and higher-level phylogeny of sauropod dinosaurs. *Journal of Vertebrate Paleontology* 18: 1-68.

Yates AM. 2003. A definite prosauropod dinosaur from the lower Elliot Formation (Norian: Upper Triassic) of South Africa. *Palaeontologia Africana* 39: 63-68.

Yates AM, 2004. The Death of a Dinosaur: dismembering *Euskelosaurus*. *Geoscience Africa* 715

Yates AM. 2007a. The first complete skull of the Triassic dinosaur Melanorosaurus Haughton (Sauropodomorpha: Anchisauria), IN: Barrett, P.M. & Batten, D.J. (eds.), Evolution and palaeobiology of early sauropodomorph dinosaurs. *Special Papers in Palaeontology* 77: 289.

Yates AM. 2007b. Solving a dinosaurian puzzle: the identity *Aliwalia rex* Galton. *Historical Biology* 19: 93-123.

Yates AM. 2008. A second specimen of *Blikanasaurus* (Dinosauria: Sauropoda) and the biostratigraphy of the lower Elliot Formation. *Palaeontologia Africana* 43: 39-43.

Yates AM. 2010. A revision of the problematic sauropodomorph dinosaurs from Manchester, Connecticut and the status of *Anchisaurus Marsh. Palaeontologia* 739-752.

Yates AM, Bonnan MF, Neveling J, Chinsamy A, Blackbeard MG. 2010. A new transitional sauropodomorph dinosaur from the Early Jurassic of South Africa and the evolution of sauropod feeding a quadrupedalism, Proceedings of the Royal Society. *Biological Sciences* 277: 787-794.

Yates AM, Bonnan MF, Neveling J. 2011. A new basal sauropodomorph dinosaur from the Early Jurassic of South Africa. *Journal of Vertebrate Paleontology* 31: 610-625.

Yates AM, Wedel MJ, Bonnan MF. 2012. The early evolution of postcranial skeletal pneumaticity in sauropodomorph dinosaurs. *Acta Palaeontologica Polonica* 57(1): 85-100.

Yates AM, Barrett PM. 2010. *Massospondylus carinatus*, Owen, 1854 (Dinosauria: Sauropodomorpha) from the Lower Jurassic of South Africa: Proposed conservation of usage designation of a neotype. *Palaeontologia Africana* 45: 7-10.

Yates AM, Kitching JW. 2003. The earliest known sauropod dinosaur and the first steps towards sauropod locomotion. *Proceedings of the Royal Society of London* 270: 1753-1758.

Young CC. 1942. *Yunnanosaurus huangi*, Young (gen. et sp. nov), a new prosauropod from the red beds at Lufeng, Yunnan. *Bulletin of the Geological Society of China* 22(1-2): 63-104.

Young CC. 1954. On a new sauropod from Yiping, Szechuan, China. *Palaeontologia Sinica* 111(4): 481-514.

Zhang Y, Yang Z. 1995. A new complete osteology of Prosauropoda in Lufeng Basin, Yunnan, China. Yunnan *Publishing House of Science and Technology, Kunming, China* 1-100.

APPENDIX

TABLES:

Table 1: Details of jackets recovered from the H5 Quarry.

Jacket:	Jacket #:	Content Description:	Collection Date:
Scapula jacket	H5-16-4	left scapula, two dorsal vertebrae, several rib fragments	2016
Humerus jacket	H5-14-24	right humerus, cervical vertebra, several rib fragments cut across by a microfault	2014-15
Hindlimb jacket	HN-14-23	left ilium, both pubes, a left femur, a left tibia, a right fibula, two dorsal vertebrae, multiple rib/gastralia fragments	2014-15
Fibula jacket	H5-16-1	left fibula, one dorsal vertebrae	2016
Small jacket 1	HN-15-1	right pedal phalanx	2015
Small jacket 2	HN-15-3	caudal vertebra	2015
Small jacket 3	HN-15-15	dorsal vertebrae, MC2	2015

Table 2: BP/1/7811 vertebral measurements.

C6?	
Anteropost length (neural arch):	183.67
Anteropost length (neural spine):	45.69
Anteropost. width of centrum:	N/A
Dorsoventral height neural arch:	78.64
Dorsoventral height centrum:	N/A
Ant. surface dorsoventral height of centra:	N/A
Ant. surface mediolateral width of centra:	N/A
Post. surface dorsoventral height of centra:	N/A
Post. surface mediolateral height of centra:	N/A

C8?	
Anteropost length (neural arch):	177.2
Anteropost length (neural spine):	36.66
Anteropost. width of centrum:	121.63
Dorsoventral height neural arch:	90.3
Dorsoventral height centrum:	58.18
Ant. surface dorsoventral height of centra:	77.47
Ant. surface mediolateral width of centra:	48.4
Post. surface dorsoventral height of centra:	74.14
Post. surface mediolateral height of centra:	57.18

D1?	
Greatest anteropost length:	N/A
Anteropost. width of neural spine:	N/A
Dorsoventral height neural arch:	85
Dorsoventral height centrum:	N/A
Anterior surface dorsoventral height of centra:	N/A
Anterior surface mediolateral width of centra:	N/A
Posterior surface dorsoventral height of centra:	N/A
Posterior surface mediolateral height of centra:	N/A

D2?	
Greatest anteropost length:	77.16
Anteropost. width of neural spine:	31.39
Dorsoventral height neural arch:	92.29
Dorsoventral height centrum:	82.3
Anterior surface dorsoventral height of centra:	84.95
Anterior surface mediolateral width of centra:	65.73
Posterior surface dorsoventral height of centra:	81.47
Posterior surface mediolateral height of centra:	67.77

D4?	
Greatest anteropost length:	92.15
Anteropost. width of neural spine:	49.99
Dorsoventral height neural arch:	54.85
Dorsoventral height centrum:	85.97
Anterior surface dorsoventral height of centra:	83.56
Anterior surface mediolateral width of centra:	54.67
Posterior surface dorsoventral height of centra:	83.89
Posterior surface mediolateral height of centra:	55.6

D5?	
Greatest anteropost length:	95.44
Anteropost. width of neural spine:	68.97
Dorsoventral height neural arch:	84.91
Dorsoventral height centrum:	119.06
Anterior surface dorsoventral height of centra:	82.71
Anterior surface mediolateral width of centra:	52.66
Posterior surface dorsoventral height of centra:	77.89
Posterior surface mediolateral height of centra:	46.87

D6?	
Greatest anteropost length:	89.4
Anteropost. width of neural spine:	64.21
Dorsoventral height neural arch:	116
Dorsoventral height centrum:	109
Anterior surface dorsoventral height of centra:	74.15
Anterior surface mediolateral width of centra:	56.11
Posterior surface dorsoventral height of centra:	92.26
Posterior surface mediolateral height of centra:	61.3

D8?	
Greatest anteropost length:	103.55
Anteropost. width of neural spine:	N/A
Dorsoventral height neural arch:	N/A
Dorsoventral height centrum:	101.21
Anterior surface dorsoventral height of centra:	82.65
Anterior surface mediolateral width of centra:	55.47
Posterior surface dorsoventral height of centra:	92.85
Posterior surface mediolateral height of centra:	65.33

D12?	
Greatest anteropost length:	87.39
Anteropost. width of neural spine:	72.79
Dorsoventral height neural arch:	116.2
Dorsoventral height centrum:	138.5
Anterior surface dorsoventral height of centra:	84.62
Anterior surface mediolateral width of centra:	82.88
Posterior surface dorsoventral height of centra:	93.41
Posterior surface mediolateral height of centra:	75.62

D13?	
Greatest anteropost length:	102.23
Anteropost. width of neural spine:	80.02
Dorsoventral height neural arch:	113.41
Dorsoventral height centrum:	133.38
Anterior surface dorsoventral height of centra:	83.95
Anterior surface mediolateral width of centra:	97.66
Posterior surface dorsoventral height of centra:	89.25
Posterior surface mediolateral height of centra:	76.78

Posterior caudal	
Greatest anteropost length:	73.35
Anteropost. width of neural spine:	64.45
Dorsoventral height neural arch:	22.58
Dorsoventral height centrum:	44.1
Anterior surface dorsoventral height of centra:	43.52
Anterior surface mediolateral width of centra:	44.91
Posterior surface dorsoventral height of centra:	40.91
Posterior surface mediolateral height of centra:	44.8

Table 3: BP/1/7811 appendicular measurements

Scapula L	
PD L:	404.58
Prox. max. W:	145.05
Distal max. W:	N/A
Min. AP W of scap:	100.82
Min. width/PD L:	0.249

Humerus L	
PD L:	428.5
DPC L:	139.48
Prox. max. W:	210.3
Distal max. W:	145.9
Min. shaft C:	181
DPC L/PD L:	0.32

Humerus R	
PD L:	432.1
DPC L:	137.16
Prox. max. W:	190.7
Distal max. W:	158
Min. shaft C:	180
DPC L/PD L:	0.317

Radius R	
PD L:	N/A
Prox. max. W:	N/A
Distal max. W:	51.94
Min. shaft C:	120

Ulna L	
PD L:	N/A
Prox. max. W:	86.58
Distal max. W:	N/A
Min. shaft C:	N/A

MC I	
PD L:	52.14
Prox. max. W:	60.26
Distal max. W:	49.83
Min. shaft D:	48.11

MCII	
PD L:	89.62
Prox. max. W:	43.39
Distal max. W:	37.62
Min. shaft D:	31.09

Ilium L	
Antpost L between pap and pop:	N/A
Antpost L between pop and ip:	283.35
Antpost L between pp amd pop:	~422.71
ACC L:	82.49
Mediolat width distal pubic peduncle:	52.73
Antpost length distal pubic peduncle:	79.22
Mediolat width distal ischial peduncle:	62.94
Antpost length distal ischial peduncle:	49.07
Dist. between pp and ip (inside of acetabulum):	152.84
Dist. between pp and ip (full):	268.53

Pubes L	
PD L:	481
ML W (mid):	135.49
ML W (prox):	62.1

Pubes R	
PD L:	444.79
ML W (mid):	124
ML W (prox):	57.01

Femur L	
PD L:	590.13
ML prox. W:	145
ML distal width:	181
Min. midshaft circum:	251
Max. midshaft circum:	266
4T height:	34.2
4T length:	112.85
PD humeral L/PD femoral L:	0.71

Tibia L	
PD Length:	459.09
Tibia PD L/Femur PD L:	0.78
Prox. maximum width:	165.24
Distal maximum width:	77.94
Min. shaft circum:	194

Fibula L:	
PD L:	421.41
Min. circ.:	123
Prox. W:	92.33
Dist. W:	49.37

Fibula R	
PD L:	416.4
Min. circ.:	12.8
Prox. W:	95.27
Dist. W:	59.56

Pedal phalanx:	
PD L:	92.37
Prox. W:	50.82

MATRIX:

Euparkeria

00000000?0000?0000000?000?1001000000000000000000?000000000100100000000000000000?0000000?00?000?
000000000?1000000000000000000?000000000000???0000??000000000?00?0?00??00000000000000000000000
?00?0?????0????000?0020000000000?0??????000000000001?0?0?0000???00?0010?0000?01100000000000100
00000000?02?000??0100000??1?000?100000?0000000??0?0?0010??0000?0????0?00?1?100000000?000

Crurotarsi

0000000000000?0(01)000000000?0001000000(01)000000000000000000001000000000000000000?0000000000
000000000000000000000000000000000000000000000???0000??000002000?00?0?00??000020000000000000
0000000000000000(01)00?0(01)0?002?000000000?00000000000000?0000000000000(01)000000010?0000?0(01)
00000000000000000000000?00?00000000000001?0000(01)00000?0000000??0?0000000000?00000000?00?001
00000000000(01)

Marasuchus

00???????0?0????????????0?00???????0???????????0?????????????????????????????00???00000??????????????
?????????00?00000000?1?1000000000100???00?0??00?000000?00???00??000?00000000?000000000??001010
0000000?000?012?1000?0000?????????????????????????????????000000000000?010001000000000000001000
0000110001000000??000000100010001001000000?0?0000000000?000??0?00?0?00?0??00???10

Aardonyx

1101?00210002?11?11?????1110?1011000??????1010??0?11010??10?1????????1?0????????????0??????1??0?
0?1?0?????11?00101011001?1??????0010?0110100101101?0000011?0011000100002000001 0?1100??0110000?
01110?0?00?????11??????????100??00??????131?01???1?10??10????????????????????1110100010011??10110?1
01?1111000011110001????????1101110?0???01???????????01201111(02)0?0010?0?2??00?0???03

Adeopapposaurus

1001100210002111?11?110110111110100001011010001 10(01)11011111001000102101(01)01100101101010101
101000001011(01)10101011111110(01)100111001111002000100101101101100(01)00111001100000000000000
1001101000100000001000000000001001
12)2110001010001101111011111001100201000001000(01)10003100000(02)0110110010?110010110010001101
000010(12)101010000000111011001001111010000111010000111100000102000110000110 01

Anchisaurus

10???00??0102?1??11?????111011?010?001010?10001100111101100?10??????01?001101?1??012110??????10
?10?000?10000000101?11?0111?0011???100?1001111011?10000?010?001100?000??0000000??01000?0???000
?00?10?0????11(01)0??2?11001011000??0??11010111?00100201000002000(01)10103100000?1111100010011?
001010010101101000010(01)1110?01000001110110?1?01?010???010111?0?0011????0?01?1?0010000010011

Antetonitrus

??
????????????????????????????0?(01)0????????????00?00?001??00(12)10002010121001000???1?????1??00?01
100?0??0?0001??3211000(01)01110??????0010?31100???1010???????0010003???0002010010001????????????
(12)110111100111111110??1000002100101010?????????????????121111120100?????(12)1200?0????(34)

Barapasaurus

??
???????????1?111211???????????1?1?????00??002??100101??002011021111201211 00?0(12)10001?1?1?1??1?
???0????101?00?21???????201????????????????????????????????111101310110001111100 11???11110010??????
?????????????1???1?1?????????1?1???????1??????????20????????????????2?1??????5

Blikanasaurus

??
??
??
???????0000?1110111?1?0100101111101110012011110011111210212000010 0?2

Camelotia

??
????????????????????????????????1???????????0??0??001??002100000000??00?0???????????1???0??011????
??1??????????1??00111?111011110111
?1??110???00000???(1 2)???000????4

Cetiosaurus

1???11???
???????????????????2??0011110111011010010002 0?2001?1??1020??1(12)11102010100???(12)??????20111?0
0100?0??0111101032110010002 01???????1?????????????????????????1111013?0210?0110?1?011??1101?00???2
11112??0???010?111??210100210010111???5

Chindesaurus

??
????????????????????????????0???????????????01?0??0?1??0?1??????000??00?????000????1?0?????1000?0?
??0???001??????0??????????????000010111000
10111000??????11111100???01?110100?????????????????????????????????????1

Chromogisaurus

??
??10000??10?0??1????????
????????????????0?????????????????????????????????0????111002102?????????????????????????0??????1???10
110????(01)00000(12)010100010?????????????????????????????????0??0???000???10

Coloradisaurus

?00?1002??10??111111?1??1110??011000?10??0??10?1001101110000100100?101001101101?110101?????1?1
001011010011?1000101010001?11?0011002000100101?01100?00?001?1001100000000000000101?????00?110
00?011???0????010010121110011?????????????????0?1???????????????0?0?131100???011?110020011001011
0000001101000010211101110000011101100??011110?001??????000011111101010200 01(01)000021002

Efraasia

100?1001?010??1?111?112?1110?100???00100100000??0?10??01?0??1??????10?000?1?????0110100??????10
010010??11?011001010100001???1?110011001001011011010000001??001?000000000000000001?0000010000
0?01100000?0?01001120120001110001101012010?1100000011101000100001001310001010000100000011001
0110100001111000010110000000000011101?001?011010?0??01?111000001??0?0?01?1?001(01)000010002

Eoraptor

0001?001?01010?0011100111010010010000110100000?1001001010??0110000(1
2)0011??11?1????????????????00000010???0?0?00?1000000001?????1100000000010?1011??000??01?00??10
0?000??00000011??10????10???001?00??0000?0100??10?10??001000??????20?000101?00010?00000(01)0100
100120002101??0??00?0???10?1011?10??0?011000010110001?00?1?0111010??1?0?00?????001????0?000????
?0?0??0010000000??000

Eucnemesaurus fortis

??
??0???01??001100(01)10000??00?0???????????10000?01100
??????????11??110???0??????????????01101110
10?1010110???000001110110??(23)

Eucnemesaurus entaxonis

??
??0?0?01??0????0???000??0000?00?1011?0?10?00?01????0?
??0?1??13?000100??1??0?0?0?11?010110?1?1?0111010
0101011010?0?????110111?1?0??0??????0??????11011112??001?(12)?0011000?????2

Glacialisaurus

??
??
??0????????????
??0011????????????????0???1010(01)0????1100?0111111?1010???????????????

Gongxianosaurus

1?????0??????????12??
??????00???1??2121????????????0?????????????1??0??001??0??????0?0??00000????????????????0?0?1?0??0
00?011???2?110????1????????????????????????????????????0?100????0????????????????????????(1
2)111?2??????0???110??1??????1?0??1???0?1?1?????1?11??01?0??????1?0??2?1112000020005

Guaibasaurus

??
??0???01??011001000000??00000??0000000?00000?01?0??0
(01)00??1??????110????1??0???????0????1?10??0?1?00??0?0?000?01(12)100210110010000000010?101100000
0100100001011010??(01)00?0?11111100100?01101?000101110000000000001?011000000000011

Herrerasaurus

00000000?0101000000000000000000000000100000010001010101000100001101000000101?0000000?1000?
00000000?1000000000000000001010001000000010000?00001000001 1??0010(01)1000000200000010000001011001001100100100?1110??0011000000000000001200000001000001101101001000001200000001000001 0???01?01010010000101110001011000001000011000100010010010100000001100000100000001000100000000?02

Isanosaurus

??0??0?????????????2??10??0??????????????????2?011000?????????????????????????????101?0???

11(01)00001001000111111111121113?00011101210010000110002?1110101010020110?01102012100000110011
1211111011001?01111110003221001001200110011011000 1?00011?0?10?1?31?11110131011?00111110011000
110100100211112??0???010?011??21010?0??0??????1010111111??????1120?1????2?1??2?121211102??05

Massospondylus

100110021000211111111121111011001000010110100011001101111000100010210100110010110101010?1010
0100101101010101 10(01)1010110011100?111002000100111101101000200111001100000000000000101110100
01(01)000000000000000?01(01)011121201011100011011110111210001012110000020000100131000(01)00011
011001001100101110(01)0101101000010(12)101010(01)000001110110010011110100?01111100001111100?01
0200011000021002

NMQR 3314

1001?1031000211111101?1110101111???1010101101011001101011?00000010220110110010??2002010011011
101?00111?1000110?10021100110?01011001?001101001011(01)10000001??0??100??0?0?10000000?01111001
?0100?0?1??00?????1????(23)01100?0?1110??????0010?21000101(12)0?00010200001001310 00(01)0(12)??????
??????1??10110?????????????1???1101110000011?011?01?0??0?0???100111001201111201001?2?011(12)0000
11003

NMQR 1551

??
??11???00?001??002100000000100000000?02?1100120000?0(01)11
000????0100??2?????00011?0???????????21?????????????????0010013100000(01)011010001????????????111
01111001110(01)1110111000001110110010 0?101010000??????11011112?000?????1120000????3

BP/1/7811

??
????????????????????????010??0????01??11???1101?0010011?00(12)10011000010000000????????????????0?1
???????00????20110?000?1?0????????10?21100??????????????00?0?13100000?011010001????????????111?1
1110011101110011100 00?1110110010??00??????(23)

Mussaurus

??
????????????????????????????001000??????10110??0000?1??00100000000?00000010??1?1??0111?00001110?
0????0110??1011000111100?1?11?0010121001101201000002 00???0?03100010?011??1001?011??10110?10101
101000010111101?100000(12)1101110100110101010??????0110111100000112001110000110 03

Neosauropoda

110001131111201101200000101011 1(02)11101112010101011(01)11110121100(0
1)10112221110010111120(01)200000102011100001201000(01)111111(02)12(01)112(01)00001110011?1101001
10020121010101(01)020111(12)0110201211000021000112011111(01)1000(01)01001110003?21001(01)0020111
00010100000?000110001??1?300111101310210001111100110011 10(01)10(01)00211012??0???010?111112101
0?0100001111101011111111011??11211100??2?10?201212111021105

Neotheropoda

00(01)1(01)002(01)010201001100001(01)000000000000110000000010(01)100(01)01000001(01)0001(012)01000
000101100000011100010000000001?0000000000000000001011001100000010000(01)10000102000010101100100
00001000000000(12)100001100100000010010000100010?110000010000100012000000?10?0001001100(12)010
101013000211101010000111110000110100001?01100010000001000(01)01111111100200101100000111110000
??0?0000000?010000000000012

Omeisaurus

110001131111201101200000101011?201001112010101011111010121100000112221110010111???0?00???1???
11100001?0?00011101111121113??0011101200011010111002?1210101011020110?011020121100?021???1?20
111100100??01111010003221001000201??????0100001?000110001001?31011110131011000111110011000111
100100211012??0???010?010??210100?1?0??111?011010?11???1????121?110??2?10?20121211102?105

Ornithischia

0010000000000?0000000?000?1011000100100?1000000100100001000000(01)000100100000000100000000010
010(01)01(01)000000100111001110100001000000000100100(0
1)0000??010000000?00?0?00?000000000000000(12)100000000000010000010000100111(02)110000010000000
000000000?00000000000000000110112100010001??000?000110000000100001?0101111020000?000000(01)10
1110002?01?(01)1000000111100000?000?00?00?0(01)0000000000010

Panphagia

??????????????????????0?1??????????????????????0??1????????1?1?0???????10?1?111??????????????????0?0?0?
1010000?10?0101000000????????001000100111?01101?000?01???01?10000?000000000??0??000??0000?0100
0?0?0??0111??0??0?11(01)0021010?00?000???11??0?110?????
??????????????????001001010100???0100?010?0????????????????0???????(01)???????????

Pantydraco

?0???0????????????(01)00?0???1??1????000100100000010?100001?00????????00?000?1?10??00100011?000?
00?01010??0000?1001010100001001??11001100101001101101?00???1????1??????????????????????????0??1?0
000100000100?????11?01?00??00100121100001?????????0011??10110?
00??????????1?1?0000??0000010?01?001??????????????????000011100000101?000000001001?

Patagosaurus

11??1?0000
1??????0??0111012111??????11001012100000110020?2001010?00201?02111120121?00?02100011(12)0?01?0?
100????0?111?00??2100100?201??????????????????????????????????1111013101000011111001100111110010?21
1112??0???0011111???10100(01)??0??5

Plateosaurus engelhardti

1001100110102011(01)1111121111001011000010010101011001100110001100100110110110110111101100010
11110010110101111110010101000011001111001100100(01)011011010002001110011000000000000001010010
0001(01)00000001000000000010011111(12)0000110001101111010111?0010010100000100001001311001020010
10001111100101111100011110000101100010100001111011001001101010000101110000111000000101100110
00010003

Plateosaurus gracilis

?00??001?0102?110111?1??1110?101??00?10?1010?0??0?10001100??10?????????????????1?????????????0?
?0110?????11100101010?001?????1100??001???01101101?00?001?10011000000000000010?10100001000000
0010000?00????????11200?011000?1011?1010101?0000???10?????0?00100131100102001010001111100101 1?
?(0 1)0001111000010110?0??10000?1??0110?????????????????????0?????????????0?0????????(23)

SAM *Plateosauravus*

??
?????????????????????????100??00100101?01101?00(12)0011?001100000000?1000000??10???011??00??11
0??0?????10???(23)011100111000????????????1????????10???????00100131100001?????????0?11??10110??0
01??110000101100010100000111011 0??????0??????????????????1100?00?????0??????????3

Pulanesaura

??
???????????10?012011????????001?111?0100??11?????0??1??00(12)(01)?0010?0120001000?????????2?111?0
11???0?0??????????????10??(12)0???0?11??1?11?????
???????????????????000002100101???1????????

PVL 3808

??
?????????????????????1?0?1111001100111101?011(01)1?00100111001100000000000000010101 01?00110000?01
10000????????103212100111000?????????????????????????????00100131100102 0?1010001????????????1?0
10101010010111?0101000001110110010???

Ruehleia

??
?????????????????????????0111001?00????01???101?0020011?00110010000011000010??1000001?0?00?0110?
??????0100111012000111000?0100??010111001000???0??00???001001311000020??11000110110?10110?1010
010100001021000??10?00?111011001?0?0010100?????????????????????????????????????3

Sarahsaurus

10?1000?10?1201??11?????1110111???0?010?0?1010010?110001(01)10010?0???001000111001?010101011??1
?10?10010?????011001010100011?0011110?10001111111011?1100200111001?00?0000000000010?110??0011
0000000?000000000100101(02)121000110001101111011?11?0?101211000002000010013 10(01)0002001011001
001100101110??101101000010010?010100000?1?01100100110101?0001111101(01)01?11200?0102000(01)000
?1100(12)

Saturnalia

10?????????????????????????1??1????00?100?0??????????????????10?????1??00???0?0??0?0000??????????01
000??????0000100000000????????00100010010??01101?000001000011001000000000000000001000010???0??1
000???0??11101111110001010?2????????????????????????????????00000111(01)0210200000000100110010010 0
0000100(01)000101100000000000101010001001001010000000010000000000000010011000?000?0010

Seitaad

??

??00?(01)?1??00??00?001????0000?????????????????????????
???0010011??110001111?011?1110011131?0?00?2110??0???0?????????????0?1000001?????????????????????
?????????????0?00?11101?0???01101010?00??11?00??11????0?010???11(01)0000010??

Sefepanosaurus

??
??????????????????????????????00??0?1100???0?10??00?001????1?00000001??0000????1??????1?0?0??011???
??0?0?0?10??1?00????1?0?1011??010131?010??1010???0?111110
000??11(01)?????000000??????0?00110101111?0001??0?????11????0???2?0???????????

Shunosaurus

11000113?11020110120000001011?201001112010101010011010120000100111210100010 11?120020???1102
00110000120100011111112121112??00011?10012?1?10010012?1100001011021?0??01??201210000?11??00?1
01?110110011?111?1?0002221001100??11000?1011001??000110000??1?3101111013101100011111?01100?11
1100100211112??0???000?011??21010?(01)1?0????110?101???1?1011??1121?110??2?00?2?12121?1021105

Silesaurus

00?0??00?0000?00100000??0?00?0?01010?????????0010??0????01?????????00?0?0?0000??000000?????1?00?
0?010???0?000001000100010?000000000000???00100000000000101000011000000000000000??100000100000
?0?0????????111?1110000010000?0?????????????????????????????????00000100000200100000000?010100?0?1
000011011000100100000100011110000000?0000000??011?1??002???00000000?0?10???000?0011

Spinophorosaurus

1????1????????????????????????????????2????????????0????01?????????0??101111110(12)00???????????1?
????????????100111012?112?????11?110101?0?01?0002?110??01????(12)?11???1?12?1010?0?????????(12)???
11011?001?1??1110?03?2(12)0?10??(12)????1?1???01(12)0?011
??001??211111110?1101??0?0??20?1002??0??11?10??0?0?01????????????????????????????????????

Staurikosaurus

00??0000000
001000?00?0000000000????????00010?????00?01001?000011?000?000000000200000 01??010?101100?001100
100????1?1???0000002001100001 10?010?00010?00000100001?
?000?0101?000??000001100000001????01???1

Tazoudasaurus

11??010??1?????????(02)011???1???1?????????????00?0
0000???0??10?1111012101???000??0010120??????0002??100001??002001010110201210 00?????????21?11?11
1?????11?????01?22100100?(12)?????????010?2100000100?0001?310?1???03101??0?111000002??11??1??1??
211011110011111011?0???001002010101 0?1101011111??011????1?????20????????1??10?1????5

Thecodontosaurus

?0????????????????????????1??1??1000??????0?0?0?0???000????????????10?0?0?1010??011000??????00?1
1010??????1100101010000?1??????0001001010?1?01101?000001??001100000000000000?10000?0101000?0
1000?0?00?0100112011000101000110001201000 1?1000010100000101000001210000 01???0?000??011??01010
?(01)000111100001011000??(01)0000010101100??011010100?????1100?0?111??0??1??000??00?0????1

Unaysaurus

100110011010??1?111??1??1010?1011000????????????0??00????001???000??0?10??0?10??110100??????010?
10110?????01100101010000???0?1?????0??1?0??????????0??0?11?00?10000?0??00000????????????0?0???0
10000?00?010011?1120000110?0??????1????11?0????211???0??0???
????????????????????????110110???011010?00????????0???1100??????0??0???0??????1

Vulcanodon karibaensis

??
??1??????01?1??0?0??????
???1?????1?0?1??0100??0?11?110010?11?0111100100
1101???0?0?10021?01??11?101?????????????111010102??001020?11110?121??5

Xingxiulong

????????????????????????1???1?1111???0?10?0????011001100110000?000101?01?00100101?0??101???????0??
???????001??000?????????110011110010001 10?01?0110100020011100110000000000?00001100110???1110000
001?????00?0000????120?01111?0????1??????11?01??????????????0010013110000(12)0?1011002??11???0?1
0010101111000010110101 0?00000(01)10?110010011010?0?0?011?001101110000001?210011000021002

Yunnanosaurus

100?1002??00??10011001??101?111????00101110?00??0?11011111001000001?01?0?00010???????????????00
0?0010???0???00010?21000?1???111100(01)100110100?0110100000011000110000000001000000?0101?10110
000?00?0???0??001?0??121200?111(01)00??01??0011?21001100201000(01)020?0010013100000001101000 10?
110010111?(01)0101101000010110101?101000110011001?0110101000011 11001?0?1110?0?011???11?0000110
?2